TECHNICAL PROGRESS REVIEWS

REACTOR CORE MATERIALS

Prepared for U. S. ATOMIC ENERGY COMMISSION by BATTELLE MEMORIAL INSTITUTE

FEBRUARY 1959 VOLUME 2 NUMBER 1

TECHNICAL PROGRESS REVIEWS

To meet the needs of industry for concise summaries of current atomic developments, the AEC is publishing this series, Technical Progress Reviews. Issued quarterly, each of the reviews digests and evaluates the latest findings in a specific area of nuclear technology and science.

The three journals currently published in this series are:

Power Reactor Technology, Walter H. Zinn and associates, General Nuclear Engineering Corporation

Reactor Fuel Processing, Stephen Lawroski and associates, Chemical Engineering Division, Argonne National Laboratory

Reactor Core Materials (covering solid material developments), R. W. Dayton, E. M. Simons, and associates, Battelle Memorial Institute

Each journal may be purchased ($2.00 per year for subscription and individual issues $0.55) from the Superintendent of Documents, U. S. Government Printing Office, Washington 25, D. C. See back cover for remittance instructions and foreign postage requirements.

●

Availability of Reports Cited in This Review

Unclassified AEC reports are available for inspection at AEC depository libraries and are sold by the Office of Technical Services, Department of Commerce, Washington 25, D. C.

Unclassified reports issued by other Government agencies or private organizations should be requested from the originator.

Unclassified British and Canadian reports may be inspected at AEC depository libraries. British reports are sold by the British Information Service, 30 Rockefeller Plaza, New York, N. Y.; Canadian reports (AECL series) are sold by the Scientific Document Distribution Office, Atomic Energy of Canada, Ltd., Chalk River, Ontario, Canada.

Classified U. S. and foreign reports identified in this journal as Secret or Confidential may be purchased by properly cleared Access Permit Holders from the Technical Information Service Extension, U. S. Atomic Energy Commission, P. O. Box 1001, Oak Ridge, Tenn. Such reports may be inspected at classified AEC depository libraries.

REACTOR CORE MATERIALS

a review of recent developments in solid materials for reactor cores

prepared by
BATTELLE MEMORIAL INSTITUTE

FEBRUARY 1959 VOLUME 2 NUMBER 1

foreword

This issue marks the beginning of the second year of publication of Technical Progress Reviews on *Reactor Core Materials*, prepared by staff members of Battelle Memorial Institute at the request of the Division of Information Services of the U. S. Atomic Energy Commission.

Emphasis has been placed on specific accomplishments and their significance in order to provide a convenient condensed source of information to two types of readers: (1) those who wish to keep abreast of developments in a general way and (2) those who are interested in sources of more detailed information in particular areas. The pertinent papers from the Second Geneva Conference which were available at the time the manuscript for this issue was prepared are reviewed herein. The remaining Geneva papers will be covered in future issues as they are received.

The editors are most anxious to make these Reviews as useful and meaningful as possible. To this end, comments and suggestions from readers will be most welcome.

R. W. DAYTON
E. M. SIMONS
Battelle Memorial Institute

contents

Issued quarterly by the U. S. Atomic Energy Commission. Use of funds for printing this publication approved by the Director of the Bureau of the Budget on November 1, 1957.

Unalloyed Uranium

The mechanism of radiation-induced dimensional changes in uranium is being studied by Sylvania-Corning Nuclear Corp.[1] The investigation is being conducted in two parts. In the first, which is discussed later in somewhat more detail under Basic Studies of Radiation Effects in Fuel Materials, p. 16, the self-diffusion coefficient of uranium is being determined for various crystallographic directions. These measurements are necessary to check the assumption that anisotropic diffusion of atoms and vacancies (produced in the lattice by fission and by fast-neutron collisions) is responsible for dimensional instability, as proposed by Seigle and Opinsky.[2] The second part involves an experiment to determine the effect of grain size on the growth of alpha uranium during irradiation. Previous evidence had shown that the effect of grain size upon growth rate is unexpectedly small; however, the uniformity of preferred orientation among the specimens had been only qualitatively established. Thus the significance of the results was uncertain. Consequently, the experiments are being repeated using specimens of a wider range of grain sizes and whose uniformity of preferred orientation has been more precisely established.

Elevated-temperature tensile tests of uranium samples irradiated to 0.018, 0.031, 0.075, and 0.10 at.% burn-up are reported by Hanford.[3] Some of these results are presented in Fig. 1. It can be seen that the effects of reactor radiation on the room-temperature tensile properties of uranium are (1) a slight decrease in ultimate strength, (2) a marked increase in yield strength, and (3) a drastic decrease in ductility. As the testing temperature rises, the ultimate strength of the unirradiated uranium is reduced at a faster rate between room temperature and 300°C than that of the irradiated uranium. Furthermore, the slopes of the ultimate-strength curves in this temperature range decrease as the radiation exposure of the uranium increases. The opposite trends in ultimate strength occur between 300 and 400°C, and above this temperature there is little difference in ultimate strength between the irradiated and unirradiated uranium.

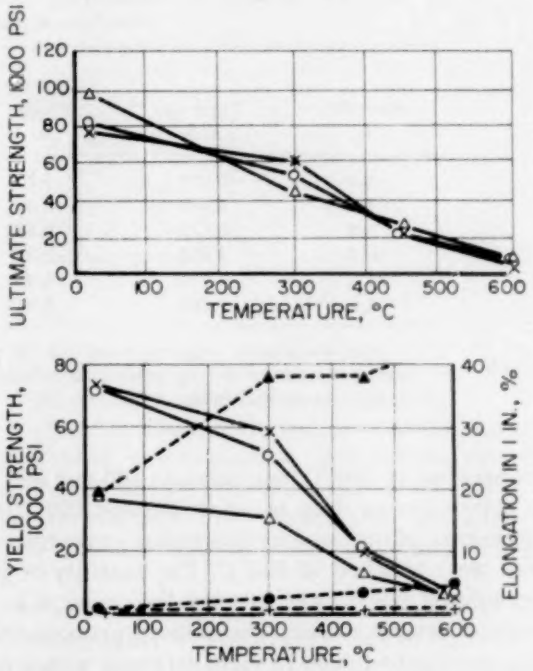

Figure 1 — Tensile properties of irradiated uranium. △▲, unirradiated; ○●, 0.031 at.% burn-up; ×+, 0.10 at.% burn-up; ---, elongation; —, strength. Data from Hanford Atomic Products Operation.[3]

The increase of yield strength at room temperature is appreciable at 0.031 at.% burn-up; however, little additional increase occurs from 0.031 to 0.10 at.% burn-up. A noticeable decrease in the yield strength with testing temperature

REACTOR CORE MATERIALS

FUEL AND FERTILE MATERIALS

Unalloyed Uranium

The mechanism of radiation-induced dimensional changes in uranium is being studied by Sylvania-Corning Nuclear Corp.[1] The investigation is being conducted in two parts. In the first, which is discussed later in somewhat more detail under Basic Studies of Radiation Effects in Fuel Materials, p. 16, the self-diffusion coefficient of uranium is being determined for various crystallographic directions. These measurements are necessary to check the assumption that anisotropic diffusion of atoms and vacancies (produced in the lattice by fission and by fast-neutron collisions) is responsible for dimensional instability, as proposed by Seigle and Opinsky.[2] The second part involves an experiment to determine the effect of grain size on the growth of alpha uranium during irradiation. Previous evidence had shown that the effect of grain size upon growth rate is unexpectedly small; however, the uniformity of preferred orientation among the specimens had been only qualitatively established. Thus the significance of the results was uncertain. Consequently, the experiments are being repeated using specimens of a wider range of grain sizes and whose uniformity of preferred orientation has been more precisely established.

Elevated-temperature tensile tests of uranium samples irradiated to 0.018, 0.031, 0.075, and 0.10 at.% burn-up are reported by Hanford.[3] Some of these results are presented in Fig. 1. It can be seen that the effects of reactor radiation on the room-temperature tensile properties of uranium are (1) a slight decrease in ultimate strength, (2) a marked increase in yield strength, and (3) a drastic decrease in ductility. As the testing temperature rises, the ultimate strength of the unirradiated uranium is reduced at a faster rate between room temperature and 300°C than that of the irradiated uranium. Furthermore, the slopes of the ultimate-strength curves in this temperature range decrease as the radiation exposure of the uranium increases. The opposite trends in ultimate strength occur between 300 and 400°C, and above this temperature there is little difference in ultimate strength between the irradiated and unirradiated uranium.

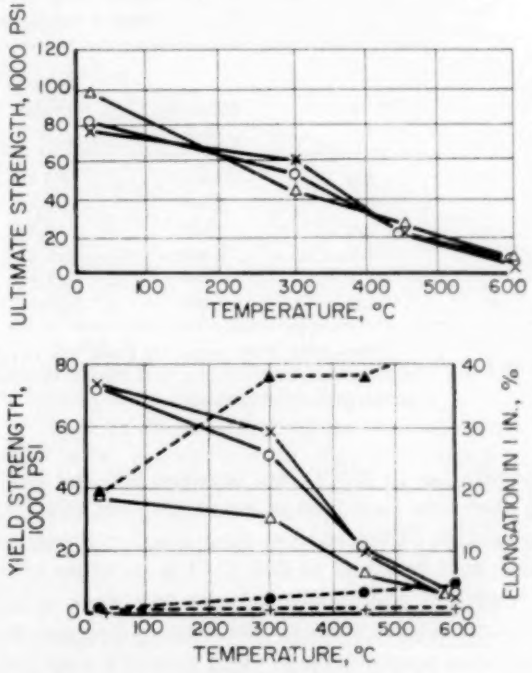

Figure 1 — Tensile properties of irradiated uranium. △▲, unirradiated; ○●, 0.031 at.% burn-up; ×+, 0.10 at.% burn-up; ---, elongation; —, strength. Data from Hanford Atomic Products Operation.[3]

The increase of yield strength at room temperature is appreciable at 0.031 at.% burn-up; however, little additional increase occurs from 0.031 to 0.10 at.% burn-up. A noticeable decrease in the yield strength with testing temperature

Table I-1 EFFECTS OF IRRADIATION ON SIDE-PRESSED* UNALLOYED URANIUM POWDER COMPACTS
(Data from Sylvania-Corning Nuclear Corp.[4])

Porosity, %	Burn-up, at.%	Calculated temp., °C		Length change, %	Growth rate, $\frac{\mu \text{ in./in.}}{\text{ppm burn-up}}$	Diameter change, %	
		Surface	Center			Parallel to pressing direction	Perpendicular to pressing direction
0.0	0.16	310	540	4.72	28	−4.69	3.26
1.2	0.16	300	530	4.77	27	−4.64	3.54
1.8	0.12	230	400	1.98	16	0.055	1.49
1.8	0.22	410	720	7.10	31	−4.49	5.65
4.2	0.11	220	360	2.04	18	−0.054	0.34
4.4	0.19	360	630	6.09	31	−0.49	5.92
5.1	0.21	390	690	7.15	33	−2.41	3.81
6.5	0.21	390	680	7.94	37	−2.74	0.54
7.5	0.058	130	210	0.85	15	0.57	3.49
8.0	0.076	160	260	0.81	11	1.56	0.37
12.4	0.080	155	250	3.4	42	1.08	1.88
12.5	0.24	380	580	10.8	43	1.41	4.10

*Specimens pressed at 600°C in side-molding die, using −12 +65 mesh powder.

Table I-2 EFFECT OF IRRADIATION ON ROLLED* UNALLOYED URANIUM POWDER COMPACTS
(Data from Sylvania-Corning Nuclear Corp.[4])

Porosity, %	Burn-up, at.%	Length change, %	Growth rate, $\frac{\mu \text{ in./in.}}{\text{ppm burn-up}}$	Diameter change, %	Hardness change, R_A
8.6	0.076	−2.78	−37	2.08	11.3
8.8	0.090	−2.43	−27	2.84	11.5
9.8	0.110	0.26	2.4	4.67	10.5
10.8	0.058	−1.15	−20	1.27	8.4
11.4	0.114	1.43	12	4.53	8.1
11.5	0.100	0.94	9.4	3.49	−0.4

*Specimens were prepared from −12 +80 mesh powder and rolled in a steel sheath at 600°C. Maximum temperature during irradiation is estimated to have ranged between 100 and 200°C, depending on the amount of burn-up.

occurs up to 300°C, but between 300 and 450°C a discontinuous drop is noted. Beyond 450°C the strengths of the various specimens converge and are well bunched at 600°C. The ductility of the irradiated specimens is very low, even at high testing temperatures. The authors propose that the pronounced drop in yield strength with temperature of the irradiated specimens above 300°C is attributable to two factors: (1) a change in deformation mechanism from predominantly twinning to predominantly slip and (2) the increasing rate of diffusion with temperature, which reduces the effectiveness of intergranular defects as slip inhibitors.

Uranium fuel with controlled, interconnected porosity is considered desirable because the pores are throught to provide a reservoir and escape path for fission gases. To test this theory, irradiation of uranium powder compacts was conducted by Sylvania-Corning.[4] The results are shown in Tables I-1 and I-2. The widely scattered results of these preliminary irradiation tests are still inconclusive and actually do not show any improvement of the porous material over the dense material in the range studied. However, it was found that side-pressed circular cylinders changed their cross section into an oval shape with very slight growth or shrinkage of the diameter in the pressing direction and consistent growth of the diameter perpendicular to the pressing direction. Rolled cylindrical specimens showed a rather uniform growth of the diameter in all directions.

Argonne[5] performed irradiation tests on two sets of three cylindrical U^{235} specimens, $\frac{1}{4}$ in. in diameter by 1 in. long. Each set contained one specimen in each of the following conditions:

Table I-3 SUMMARY OF PROPERTY CHANGES IN IRRADIATED U^{235} SPECIMENS*

Property changed	Degree of change at indicated per cent average depletion of U^{235}		
	Vertical capsule irradiation		Horizontal capsule irradiation
	0.011 at.%	0.019 at.%	0.019 at.%
Alpha annealed			
Length change, %		2.5	4.1
Diameter change, %		−0.8	−0.8
Density change, %		−0.10	−0.09
Hardness (R_A) increase		6.0	13.5
% change in roughness referred to diameter		−1.04	−0.64
Beta annealed			
Length change, %	0.34		0.4
Diameter change, %	0.36		2.4
Density change, %	−0.09		−0.10
Hardness (R_A) increase			
% change in roughness referred to diameter	0.56		1.28
Beta quenched			
Length change, %		0.5	0.5
Diameter change, %		0.9	0.7
Density change, %		−1.0	−0.10
Hardness (R_A) increase			
% change in roughness referred to diameter		0	0.08

*Data from Argonne National Laboratory.[5]

1. Alpha annealed; fine-grained material having a strong rolling texture.

2. Beta annealed; coarse-grained material, rolling texture removed by heat-treatment.

3. Beta quenched; fine-grained material, rolling texture removed by heat-treatment.

These specimens were irradiated both in vertically and horizontally positioned capsules. Burn-ups of 0.01 to 0.02 at.% were obtained at temperatures calculated to be below 75°C. The results, presented in Table I-3, may be summarized as follows:

1. Irradiation in a thermal flux caused alpha-annealed U^{235} cylinders to elongate markedly; beta-annealed specimens showed little or no dimensional change; beta-quenched specimens showed slightly more. Surface roughening correlated with grain size and preferred orientation in the specimens.

2. The irradiation changes are qualitatively similar to those noted in comparable specimens which have been thermally cycled, but no basis for quantitative correlation is apparent.

3. The irradiation elongation behavior correlates with preirradiation thermal-expansion-coefficient measurements made on the specimens. Sensitivity of this correlation appears good, and it should be investigated more carefully.

Detailed descriptions and discussions of the metallographic techniques utilized by Hanford[6,7] to study unirradiated and irradiated uranium have been published. (M. S. Farkas)

Alpha-Uranium Alloys

Argonne[8,9] has conducted "pin-cushion" irradiation tests on $\frac{1}{16}$-in.-diameter by $\frac{3}{16}$-in.-long specimens of fully enriched uranium, U^{235}-zirconium, and U^{235}-chromium alloys. The uranium-zirconium alloys ranged in composition from 2 to 20 wt.% zirconium, and the uranium-chromium alloys contained 0.03, 0.07,

and 0.22 wt.% chromium. The small pins were mounted in heat-transfer blocks, or "cushions," in such a way that surface roughening and length changes could be observed, recorded, and compared for various heat-treatments and burn-ups. Up to 1 total at.% burn-up occurred in the case of the zirconium alloys, and 0.45 at.% burn-up occurred in the chromium alloys.

The pin-cushion method was devised to allow for periodic examination of irradiation specimens from a qualitative viewpoint. In addition this method permits periodic length measurement at various calculated burn-ups, the final burn-up being determined by radiochemical analysis for Cs^{137}.

Results of the uranium-zirconium irradiation under the conditions of the test indicate that:

1. The addition of 2 to 20 wt.% zirconium to uranium improves dimensional stability under irradiation, as measured by the anisotropic elongation behavior. The improvement, in general, appears to increase with zirconium content. There are two reservations to this statement, mentioned in items 2 and 4.

2. The behavior of 725°C quenched specimens appears erratic. The most stable specimens show a trend toward improvement with zirconium content, but above 2 wt.% zirconium, anomalous scatter occurs and some specimens actually appear less stable than beta-quenched unalloyed uranium.

3. The 4 wt.% zirconium as-cast specimens are not quite so stable as the 2 wt.% specimens, but stability improves with increasing zirconium between 4 and 20 wt.%.

4. The following metallurgical treatments are consistently beneficial: as-cast (2 to 20 wt.% zirconium); cast, 800 to 850°C isothermal treatment (2 wt.% zirconium only); alpha-rolled, 800°C slow cool (2 to 6 wt.% zirconium); alpha-rolled, 800 to 850°C isothermal treatment (2 to 6 wt.% zirconium).

5. The following inversions in growth behavior under irradiation were observed as the zirconium content was increased from 2 to 4 wt.%: as-cast material changed from shrinkage to swelling; alpha-rolled, 800°C slow cooled material changed from swelling to shrinkage; alpha-rolled, 800 to 850°C isothermally treated material changed from swelling to shrinkage.

6. Visual appearance of the irradiated specimens is compatible with the thesis that surface stability is associated with grain refinement. As-cast surfaces were smoothest, and those that had undergone modified or interrupted cooling were intermediate. Increasing the zirconium content from 2 to 4 wt.% noticeably improved the surface stability for all treatments; further increases caused little, if any, added benefit except in the as-cast conditions.

Radiation damage to the uranium −0.03, −0.07, and −0.22 wt.% chromium specimens in the alpha-annealed and beta-quenched conditions was very similar to that observed in unalloyed uranium of comparable history. The uranium-chromium specimens that were treated isothermally gave irradiation results similar to those of beta-annealed uranium. In spite of this essentially null result, which is associated with failure to obtain grain refinement in the specimens, there is evidence that, under other conditions, chromium additions to uranium may be beneficial.

The high-temperature mechanical and physical properties and transformation behavior of uranium alloys containing up to 4 at.% additions of a second element were reported by the British[10,11] at the Second Geneva Conference. Another Geneva paper[12] presents a survey of the advances in physical metallurgy of uranium and its alloys. Also of general interest is a recent book by Wilkinson and Murphy[13] on uranium and uranium alloys, which includes chapters on production, physical and mechanical properties, metallography, fabrication, powder metallurgy, corrosion, cladding, and radiation damage.

(M. S. Farkas)

Gamma-phase Uranium Alloys

At the Second Geneva Conference, Bettis presented[14] results obtained on the irradiation-induced gamma-phase reversion phenomenon. This is discussed under Radiation Effects in Metallic Fuels, p. 16. Briefly, on the basis of electrical-resistivity measurements, the kinetics of the neutron-induced phase reversal at low temperature have been described. A diffusion coefficient was determined for the process of concentration homogenization by displacement spikes which produce the gamma phase. In more recent studies[15] the reversion of alpha plus epsilon in uranium-molybdenum alloys was found to occur more rapidly than reversion of alpha plus gamma in uranium-niobium alloys. Results showing the effect of enrichment and

interlamellar spacing in uranium–9 wt.% molybdenum[16] are also reported.

Uranium-Molybdenum Alloys

Irradiation and postirradiation test results on the uranium–10 wt.% molybdenum alloy are reported in a joint APDA-Battelle Geneva Conference paper.[17] Density changes for irradiations to 2.7 total at.% burn-up and to temperatures of 745°C are shown in Fig. 2. No significant

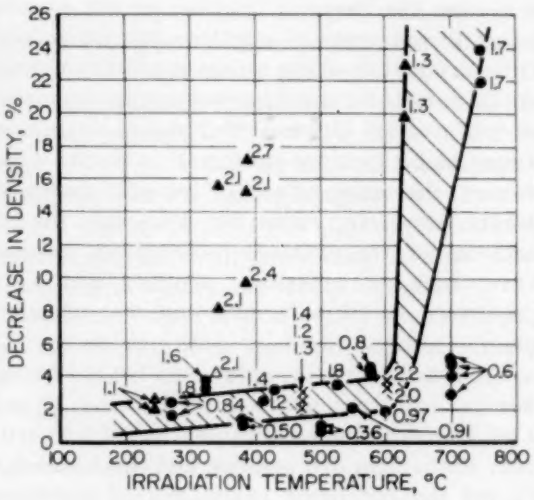

Figure 2—Density change as a function of irradiation temperature and burn-up in uranium–10 wt.% molybdenum alloy. Curves drawn from data obtained at less than 2.0 total at.% burn-up; all values are total at.% burn-up. ●, hot-rolled, unclad; ×, coextruded, unclad; ▲, coextruded, clad. Data from Atomic Power Development Associates; Battelle Memorial Institute Geneva Conference paper.[17]

effect of variations in composition between 9 and 11 wt.% molybdenum was noted. Samples irradiated in the gamma-quenched condition of heat-treatment exhibited smaller changes than did samples either partially or fully transformed. In specimens which cracked at burn-ups of 2.0 to 2.7 at.%, the severity of cracking increased with increasing zirconium-cladding thicknesses of 4 to 11 mils.

Postirradiation instrumented bend tests showed that a marked reduction in strength and ductility accompanied irradiations to less than 1 at.% burn-up. Elastic modulus decreased both with increasing burn-up and with decreasing temperature of irradiation. Hardness increased slightly as a result of irradiation. Electrical-resistivity changes accompanying irradiation were noted for specimens irradiated in the gamma-transformed condition. The changes are attributed to reversion to the gamma phase as a result of irradiation. An increased rate of thermal expansion on heating to 500 and 800°C is reported. The change is believed to reflect swelling. Microstructural changes accompanying irradiations to burn-ups of 2.0 to 2.7 at.% are reported. Homogenization and recrystallization effects and evidence for either fission-gas void formation or gamma transformation have been noted.

The known properties of uranium–10 wt.% molybdenum alloys have been compiled[18] by APDA. Physical properties include thermal conductivity, thermal expansion, electrical resistivity, density, melting point, and specific heat. Mechanical properties reported include ultimate strength, yield point, Young's modulus, elongation, and hardness. Properties measured for irradiated alloy materials include thermal conductivity, electrical resistivity, density, dimensional changes, and fission-gas release. Methods of fuel-core element and fuel-blanket element fabrication are presented and discussed.

The rate of growth of the diffusion layer in zirconium-clad uranium–10 wt.% molybdenum pins was examined at Nuclear Metals.[19] The increase in thickness was found to follow the relation $x = kt^{1/2}$, where x is thickness of the layer, t is the time, and k is a constant.

The British report[20] on the mechanical properties of uranium–0 to 14 wt.% molybdenum alloys, including hot hardness, Young's modulus, tensile and ultimate strengths, and Poisson's ratio. Data for room and elevated temperatures are given. Changes in properties with heat-treatment were found to be pronounced. Some qualification of the strength and ductility data is indicated due to the high nonmetallic impurity content of the alloy material employed.

A British investigator, Loasby, found[21] the magnetic susceptibility of a uranium–25 at.% molybdenum alloy to be $1.82 \pm 0.02 \times 10^{-6}$ emu/g at 20°C after quenching from 1000°C. The susceptibility was found to be independent of temperature between 90 and 300°K. Loasby also presented resistivity changes as a function of temperature and of transformation effected by various annealing conditions.

Ternary Alloys

Armour[22] reports corrosion rates in 680°F water for bare samples of uranium–7 wt.% niobium containing ternary additions of 1 and 2 wt.% zirconium; uranium–8 wt.% niobium containing ternary additions of 0.12 and 0.74 wt.% chromium, 0.90 and 1.94 wt.% titanium, 0.14 and 0.68 wt.% silicon, 0.14 wt.% nickel, 0.49 wt.% ruthenium, 0.98 and 2.02 wt.% vanadium; and of binary alloys of uranium–7, 125, and 15 wt.% niobium. All specimens failed within 10 days. Edge-exposed Zircaloy-2–clad sections of these same alloys in the as-rolled condition failed within 4 to 7 days. After heat-treatment at 450°C to produce 5 per cent transformation in the grain boundaries, all specimens failed within 1 day.

Battelle reports[23] the results of a survey of the effects of ternary and quaternary alloying on the stability and properties of uranium-zirconium, -niobium, and -molybdenum-base gamma-phase alloys. The effects of ternary and quaternary additions of chromium, molybdenum, niobium, ruthenium, vanadium, and zirconium on transformation kinetics, transformation temperature, hot hardness, and corrosion resistance were investigated.

Niobium or molybdenum additions to uranium-zirconium-base alloys increased thermal stability and hot hardness of the gamma phase and lowered transformation temperatures. These additions also generally resulted in improved corrosion resistance. Chromium, ruthenium, and vanadium additions also increased the thermal stability of the gamma phase and lowered transformation temperatures.

Zirconium increased the gamma-phase stability in uranium-niobium-base alloys, lowered transformation temperatures, and in some amounts increased hot hardness and improved corrosion resistance. Variable corrosion behavior of the uranium-niobium-zirconium alloys is probably attributable to lack of homogeneity. Molybdenum additions had either a negligible or detrimental effect on the thermal stability of the uranium-niobium gamma phase, although molybdenum did lower the temperature at which alpha uranium begins to decompose on heating. The addition of 1 wt.% molybdenum to the 10 wt.% niobium alloy or of 3 wt.% molybdenum to the 20 wt.% niobium alloy resulted in maximum hardness of the gamma phase at elevated temperatures, the hot hardness decreasing with larger additions. Little effect of molybdenum on the corrosion resistance of uranium-niobium-base alloys was noted, although a 3 wt.% addition was found to increase the corrosion life of the 10 wt.% niobium alloy. Chromium, ruthenium, and vanadium additions, while slightly depressing the temperature of transformation on heating, exhibited little effect on other properties of the gamma phase.

Niobium additions of up to 3 wt.% to the 7.5 wt.% molybdenum-base alloy and of 1 wt.% to the 10 and 12 wt.% molybdenum-base alloys increased the thermal stability of the gamma phase; larger niobium additions decreased stability. A possible slight increase in the temperature of gamma formation on heating accompanied the addition of niobium. Ruthenium increased gamma stability more effectively, whereas it depressed the temperature of transformation to gamma. However, ruthenium decreased the hot hardness of the uranium-molybdenum gamma phase, both as a ternary addition and as a quaternary addition to uranium-molybdenum-niobium alloys. Niobium additions to the 7.5 wt.% molybdenum alloy increased hot hardness, whereas additions above 1 wt.% to the 10 and 12 wt.% molybdenum alloys decreased hot hardness. Ruthenium and niobium additions both increased the corrosion resistance of uranium-molybdenum alloys.

Zirconium additions were found to be generally detrimental to thermal stability, hot hardness, and corrosion resistance of the uranium-molybdenum gamma phase, while vanadium and chromium additions exhibited a negligible effect.

Epsilon-phase Alloys

Uranium-Zirconium Alloys

A joint Battelle-Bettis paper[24] presented at Geneva summarized the constitution, transformation behavior, physical and mechanical properties, corrosion, and irradiation behavior of zirconium-uranium alloys, principally in the range to 70 wt.% uranium. Trends with composition and the effect of constitution as influenced by heat-treatment and impurities are noted. A Russian summary[25] of the results of American investigations, showing the stability of the uranium-zirconium epsilon phase and the effect of oxygen on the epsilon phase, has been published.

A complete hardness survey[26] of the zirconium-uranium system from room temperature to 900°C has been published by Chubb et al.

Loasby reports[21] that the magnetic susceptibility of a uranium–70 at.% zirconium alloy, annealed at 580°C, is $1.57 \pm 0.01 \times 10^{-6}$ emu/g at 20°C. Changes with temperature are presented. Resistivity measured at 0°C was $184 \pm 2 \times 10^{-6}$ ohm-cm; the temperature coefficient of resistivity over the range 90 to 300°K was -1.1×10^{-4}/°C.

Bettis[27] has issued a report describing the corrosion behavior of uranium-zirconium alloys in 600 and 680°F water and in 750°F steam. The uranium–50 wt.% zirconium alloy is unaffected by heat-treatment. The alloy exhibits a linear corrosion rate at 680°F, with corrosion rate increasing with increasing temperature according to the Arrhenius relation. Corrosion rates increase with increasing uranium content and decrease with increasing zirconium content.

Uranium–40 and –50 wt.% zirconium specimens, irradiated to less than 0.5 at.% burn-up, were found to exhibit less than 1 per cent swelling.

Uranium-Silicon Alloys

Chalk River[28] reports on studies of uranium-silicon epsilon-phase (U_3Si) alloys. Epsilon forms rapidly initially at 800°C from uranium and U_3Si_2, the rate decreasing with time. In as-cast alloys after 24 hr, 90 per cent epsilon has formed, and 95 per cent has formed after 156 hr. Epsilonization at 500°C and above is reported. De-epsilonization of extruded material on heating to temperatures of 900°C and above was found to be markedly dependent on carbon content, de-epsilonization proceeding more rapidly at lower temperatures in high-carbon materials. Similarly the amount of epsilon formed during extrusion at 850°C is dependent on carbon content. These effects are believed to be due to a lowering of the epsilon peritectoid temperature. Density increases, hardness decreases, and resistivity decreases as a function of per cent epsilon present are given.

Corrosion results in 300°C water for arc-melted epsilonized material show that corrosion rates are dependent on silicon content. Below 3.65 wt.% silicon, samples tend to crack and gain weight. Between 3.65 and 3.77 wt.%, the corrosion rate is constant and of the order of 15 mg/(cm^2)(day). At 4.09 wt.% silicon the corrosion rate is much higher again. Results are erratic, however, and conclusions are based on statistical results.

On bare extruded material containing 3.9 to 4.0 wt.% silicon which has been given an epsilonization heat-treatment, no effect of carbon contents from 160 to 1400 ppm is evident, corrosion rates varying between 3.0 and 31.0 mg/(cm^2)(day). However, without the epsilonization treatment, carbon has a detrimental effect, presumably because of partial de-epsilonization resulting from a lowering of the peritectoid temperature with increasing carbon content.

Preirradiation electrical resistivities of uranium-silicon epsilon-phase specimens have been measured.[29] They vary from 42.54 to 25.97 μohm-cm at –200°C and from 84.14 to 70.58 μohm-cm at 400°C in specimens heat-treated to contain 0 to 90 per cent epsilon, respectively.

(A. A. Bauer)

Dilute Uranium Alloys

Aluminum-Uranium Alloys

Segregation in aluminum-uranium alloys and the effect on fuel loading of aluminum-base fuel elements has been the subject of an extensive study at Oak Ridge.[30] It was found that chemical assay of the alloys by potentiometric titration of the tetravalent uranium ion yields results which are, on the average, within 0.4 per cent of the true uranium content. Alloy castings containing up to 55 wt.% uranium which are prepared by conventional casting techniques exhibit inverse segregation. Results of the study show that the segregation persists in castings solidified over a fairly wide range of cooling rates. It is interesting to note that gravity segregation patterns are not important. This effect was the same in both bottom and lip-poured castings, but it was greatly overshadowed by the inverse segregation.

Increased mold temperatures were found to improve homogeneity, but the required temperatures are sufficiently high to be undesirable in terms of other production considerations. Dip sampling of the melt permits accounting for the weight of U^{235} in subsequently manufactured fuel elements of alloys containing from 13 to 19 wt.% uranium. This eliminates the need for sampling and analyzing the rolled stock. However, the method cannot be used for alloys containing

more than 19 wt.% uranium because uranium gradients become steeper as the alloy composition deviates from the eutectic composition (about 13 wt.% uranium).

Alloy shot having a nominal composition of 75 wt.% aluminum–25 wt.% uranium has been successfully produced by National Lead Co.[31] as a homogeneous feed material for such fabrication techniques as extrusion, arc melting, compression rolling, and compacting. The shot is produced by vacuum melting and pouring slowly through a $^{3}/_{32}$-in. hole onto a rapidly spinning disk. The disk design is important. Best results have been obtained with a 5-in.-diameter concave disk made of graphite, flame-spray coated with a layer of stabilized zirconia and then a layer of alumina. Optimum conditions appear to be a speed of rotation for the disk of 2400 rpm under helium at a pressure greater than $^{1}/_{2}$ atmosphere. There was no porosity in the shot, and spot analyses varied between 24.6 and 25.1 wt.% uranium. Nuclear Metals[32] workers have prepared very good alloy rod from powder of this type with front, center, and rear analyses of 24.19, 24.19, and 25.29 wt.% uranium, respectively. The shot was hot-compacted at 850°F under 450-ton pressure in a steel can; the can was machined away and the billet canned in 2S aluminum. This was then extruded at 950°F at a reduction ratio of 32:1. Data indicate that alloys prepared by this technique are homogeneous and are harder and stronger than similar cast alloys. Microstructures show that the UAl_4 particle size is smaller than it is in normal cast material.

Battelle[33,34] is experimenting with a moving pouring spout in the centrifugal casting of aluminum–35 wt.% uranium alloy extrusion blanks. This technique lays the molten metal into the mold continuously along its length. The problem of excessive metal solidification in the spout is solved by heating it to a temperature of 1500°F. Long castings can be produced by this technique with excellent outside surfaces and no internal porosity. The addition of 3 at.% palladium to the alloy stabilizes the UAl_3 and thus prevents formation of UAl_4. This addition was also found to improve fabricability. Wilkinson and Murphy[35] describe a technique for making aluminum-uranium alloys in which powdered UAl_4 and UAl_2 are mixed with powdered aluminum, cold-pressed, and sintered at 450 to 600°C.

Zirconium-Uranium Alloys

In connection with a study of the effect of transient temperature excursions in a reactor on swelling of Zircaloy-2–base 6 to 12 wt.% uranium alloys, Bettis[15] reports that a Zircaloy-2–clad alloy containing 10 wt.% uranium irradiated to a burn-up of 25 per cent of the uranium atoms (about 0.97 total at.%) exhibited a thickness increase of 213 per cent after $^{1}/_{2}$-hr post-irradiation anneal at 760°C (1400°F). Metallographic examination showed that there was a large void present in the fuel. It is postulated that fission gases collected in a crack or cracks caused by either fabrication or thermal stresses induced by quenching. Postirradiation annealing studies in progress at Knolls[36] on zirconium-base alloys containing 6 to 8 wt.% uranium indicate that when volume increases exceed the normal rate of increase per per cent burn-up (that caused only by the extra volume of fission products) the resistivity increase drops below normal. This leads to the general conclusion that the resistivity is depressed by the same phenomena responsible for swelling and thus is related to irradiation temperature and concentration of fission products. There may be two opposing factors—one tending to increase resistivity and the other tending to decrease it. The increase could be caused by the introduction of foreign atoms into the lattice and the decrease caused by recrystallization or precipitation of these atoms to form gas bubbles.

Knolls also found that 7 wt.% uranium alloys having 1, 1.3, and 6 total at.% burn-up swelled slowly during a 6-hr postirradiation heat-treatment at 620°C. However, Bettis noted that zirconium-base alloys containing 5 to 6 wt.% uranium, having 1.0 and 1.5 total at.% burn-up, showed no volume changes until they were post-irradiation annealed for $^{1}/_{2}$ hr at 700°C; at this point the material having 1.0 at.% burn-up exhibited a volume change of 3.2 per cent, and the material having 1.5 at.% burn-up showed a volume change of 7.5 per cent.

Evaluation of qualitative data obtained by Knolls[36] by a 3-point-loaded bend test on irradiated zirconium-base uranium alloys resulted in the following conclusions:

1. Ductility decreases with increased burn-up.
2. Load carrying capacity generally increases with increasing burn-up.

3. During elevated-temperature tests, the maximum load is reached at lower strain than in the room-temperature tests.

It is interesting to note that initial studies of energy absorbed versus burn-up indicate that radiation change tends to saturate at about 1.2 at.% burn-up.

Merten et al.[37] report results of studies with zirconium-uranium-hydrogen alloys. These alloys are produced by first preparing a binary alloy of zirconium and 8 wt.% uranium by arc melting and normal fabrication. The hydrogen is then added slowly at temperatures in excess of 750°C until the desired hydrogen content has been attained. Two forms of cracking may occur in these alloys. The first is a surface crack caused by a high hydrogen concentration at the surface which produces a hydride precipitate. This precipitate cracks as the center of the piece expands with increase in hydrogen. The other form of cracking is associated with the formation of beads of the uranium phase on the surface. This is not fully understood. General specimen distortion is closely related to the uniformity of hydrogen distribution which, in turn, is a function of the temperature uniformity maintained during hydriding.

The thermal conductivity of the zirconium–8 wt.% uranium–1 wt.% hydrogen alloy at 100°C is less than that of unalloyed zirconium but is half again that of the uranium-zirconium alloy before hydriding. The electrical resistivity at room temperature is 53 μohm-cm, that of zirconium is 45 μohm-cm, and the 8 wt.% uranium binary alloy before hydriding has a resistivity of 73 μohm-cm. The ternary is brittle at room temperature. The ultimate strength is about 30,000 psi. Reported weight loss after 90 days of exposure in boiling water is 0.2 mg/cm^2.

Kalish[38] has produced zirconium-uranium alloys, rich in zirconium, by powder metallurgy. These alloys had high density when sintered at temperatures on the order of 1170°C. They were prepared from minus 325-mesh uranium and minus 325-mesh zirconium-hydride powder, compacted at 50 tsi, and vacuum sintered.

Niobium-Uranium Alloys

Battelle has irradiated two niobium-uranium alloy specimens containing 20 wt.% uranium to a burn-up of about 10 per cent of the uranium atoms at a temperature of 1100°F. Postirradiation examination showed that there was very little change in the specimens. One of these specimens was heat-treated at 1300, 1500, and 1800 to 1900°F for ½ hr at each temperature. As a result of the 1300°F treatment, the density decreased 1.1 per cent; the density change after the 1500°F treatment was 1.7 per cent; and, after the 1800 to 1900°F treatment, the change was 3.2 per cent. A final heat-treatment, carried out at a temperature above 2000°F (actual temperature unknown), caused the specimen density to decrease by 13.6 per cent of its value prior to any heat-treatment but after irradiation.

Unirradiated samples have been heated in NaK at 1800°F for one week. Although there was no severe attack on the specimens, weight losses were on the order of 0.1 to 0.2 per cent. A study of the properties of niobium-uranium alloys is also in progress.[34] Fabricability, mechanical and physical properties, and corrosion characteristics of binary alloys containing from 10 to 60 wt.% uranium are being investigated. To determine the effect of impurities on these properties, alloys have been prepared from three grades of niobium having the following oxygen and zirconium analyses:

1. 400 ppm oxygen and <100 ppm zirconium.
2. 700 ppm oxygen and 0.17 wt.% zirconium.
3. 600 ppm oxygen and 0.7 wt.% zirconium.

These alloys are being fabricated for the testing program. (R. F. Dickerson)

Plutonium Alloys

Plutonium Metal

Attempts to zone refine plutonium at Los Alamos have shown that concentrations of aluminum, chromium, cobalt, iron, manganese, nickel, and silicon can be reduced by zone-refining techniques.[39] Movement of impurities was found to be dependent upon rate of zone travel and width of zone. Speeds in excess of 0.5 in./hr did not prove to be very effective.

Transformation kinetics of alpha and beta plutonium were studied at Hanford, using a fluid-displacement technique.[40] Time-temperature transformation curves of the beta-to-alpha reaction have the form of typical C curves, with the maximum rate of transformation at approximately –20°C. Impurities were found to shift the curve to the right, as shown in Fig. 3.

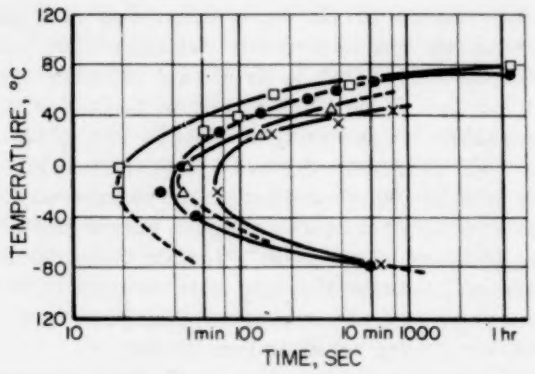

Figure 3 — Time-temperature-transformation curves for beta-alpha plutonium (50 per cent transformed), showing the effect of impurities. □, 200 ppm; ●, 400 ppm; Δ, 500 ppm; ×, 1500 ppm. Data from Hanford Atomic Products Operation.[40]

Plutonium-Uranium Alloys

The plutonium-rich portion of the plutonium-uranium diagram has been redetermined. The new version, as shown in Fig. 4, differs from the earlier one in a number of ways: (1) a peritectoid reaction occurs at 125°C involving the alpha, beta, and gamma phases rather than the eutectoid at 115°C previously reported; (2) the narrow gamma-plus-zeta region between 271 and 297°C has been eliminated; and (3) solid solubilities of uranium in beta, gamma, and delta phases appear to be lower than previously reported. Also, about 1.2 at.% uranium appears to be soluble in the delta-prime phase at 442°C.

Cast uranium alloys containing up to 13 wt.% plutonium were irradiated by Argonne[42] to burn-ups ranging up to 0.84 at.% with central temperatures ranging up to 490°C. The cast specimens all developed severe surface roughening during irradiation, probably because of excessively large grain sizes. The as-extruded alloys, having small grains, maintained good surface smoothness but showed elongations which were dependent on plutonium content. At 14.1 wt.% plutonium alloy elongated 96 per cent with 0.4 at.% burn-up, whereas an 18.7 wt.% plutonium alloy elongated only 8.4 per cent. Pre-irradiation heat-treatment of the extruded alloys increased the grain size and resulted in excessive surface roughening during irradiation.

Plutonium-Thorium Alloys

The plutonium-thorium diagram has been redetermined at Los Alamos.[43] From evidence

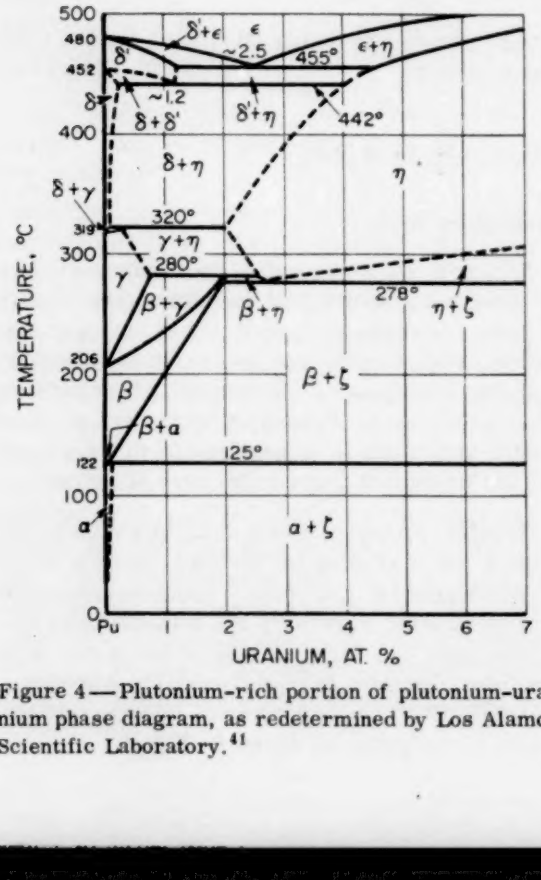

Figure 4 — Plutonium-rich portion of plutonium-uranium phase diagram, as redetermined by Los Alamos Scientific Laboratory.[41]

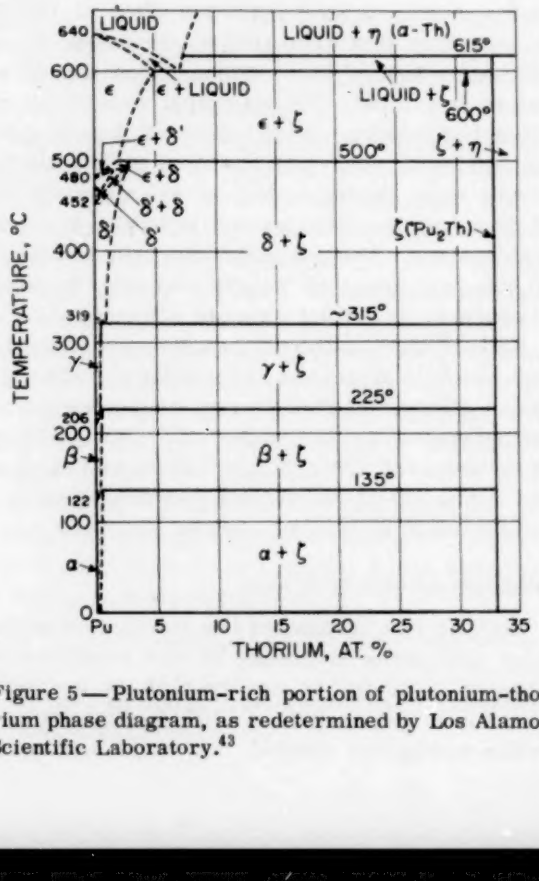

Figure 5 — Plutonium-rich portion of plutonium-thorium phase diagram, as redetermined by Los Alamos Scientific Laboratory.[43]

gathered for a plutonium–30 wt.% thorium alloy, it appears that the zeta phase decomposes peritectically on heating at 615°C to form liquid and an eta phase. A plutonium–15 at.% thorium alloy showed diffraction patterns of the epsilon and zeta phases below 600°C, with the epsilon phase disappearing above 600°C. Solid solubility of thorium in delta plutonium is 3 to 4 at.% at 500°C, in epsilon plutonium it is 5 at.% at 600°C, and in delta-prime plutonium it is 1 to 1.5 at.% near 485°C. The diagram, as constructed to conform with the new evidence, is shown in Fig. 5. (V. W. Storhok)

Thorium Alloys

Two historical reviews of the technological development of thorium have been published recently. The book by Wilkinson and Murphy[44] contains a chapter describing, in abbreviated form, the handling of thorium from ore deposit to finished product. A report from Du Pont describes in historical fashion the development of high-purity thorium metal for reactor applications. The latter report contains corrosion, irradiation, and reprocessing data obtained through 1956.

Murray[45] of the British Atomic Energy Research Establishment has provided additional details on the nature of the constitution of thorium-uranium alloys and has presented information on the constitution of the ternary system, thorium-uranium-zirconium. Murray's data on the binary thorium-uranium system are in excellent agreement with previously published data. New data on the solubility of thorium in uranium give values of 0.30 at.% thorium at 900°C and less than 0.05 at.% thorium at 700°C. For the ternary system it is reported that the addition of zirconium raises the thorium-uranium eutectic temperature above 1100°C. The addition of about 8 at.% zirconium eliminates the liquid miscibility gap between thorium and uranium above 1380°C. The addition of zirconium should and apparently does result in increased terminal solid-solution regions. Alloys of 7.4 at.% thorium plus 10 to 14 at.% zirconium possess an acicular structure when quenched from 900°C, showing that they were largely gamma-uranium solid solution at 900°C.

A revised and enlarged edition of a compilation of uranium and thorium constitution diagrams has been issued by Battelle.[46] Many minor revisions will be noted in this edition as compared with the earlier edition. A new version of the thorium-carbon diagram shows a minimum in the liquidus between thorium and thorium monocarbide at about 0.4 wt.% carbon and 1680°C. The diagram continues to show complete solid solubility at high temperatures between thorium and thorium dicarbide, with the intermediate phase, thorium monocarbide, having a congruent melting point on the liquidus curve. It appears that one or more peritectic or eutectic reactions have been overlooked and that much additional work is needed on this diagram. With the discovery of the phases ThPb, $ThPb_2$, and $ThPb_3$ and with a description of part of the liquidus curve, the thorium-lead constitution diagram begins to take on a resemblance to the thorium-bismuth diagram. However, a ternary section of the thorium-bismuth-lead system at 1000°C shows no indication of solubility between the phases ThBi and ThPb. The solutiliby of oxygen in thorium is reported to be less than 0.03 wt.% at 1415°C.

Problems encountered in melting and casting aluminum-thorium alloys appear to be identical with those encountered in preparing aluminum-uranium alloys. Atomic Energy of Canada, Ltd.,[47] reports that a pouring temperature of 1050°C gives the best compromise between porosity and segregation in casting of aluminum–30 wt.% alloys. The pouring temperatures investigated ranged from 900 to 1050°C, the pouring funnel was preheated to 550°C, and the mold was graphite.

Hanford has reported additional details of its studies of thorium-uranium alloys.[3] After cold reductions of 60 per cent, low-carbon thorium alloys containing 1 to 5.4 wt.% uranium had hardnesses ranging from 125 to 130 DPH. After annealing for 2 to 4 hr at 800°C, these same materials had hardnesses ranging from 83 to 108 DPH and were completely recrystallized. Annealing at 900°C resulted in some hardness increases over the minimums achieved, and this effect was attributed to the increased solubility of uranium in thorium at 900°C and to precipitation of uranium from the thorium on furnace cooling. No additional information is available on the series of thorium–2 wt.% uranium alloys being irradiated at 560°C to a burn-up of 3 at.%. Samples examined at ½, 1, and 1½ at.% burn-up have been harder and less ductile than control

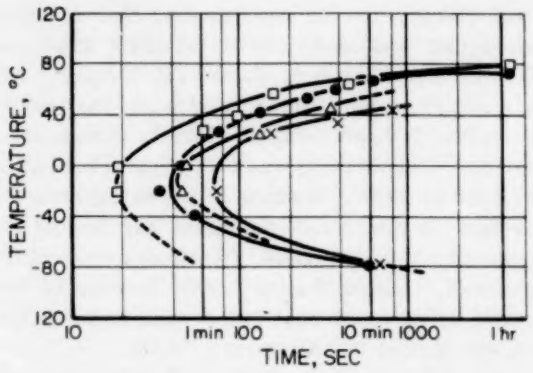

Figure 3 — Time-temperature-transformation curves for beta-alpha plutonium (50 per cent transformed), showing the effect of impurities. □, 200 ppm; ●, 400 ppm; Δ, 500 ppm; ×, 1500 ppm. Data from Hanford Atomic Products Operation.[40]

Plutonium-Uranium Alloys

The plutonium-rich portion of the plutonium-uranium diagram has been redetermined. The new version, as shown in Fig. 4, differs from the earlier one in a number of ways: (1) a peritectoid reaction occurs at 125°C involving the alpha, beta, and gamma phases rather than the eutectoid at 115°C previously reported; (2) the narrow gamma-plus-zeta region between 271 and 297°C has been eliminated; and (3) solid solubilities of uranium in beta, gamma, and delta phases appear to be lower than previously reported. Also, about 1.2 at.% uranium appears to be soluble in the delta-prime phase at 442°C.

Cast uranium alloys containing up to 13 wt.% plutonium were irradiated by Argonne[42] to burn-ups ranging up to 0.84 at.% with central temperatures ranging up to 490°C. The cast specimens all developed severe surface roughening during irradiation, probably because of excessively large grain sizes. The as-extruded alloys, having small grains, maintained good surface smoothness but showed elongations which were dependent on plutonium content. At 14.1 wt.% plutonium alloy elongated 96 per cent with 0.4 at.% burn-up, whereas an 18.7 wt.% plutonium alloy elongated only 8.4 per cent. Pre-irradiation heat-treatment of the extruded alloys increased the grain size and resulted in excessive surface roughening during irradiation.

Plutonium-Thorium Alloys

The plutonium-thorium diagram has been redetermined at Los Alamos.[43] From evidence

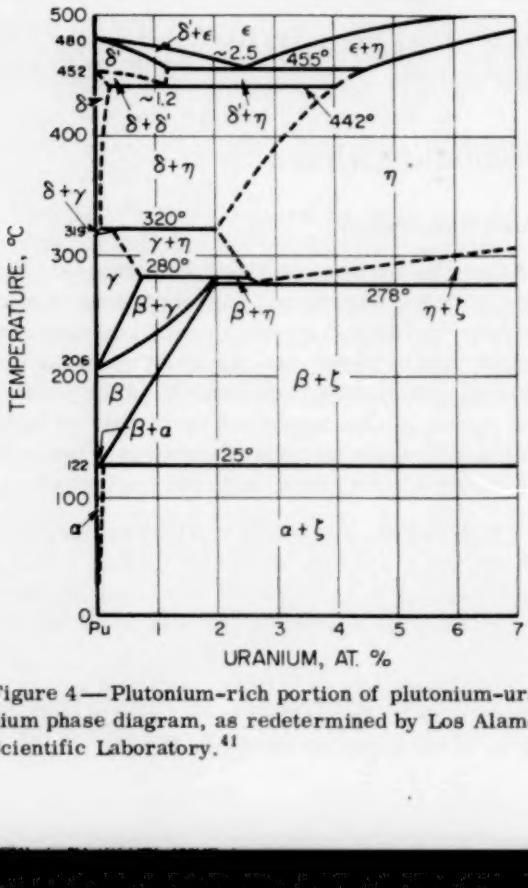

Figure 4 — Plutonium-rich portion of plutonium-uranium phase diagram, as redetermined by Los Alamos Scientific Laboratory.[41]

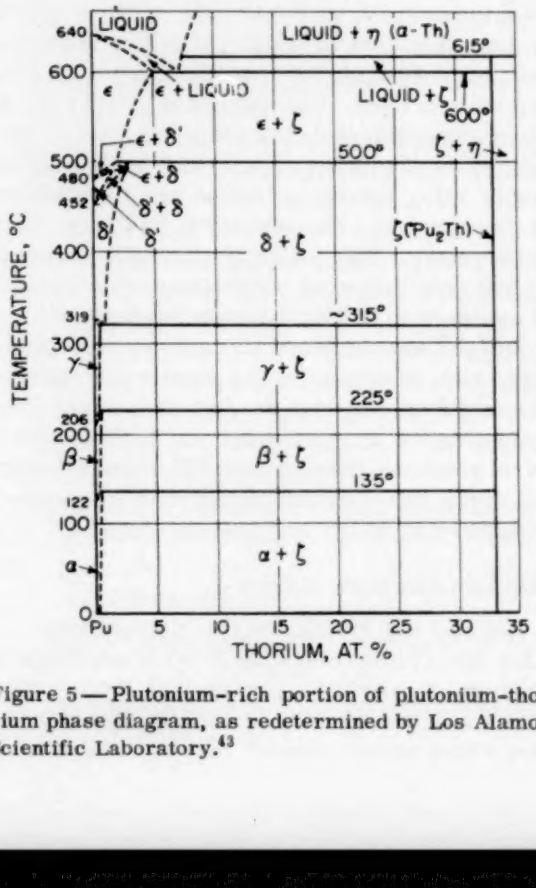

Figure 5 — Plutonium-rich portion of plutonium-thorium phase diagram, as redetermined by Los Alamos Scientific Laboratory.[43]

gathered for a plutonium–30 wt.% thorium alloy, it appears that the zeta phase decomposes peritectically on heating at 615°C to form liquid and an eta phase. A plutonium–15 at.% thorium alloy showed diffraction patterns of the epsilon and zeta phases below 600°C, with the epsilon phase disappearing above 600°C. Solid solubility of thorium in delta plutonium is 3 to 4 at.% at 500°C, in epsilon plutonium it is 5 at.% at 600°C, and in delta-prime plutonium it is 1 to 1.5 at.% near 485°C. The diagram, as constructed to conform with the new evidence, is shown in Fig. 5. (V. W. Storhok)

Thorium Alloys

Two historical reviews of the technological development of thorium have been published recently. The book by Wilkinson and Murphy[44] contains a chapter describing, in abbreviated form, the handling of thorium from ore deposit to finished product. A report from Du Pont describes in historical fashion the development of high-purity thorium metal for reactor applications. The latter report contains corrosion, irradiation, and reprocessing data obtained through 1956.

Murray[45] of the British Atomic Energy Research Establishment has provided additional details on the nature of the constitution of thorium-uranium alloys and has presented information on the constitution of the ternary system, thorium-uranium-zirconium. Murray's data on the binary thorium-uranium system are in excellent agreement with previously published data. New data on the solubility of thorium in uranium give values of 0.30 at.% thorium at 900°C and less than 0.05 at.% thorium at 700°C. For the ternary system it is reported that the addition of zirconium raises the thorium-uranium eutectic temperature above 1100°C. The addition of about 8 at.% zirconium eliminates the liquid miscibility gap between thorium and uranium above 1380°C. The addition of zirconium should and apparently does result in increased terminal solid-solution regions. Alloys of 7.4 at.% thorium plus 10 to 14 at.% zirconium possess an acicular structure when quenched from 900°C, showing that they were largely gamma-uranium solid solution at 900°C.

A revised and enlarged edition of a compilation of uranium and thorium constitution diagrams has been issued by Battelle.[46] Many minor revisions will be noted in this edition as compared with the earlier edition. A new version of the thorium-carbon diagram shows a minimum in the liquidus between thorium and thorium monocarbide at about 0.4 wt.% carbon and 1680°C. The diagram continues to show complete solid solubility at high temperatures between thorium and thorium dicarbide, with the intermediate phase, thorium monocarbide, having a congruent melting point on the liquidus curve. It appears that one or more peritectic or eutectic reactions have been overlooked and that much additional work is needed on this diagram. With the discovery of the phases ThPb, $ThPb_2$, and $ThPb_3$ and with a description of part of the liquidus curve, the thorium-lead constitution diagram begins to take on a resemblance to the thorium-bismuth diagram. However, a ternary section of the thorium-bismuth-lead system at 1000°C shows no indication of solubility between the phases ThBi and ThPb. The solutiliby of oxygen in thorium is reported to be less than 0.03 wt.% at 1415°C.

Problems encountered in melting and casting aluminum-thorium alloys appear to be identical with those encountered in preparing aluminum-uranium alloys. Atomic Energy of Canada, Ltd.,[47] reports that a pouring temperature of 1050°C gives the best compromise between porosity and segregation in casting of aluminum–30 wt.% alloys. The pouring temperatures investigated ranged from 900 to 1050°C, the pouring funnel was preheated to 550°C, and the mold was graphite.

Hanford has reported additional details of its studies of thorium-uranium alloys.[3] After cold reductions of 60 per cent, low-carbon thorium alloys containing 1 to 5.4 wt.% uranium had hardnesses ranging from 125 to 130 DPH. After annealing for 2 to 4 hr at 800°C, these same materials had hardnesses ranging from 83 to 108 DPH and were completely recrystallized. Annealing at 900°C resulted in some hardness increases over the minimums achieved, and this effect was attributed to the increased solubility of uranium in thorium at 900°C and to precipitation of uranium from the thorium on furnace cooling. No additional information is available on the series of thorium–2 wt.% uranium alloys being irradiated at 560°C to a burn-up of 3 at.%. Samples examined at ½, 1, and 1½ at.% burn-up have been harder and less ductile than control

samples, but density changes have been less than 1 per cent.

Battelle has reported[48] additional information on the results of its examinations of thorium–11 wt.% uranium alloy samples which were irradiated while incompletely covered with NaK. The intended irradiation temperature was 540 to 650°C; the intended burn-up was 1 at.%. Of 12 specimens in separate NaK capsules, 6 showed severe bulging or disintegration on the uncovered end. Metallic luster was observed on most of the specimens, however, and density decreases of 2.6 to 4.3 per cent were measured on sections of the specimens remote from the bulged ends. These data suggest that the average specimen temperature was above 600°C.

(W. Chubb)

Dispersion Fuel Elements

Knolls[49] has irradiated specimens of ferritic stainless steel–UO_2 in the MTR to an 11 at.% burn-up to see how the fuel operating temperature compares with that of dispersions having an austenitic stainless-steel matrix. The specimens were prepared by the cold-binder extrusion of a plastic powder dispersion, fired in dry hydrogen, fitted with end caps, and electroplated with nickel before being fitted into a type 430 stainless-steel tube and bonded by hot swaging at 800°C. Postirradiation examinations indicate that the desired lowering of the UO_2 particle operating temperature was realized and that the ferritic stainless-steel matrix was not unduly susceptible to radiation damage. (D. L. Keller)

Refractory Fuel and Fertile Materials

Reviews of UO_2 Fuel Status and Technology

Several good summaries of Argonne, Canadian, Knolls, and Bettis work on the properties,[50–52] technology,[52] and irradiation performance[53,54] of uranium oxide were presented at the Geneva Conference. Canadian work in the latter category has also been reviewed in another paper.[55] Another Knolls paper,[36] covering the same topic as the Geneva paper, summarizes the irradiation performance of high-burn-up annularly loaded UO_2 pins and UO_2 dispersions in stainless steel. (W. S. Diethorn)

Fabrication of UO_2-containing Ceramics

The process used in Sweden for the fabrication of UO_2 fuel elements was described at Geneva.[56] Precipitated ammonium diuranate powder was calcined to form UO_3, which then was reduced in hydrogen to UO_2. It was found that low reducing temperatures were necessary to produce sinterable powders. The techniques for preparation of sinterable powder are similar to techniques reported previously by Mallinckrodt[57a] and by Chalk River.[57b]

Pellets pressed at about 65,000 psi to about 50 per cent of theoretical density were sintered in hydrogen at 1500°C to about 95 per cent of theoretical density. Specimens sintered in hydrogen saturated with water vapor at room temperature appeared to be denser than those sintered in dry hydrogen.

Hanford[3] investigated the effects of processing variables on the density of swaged UO_2. The density obtained was found to depend on the type of UO_2 powder and on the choice of cladding. Hot swaging (up to 600°C) was found to give higher density than cold swaging. (H. D. Sheets)

Properties and Behavior of Uranium Oxides

As reported in previous reviews in this series, there is considerable interest in the effect of radiation and the oxygen-to-uranium ratio on the thermal conductivity of uranium oxide. In a recent Oak Ridge paper,[58] the effect of impurities on the thermal conductivity of uranium oxide is treated theoretically, and all existing thermal conductivity data are reviewed in some detail. Low-temperature measurements on nonirradiated uranium oxide reported by Belle[50] of Bettis show that the thermal conductivity decreases with oxygen content. At 50°C the thermal conductivity of a hydrogen-fired $UO_{2.18}$ body was only about half of that for a steam-sintered body, after correction of the values to zero porosity. Harwell[59] measurements on stoichiometric UO_2 specimens at high temperature support the thermal conductivity data reported by Armour and Kingery. Cored specimens were heated by an axial electric heater. Frequent specimen failure reported in this work suggests that a surface to centerline temperature gradient greater than 150°C will cause specimen fracture. On the basis of this observation, Scott questions the merit of grinding UO_2 fuel pellets to close tolerances prior to fuel-element fabrication.

Bettis has reported[60] in-pile measurements of the effective thermal conductivity of cold-pressed and sintered natural Mallinckrodt UO_2. A thermocoupled stack of pellets, having a theoretical density of 94 per cent, was irradiated to an estimated exposure of 0.7×10^{20} nvt in the MTR. During irradiation the pellets were surrounded by a helium annulus. Centerline temperature varied from 300 to 1100°F. The reactor power was raised from 0 to 40 Mw in 10-Mw increments four times during the two-week irradiation. No postirradiation examination of the pellets is reported.

Above 600°F there is no evidence of a change in thermal conductivity during irradiation. No firm conclusion can be drawn about the change with time at temperatures less than 600°F because the scatter in the data is large at these lower temperatures. At all temperatures the in-pile thermal conductivity is, however, lower than the thermal conductivity of nonirradiated UO_2. Instantaneous values calculated from the raw in-pile data are compared with the Kingery and Armour data in Fig. 6. The in-pile data support the use of 1.0 Btu/(hr)(ft)(°F) for the thermal conductivity of UO_2 pellets in the PWR Core 1 blanket rods. Preliminary in-pile studies with UO_2, as reported by Flinta,[61] confirm the low thermal conductivity observed by Bettis.

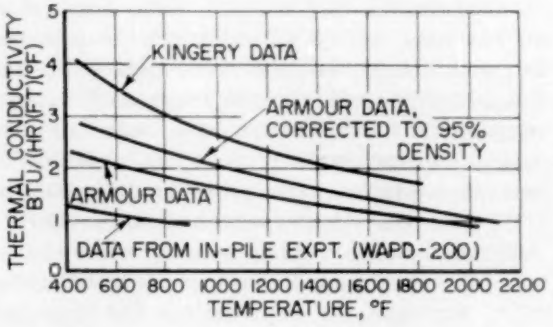

Figure 6 — Thermal conductivity of UO_2 versus temperature. Data compiled by Bettis Plant of Westinghouse Electric Corp.[60]

Belle has summarized[50] Bettis and Canadian data on the diffusion of rare gases in UO_2. This information is given in Fig. 7.

In experiments by Knolls[62] the thermal expansion of UO_2 bodies subjected to transient temperature increases has been studied as part of a fast-reactor program. UO_2 rods, 0.4 in. in outside diameter by 1 in. long, were electrically

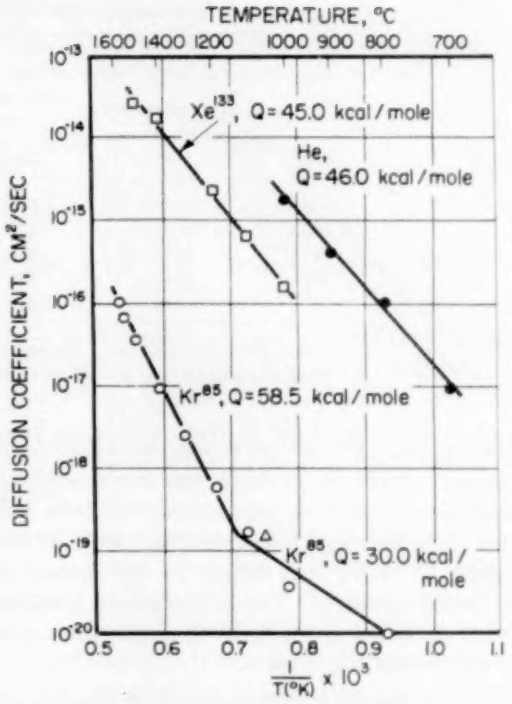

Figure 7 — Rare-gas diffusion in UO_2. ●, He in UO_2 powder, a = 0.083 μ; ○, Kr^{85} in 97.4% theoretical density solid UO_2, a = 0.043 cm; △, Kr^{85} in UO_2 powder, a = 0.22 μ; □, Xe^{133} in fused UO_2, a = 0.002 cm, a = radius of equivalent sphere in diffusion model. Data from Geneva Conference paper by J. Belle.[50]

heated in an inert atmosphere for 1 to 3 sec at a rate of 250 to 650°C/sec. Rod densities were 70 per cent of theoretical. Expansion coefficients fell in the range of 2.3 to 7.7×10^{-6}/°C. These values are similar to those reported for single crystals and dense bodies measured under equilibrium conditions.

The thermal contact conductance between nonirradiated UO_2 and cladding materials is being investigated by Hanford. A UO_2 wafer, 1 in. in outside diameter by 70 mils thick, is sandwiched between the ends of two 1-in.-diameter cylinders of the cladding material. Results for aluminum are reported in Table I-4. (W. S. Diethorn)

Fabrication of Uranium and Thorium Carbides

The fabrication of mixtures of uranium carbides with other carbides is being studied extensively at various laboratories. The most common fabrication technique is hot pressing of mixtures of the carbides or of the elements.

Table I-4 THERMAL CONTACT CONDUCTANCE OF UO_2-ALUMINUM JOINTS*

Run	Unit pressure on the joint, psi	Aluminum temp. at joint, °C		*Thermal flux, Btu/(hr)(ft²)	Average contact conductance, Btu/(hr)(ft)(°F), ½ (hot joint + cold joint)
		Hot	Cold		
1 and 2	323	320	170	163,000	1500 to 1700
3 and 4	232	175	95	92,000	1500 to 1700
5	424	280	180	155,000	3000
6	424	155	100	76,000	2600
7	64†	320	150	11,400	950

*Data taken from Hanford Atomic Products Operation.
†Run made after the 424 psi run without breaking joint.

Nowotny et al.[63] hot-pressed, at 1800°C, mixtures of uranium carbide and monocarbides of titanium, vanadium, zirconium, niobium, tantalum, chromium, molybdenum, and tungsten. Cobalt (1 wt.%) was added to the mixtures to facilitate reaction. The hot-pressed specimens were annealed for 4 hr in an argon atmosphere at approximately 2000°C.

Cold pressing followed by sintering in a purified argon atmosphere, as well as hot pressing, was employed at Harwell in the fabrication of UC_2, ThC_2, and mixtures of the two carbides.[64] The hot-pressed compacts were subsequently fused under an argon arc, with a zirconium getter heated simultaneously with the specimen to avoid oxygen pickup. The fused specimens were annealed under argon at 1800°C. The UC_2 specimens were contaminated by traces of UO_2, probably arising from oxidation on cooling. Pure ThC_2 was obtained by sintering in argon at 1800°C, transferring directly from the furnace tube to an argon box, and imbedding in molten paraffin when cool.

In experiments with a carbon-arc-image furnace at Hanford, UC was melted under helium and at reduced pressures.[3] Uranium monocarbide melted at approximately 2100°C in an electron-beam furnace to yield a white, metallic-ceramic body with better thermal-shock resistance than UO_2.

The preparation of UC by arc melting of uranium metal and carbon in an argon atmosphere was described by Gray et al.[65]

Work continued at Battelle on the fabrication of various refractory uranium compounds.[34] The effect of forming pressure during hydrostatic pressing on the green density of compacts of UC was studied. It was found that the green density was directly proportional to the forming pressure over the range investigated (20,000 to 100,000 psi). (M. J. Snyder)

Properties of Refractory Fuels Other Than Uranium Oxides

Compounds of uranium, plutonium, and thorium are being elevated at high temperatures as potential fuel materials. The uranium-carbon-nitrogen system was studied[66] by Battelle at 1800°C and 2000°C. Complete solid solubility was observed by X-ray diffraction in the UC-UN system. However, there was essentially no solubility of nitrogen in UC_2 or U_2C_3 or of carbon in U_2N_3. The phases UC_2 and U(C,N) are stable in vacuum or argon at 1800°C, whereas in nitrogen the nitrides are more stable than the carbides. At 200°C in nitrogen the carbides, UC_2 and U(C,N), become more stable. UC-NaK compatibility studies are in progress.[34] To date, very small weight losses have been observed during thermal cycling up to 1100 and 1300°F. Several capsules have been irradiated at the MTR and Battelle Research Reactor (BRR). Preliminary observations indicate some cracking of the specimens in one capsule irradiated at MTR. However, the examinations and physical-property measurements are not complete. Fission-gas release will be measured, using these irradiated specimens. Theoretical calculations of the swelling of UC due to fission-fragment retention indicate that the maximum swelling would be about 3.4 per cent per at.% burn-up. However, at elevated temperatures the degree of swelling would be lower, about 1.36 per cent per at.% burn-up.

Harwell[64] investigated the structure and stability of the solid-solution carbides of uranium and thorium. Complete solid solubility was ob-

served for cubic UC in cubic ThC and tetragonal UC_2 in monoclinic ThC_2. The structure change in the dicarbide occurred at approximately 50 mole %. In this composition range the dicarbide solid solution was poorly crystalline, indicating a highly strained lattice. The solid solutions are stable up to 400°C in inert atmosphere but oxidize in oxygen to the solid-solution oxide $(U,Th)O_2$.

Plutonium oxides have been prepared[67] by ignition of metal, hydrides, nitrides, carbides, and Pu^{+3} and Pu^{+4} salts. Oxides prepared by ignition below 500°C dissolve slowly in mineral acids, whereas the high-fired oxide is attacked only by H_2SO_4 and hot HNO_3 containing some HF. The crystal structures of the four plutonium oxides are given.[68] In this study of the plutonium-oxygen phase diagram, the compound PuO was not observed. The hexagonal Pu_2O_3 exists over a very narrow compositional range, slightly below the stoichiometric composition; the cubic modification of Pu_2O_3 has a variable lattice parameter, 10.98 to 11.00 A, indicating some range in composition. PuO_2, the most stable of the oxides, has a variable composition also, the lattice parameter increasing from 5.395 to 5.47 A as the oxygen content decreases below that of the stoichiometric compound. Three carbides of plutonium, PuC, Pu_2C_3, and PuC_2, have been prepared.[69] Carbon reacts with plutonium metal or $PuH_{2.7}$ at 900°C to form PuC or with PuO_2 at 1800 to 1900°C to form Pu_2C_3. PuC_2 is obtained by heating the metal in an excess of carbon at temperatures above 2000°C. The crystal structure of PuC is isomorphous with UC, while the structures of the other two carbides, Pu_2C_3 and PuC_2, are unknown. The carbides are easily hydrolyzed in dilute acid or water.

(D. A. Vaughan)

Mechanism of Corrosion of Fuel Alloys

Los Alamos has proposed a mechanism for the aqueous corrosion of uranium which they believe to be more compatible with experimental evidence than the generally accepted "hydride" theory.[70] In the latter a uranium hydride is formed as an intermediate reaction product and is then converted to UO_2 by reacting with more water. In the Los Alamos theory the U^{+3} hydroxide occupies the pivotal position formerly accorded the hydride. The stepwise nature of the anodic reactions is indicated below:

$$U + 3\ OH^- + 3\oplus \rightarrow U(OH)_3$$

$$U + 2\ O^{-2} + 4\oplus \rightarrow UO_2$$

$$U(OH)_3 + OH^- + \oplus \rightarrow U(OH)_4 \text{ or } UO_2 \cdot 2H_2O$$

where $\oplus$ is a space charge of positive holes. Battelle has previously reported evidence of U^{+2} or U^{+3} in the uranium corrosion product formed in water, which lends support to the concept of hydroxides as intermediate reaction products.[71]

Westinghouse Research Laboratory has conducted further oxidation experiments which support an earlier theory of the oxidation process of uranium,[72] namely, UO_2 oxidizes by the immediate formation of a second phase, tetragonal U_3O_7, around the UO_2 particle; further reaction occurs by the diffusion of oxygen through the U_3O_7 to form additional U_3O_7 at the UO_2-U_3O_7 interface, until the UO_2 is completely converted to U_3O_7; further oxidation occurs by the nucleation and growth of U_3O_8 on the U_3O_7 particles. This proposed mechanism differs from the generally accepted theory that oxygen initially dissolves in the UO_2 particle without change of parameter or structure and that this initial stage of oxidation is followed by the formation of a second tetragonal phase. The Westinghouse work conducted at temperatures below 300°C supports their theory by indicating that (1) the oxygen solubility in UO_2 is less than 1 at.% per mole of UO_2, (2) U_3O_7 X-ray spectra appear at $UO_{2.06}$, and (3) linear increase in density with oxygen concentration is about the same as that calculated for the formation of U_3O_7.

Recent work performed at Bettis has provided additional proof that the mechanism of failure of zirconium-uranium epsilon alloys is not associated with hydrogen.[27] This conclusion is based on the observations that (1) corrosion behavior in dry oxygen (no hydrogen present) is similar to that in water and (2) a hydride of zirconium is formed in this system rather than a hydride of uranium. The latter hydride has been associated with failure in gamma-phase uranium alloys.

(W. E. Berry)

Basic Studies of Radiation Effects in Fuel Materials

Radiation Effects in Metallic Fuels

Several related articles concerned with radiation damage of uranium-containing alloys are reported. These include articles on the mechanism of anisotropic growth in uranium, nucleation and swelling experiments on uranium and uranium-containing alloys, and diffusion of xenon in uranium. In addition, two studies analyzing reversion phenomena in uranium alloys are described.

At Sylvania,[1,73] the mechanism of anisotropic growth of uranium when subjected to radiation is being studied, and a comparison of diffusional and stress-relaxation mechanisms is made. Current work is directed toward improving the diffusional model by considering the interaction of vacancies and interstitials generated by radiation with subgrain boundaries and with dislocations. The structure of alpha uranium leads one to expect that the migration of interstitials will be almost isotropic and that of vacancies confined to the [1 0 0] and [0 0 1] directions. Hence extension occurs in the [0 1 0] direction and shrinkage in one or both of the [1 0 0] and [0 0 1] directions. Additional research is needed to better define the model for the observed growth effects. Values of the diffusion coefficient are reported as 5×10^{-15} cm^2/sec along the [0 1 0] and 4×10^{-15} cm^2/sec along the [0 0 1], both measurements being made at 640°C. These values are being rechecked, and irradiation experiments are being planned.[1]

Atomics International[74] proposes mechanisms of swelling to account for the varied behavior of uranium, various alpha-phase alloys, and uranium−10 wt.% molybdenum. Their concept suggests different behavior in three temperature ranges. For alpha uranium and alpha alloys below 350°C, it is proposed that the causes of swelling are ineffective because vacancies are less mobile than interstitial atoms and the vacancies are annihilated by movement of the interstitials to the vacancies. Gas atoms are also immobile relative to the interstitial atoms in this temperature range.

In the range of 350 to 500°C, appreciable swelling occurs, due primarily to vacancy agglomeration on the fission-gas atoms. As the temperature is increased above 350°C, the mobility of vacancies must increase relative to the mobility of the interstitial atoms for this to occur. This increased mobility of the vacancies maintains the vacancy concentration lower than in the range below 350°C, and the fraction of those vacancies annihilated by interstitial-vacancy recombination is reduced. At 350 to 500°C the concentration of vacancies is still high, relative to the number in thermal equilibrium. Since the lattice strain associated with the gas atoms is higher than that with interstitials, vacancies are attracted to the gas atoms. Several vacancies may condense on a single gas atom, immobilizing it and furnishing a site for easy bubble nucleation. This will occur only under a high vacancy supersaturation since surface tension opposes this agglomeration. This vacancy agglomeration does not build up pressure; thus it is concluded that any volume change due to agglomeration of vacancies is independent of restraining forces.

Appreciable swelling occurs above 500°C. In this range it is suggested that swelling is due to fission-gas agglomeration. The thermal-equilibrium vacancy concentration approaches the irradiation-induced concentration. Since the concentration is not so high, surface tension prevents condensation of vacancies. One or two vacancies should remain attached to the gas atom, however, because of the high strain energy of the gas atom as a positive dilation center. Such a combination is still mobile, and the tendency is for diffusion and agglomeration of gaseous bubbles to occur. The swelling in this temperature range is creep dependent. At 350 to 500°C the bubbles will be small and of nearly equal size, whereas above 500°C the bubbles will vary in size.

Increases in irradiation rate would probably increase the rate of volume change in the 350 to 500°C range, due to higher supersaturation of vacancies. The opposite is thought to be true above 500°C because the swelling is dependent on creep.

Uranium-molybdenum alloys are probably better than uranium due to inhibition of vacancy agglomeration at 350 to 500°C by such factors as increased surface tension, stabilization of the gamma phase, and reduced uranium self-diffusion rates.

Willis, of Knolls,[75] has analyzed various aspects of damage to fuel elements, especially the allowable concentration of rare gases that can be expected to reside in a metal lattice and the size and number of bubbles that can be expected.

It is proposed that the allowable concentration of gases in solution is proportional to $(F/D)^{1/2}$, where F is the fission rate and D the diffusion coefficient of the gas in the metal. It is also predicted that an equilibrium bubble size of about 10^{-6} cm will exist with 10^{16} to 10^{17} bubbles per cm^3, unless very low power densities are being investigated.

Isothermal annealing and transient postirradiation heating studies are also reported by Knolls[76] for zirconium −7 and −8 wt.% uranium alloys. These alloy samples had burn-ups of 0.6 to 1.4 at.%. Studies being made include determination and mechanistic interpretation of the number and size of gas bubbles formed. Carbon-shadowed Faxfilm replicas from samples of 8 wt.% uranium, having various heat-treatments, contained 10^{14} to 10^{15} bubbles per cm^3 between 0.015 and 0.1 μ in diameter. Swelling occurred rapidly at high temperatures.

Various experiments on the swelling of uranium have been conducted by Harwell.[77] Small pieces of natural uranium, after irradiation below 300°C, were heated to higher temperatures under various pressures. The spacing and size of the bubbles produced when uranium is heated after irradiation are smaller than those produced when it is heated during irradiation. This is believed to be due to the formation of numerous nuclei during heating as soon as mobility of the gas atoms will permit. These nuclei and small bubbles are constrained by surface tension and, being numerous, prevent diffusion of the gases to pre-existing large nuclei, such as inclusions and cracks. Heating in vacuum between 575 and 1000°C produced changes in volume of 2 to 20 per cent. In material which was thermally cycled repeatedly and heated at low pressure to 810 to 835°C, swelling of 10 to 20 per cent occurred. Bubbles between 10^{-2} and 5×10^{-6} cm in diameter were observed in uncycled material. Cracks were also observed and were often associated with nonmetallic inclusions. They were most prevalent in the thermally cycled samples. A theory of the creep dependency of growth of bubbles is described. It is reported that the swelling at 575°C is greater than expected for spherical bubbles growing against the mechanical strength and surface tension of the metal; this may be due to neglect of anisotropic effects of surface tension and mechanical strength.

At Harwell[78] studies of bubble formation of helium in copper indicate that coalesence of bubbles occurs at the expense of other bubbles, showing that helium can be taken back into solution. It is suggested that this is unlikely for xenon or krypton in metals because of the higher strain associated with solution of these gases.

At Stockholm[79] the diffusion of Xe^{133} in uranium has been determined in the range of 570 to 1000°C. The diffusion process can be described by means of an activation energy of 59,600 cal/mole and a diffusion coefficient of

$$D = 2.4 \exp(-59{,}600/RT) \text{ cm}^2/\text{sec}$$

At higher temperatures other isotopes, principally iodine, also diffuse out of uranium in increasing quantities. It is pointed out that the results can be applied with accuracy only if the ratio of sample dimension to grain size remains the same since grain-boundary diffusion appears to be important.

At Bettis[14] effects of irradiation at low temperatures, −90 to +17°C, on the resistivity of uranium−9 wt.% molybdenum, both gamma-treated and transformed to alpha plus epsilon, are reported and analyzed. Using predicted molybdenum concentration gradients produced by irradiation of alpha-plus-epsilon interfaces, resistivities were calculated that compare well with experimental values for the alpha-plus-epsilon sample. The gamma-phase sample was affected only during the early stages of irradiation. Detailed comparison is made between two suggested mechanisms for the reversion from alpha plus epsilon to gamma. These are the displacement-spike mechanism and the thermal-pulse mechanism proposed by Russian scientists. While the same kinetics equation is proposed, based on each model, predicted results depend upon the number of atoms displaced per fission in the displacement-spike model and the amount of energy available for thermal effects in the thermal-pulse model. Thus it is still not known which model is more valid, and additional tests are to be performed with additional uranium-molybdenum and uranium-niobium alloys.

At Harwell[80] calculations have been made to determine what induction period might be required for the transformation of a beta-uranium alloy to alpha uranium at high-alpha temperatures, in order to maintain it in the metastable beta condition by irradiation. It is concluded, for the specific case considered, that a uranium alloy with induction periods of the order of 5 min

or more might be suitable. The objective of this study is to maintain a uranium alloy in the beta condition at high-alpha temperatures in order to utilize its greater strength to resist swelling.

(F. A. Rough)

Radiation Effects in Ceramic and Cermet Fuels

The formation of fission-gas bubbles in metallic fuels was discussed in an earlier issue of the *Reactor Core Materials*.[81] Recent reports by Knolls[54,82,83] indicate that a similar phenomenon occurs in the case of irradiated UO_2. Results are reported on both unconfined UO_2 (powders) and confined UO_2 (dispersions) over a wide range of burn-ups and other irradiation conditions. The results may be summarized as follows. The size and distribution of the gas pores appear to be influenced by burn-up, irradiation temperature, initial porosity, degree of restraint of the UO_2, and fission density. The manner in which these factors influence pore characteristics has not been defined quantitatively. In general, for low-temperature irradiations, the pores are small and uniformly distributed, whereas high-temperature irradiation produces larger pores of varying size and nonuniform distribution.

In many respects the formation of gas-filled pores appears to be similar to the formation of gas bubbles in metallic fuels. An important difference arises, however, due to the difference in plasticity of metallic fuels and UO_2. During postirradiation annealing of unconfined UO_2, gas pores burst at temperatures below the irradiation temperature and produce a sporadic type of gas release. It is believed that, during irradiation, radiation-induced plasticity reduces fracture of the fuel particles. Evidence of plastic flow can be seen clearly in metallographs of irradiated dispersions.

The evidence thus far indicates that gas pores are not restricted to the closed porosity initially present in the material but that the pores can be formed during irradiation, perhaps at point defects or defect clusters. It is interesting to speculate on the effect of gas-filled pores on measurement of fission-gas release, particularly in attempting to relate such data to diffusion coefficients. For example, Bettis[84] has computed diffusion coefficients (as in Fig. 7) from gas release data, based on the size of an equivalent sphere as determined from surface area measurements which include the surface area due to open porosity. However, if appreciable quantities of fission gas collect in closed pores, this gas is no longer free to diffuse to open pores since the fission gases are essentially insoluble in UO_2. Accordingly, the Bettis method of calculation would yield diffusion coefficients which are too low if the closed pores do not rupture since the quantity of gas available to escape to the surface by diffusion is less than the amount produced. However, if all the closed pores rupture during the irradiation experiment, the calculated diffusion coefficient is too high since the radius of the equivalent spheres as determined by pre-irradiation surface measurements is greater than the average diffusion path. It is apparent that gas pore formation must be understood in more detail before accurate diffusion coefficients can be established.

Results on an interesting Harwell study of the nature of thermal spikes have been reported recently.[85] A U_3O_8 film placed 1 mm from the (1 0 0) cleavage plane of a LiF single crystal was irradiated to produce 1×10^7 and 1×10^{12} fission recoils per cm^2. The crystal plane was subsequently treated with a hydrofluoric acid–acetic acid–ferric fluoride etchant which does not attack the undamaged portion of the crystal surface. Etch pits were formed at the site of the recoil track. The density of etch pits was estimated to be 8 to 9×10^6 etch pits per cm^2 for the crystal irradiated to a calculated value of 1×10^7 fission recoils per cm^2. Pits are not formed after a pre-etching anneal at 450 to 500°C.

The etch pits had a general pyramidal shape, although those that grew as regular square pyramids were in the minority. The majority of the pits had terraced sides which became steeper toward the bottom of the pit. Some also had flat bottoms with an area much smaller than that of the base of the pyramid.

D. A. Young, author of this report, postulates that dissolution proceeds along the highly disordered region of the recoil track and finally permits development of crystal faces of low, but not necessarily the lowest, surface energy. He concludes that the diameter of a fission-recoil track may be as much as 5000 A, as indicated by the size of the etch pits. However, there is no assurance that the width of the base

of the etch pit is an accurate reflection of the diameter of the recoil track. It seems reasonable that, once the etchant has removed the damaged volume, the exposed crystal surfaces may have sufficiently high surface energy to permit appreciable dissolution of undamaged crystal before a surface resistant to further attack is produced. It is conceivable that the undamaged volume dissolved under these circumstances could be many times greater than the damaged volume. Although there is some question regarding the correlation of etch-pit and thermal-spike volume, the technique appears to be extremely useful, particularly if it can be shown that the etchant does not dissolve excessive amounts of undamaged crystal.

(P. Schall)

References

1. R. Resnick, L. S. Castleman, and L. Resnick, Dimensional Instability of Uranium-III. Third Annual Progress Report for June 30, 1957, to June 30, 1958, SEP-249, June 30, 1958. (Unclassified AEC report.)
2. L. L. Seigle and A. J. Opinsky, Mechanism of Dimensional Instability of Uranium, *Nuclear Science and Engineering*, 2(1): 38 (February 1957).
3. Fuels Development Operation Quarterly Progress Report for January, February, and March, 1958, HW-56029, Apr. 15, 1958. (Secret AEC report.)
4. I. Sheinhartz, Methods of Fabrication and Properties of Porous Uranium Fuel Elements, SCNC-259, May 1958. (Unclassified AEC report.)
5. S. H. Paine, P. J. Persiani, and W. F. Murphy, Irradiation of Prototype CP-4 (EBR-1) Reactor Fuel Slugs in the CP-3′ Goat Hole, ANL-5855, August 1958. (Unclassified AEC report.)
6. T. K. Bierlein and B. Mastel, Metallographic Studies of Uranium, HW-56412, June 2, 1958. (Unclassified AEC report.)
7. * T. K. Bierlein and B. Mastel, Metallographic Studies of Uranium, A/CONF./15/P/1855.
8. S. H. Paine and F. L. Brown, Pin-cushion Irradiation Tests of Uranium and Its Zirconium Alloys, ANL-5538, July 1958. (Unclassified AEC report.)
9. S. H. Paine and F. L. Brown, Pin-cushion Irradiation Tests of Uranium-Chromium Alloys, ANL-5854, July 1958. (Unclassified AEC report.)
10. * T. J. Heal and A. B. McIntosh, High-temperature Properties of Uranium and Its Alloys, A/CONF./15/P/49.
11. * M. D. Jepson et al., The Transformation Behavior of Some Dilute Uranium Alloys, A/CONF./15/P/27.
12. * H. H. Chiswick et al., Advances in the Physical Metallurgy of Uranium and Its Alloys, A/CONF./15/P/713.
13. W. D. Wilkinson and W. F. Murphy, "Nuclear Reactor Metallurgy," D. Van Nostrand, Inc., 1958.
14. * M. L. Bleiberg, Irradiation Induced Phase Changes in Uranium-base Alloys, A/CONF./15/P/619.
15. Technical Progress Report, Pressurized Water Reactor (PWR) Project for the Period Apr. 24, 1958, to June 23, 1958, WAPD-MRP-74. (Unclassified AEC report.)
16. Technical Progress Report, Pressurized Water Reactor (PWR) Project for the Period June 24, 1958, to Aug. 23, 1958, WAPD-MRP-75. (Unclassified AEC report.)
17. * D. O. Leeser, F. A. Rough, and A. A. Bauer, Radiation Stability of Fuel Elements for the Enrico Fermi Power Reactor, A/CONF./15/P/622.
18. A. Del Grosso, Compilation of Uranium–10 wt.% Molybdenum Fuel Alloy Properties, AECU-3679, June 7, 1957. (Unclassified AEC report.)
19. R. Aronin and J. J. Pickett, Core-to-Clad Interdiffusion Studies on Zirconium-clad U–10 Wt.% Mo Alloy Fuel Pins, NMI-4403, Jan. 10, 1958. (Unclassified AEC report.)
20. M. B. Waldron, R. C. Burnett, and S. F. Pugh, The Mechanical Properties of Uranium-Molybdenum Alloys, AERE-M/R-2554, 1958. (Unclassified British report.)
21. R. G. Loasby, The Gamma Phase in Uranium Alloys, *Proceedings of the Physical Society*, 72 (465): 425-428 (Sept. 1, 1958).
22. U. S. Atomic Energy Commission, Sept. 5, 1957. (Unpublished.)
23. V. W. Storhok, A. A. Bauer, and R. F. Dickerson, Survey of Ternary and Quaternary Metastable Gamma-phase Uranium Alloys, BMI-1278, July 15, 1958. (Unclassified AEC report.)
24. * A. A. Bauer, S. Kass, and K. M. Goldman, Physical Metallurgy and Properties of Zirconium-Uranium Alloys, A/CONF./15/P/1785.
25. On Uranium-Zirconium Alloys, *Atomnaya Energiya*, 3(8): 176-177 (1957).
26. W. Chubb, G. T. Muhlenkamp, and A. D. Schwope, A Hot-hardness Survey of the Zirconium-Uranium System, *Transactions of the American Society for Metals*, 50: 298-304 (1958).
27. S. Kass and K. M. Goldman, Corrosion Behavior of U-Zr Alloys in High-temperature Water and Steam, WAPD-T-416, April 1958. (Unclassified AEC report.)
28. L. M. Howe and L. G. Bell, Preirradiation Tests of Uranium-Silicon Alloys, CR-MET-763, May 1958. (Unclassified Canadian report.)

29. Atomic Energy of Canada, Ltd., 1957. (Unpublished.)
30. W. C. Thubber and R. J. Beaver, Segregation in Uranium-Aluminum Alloys and Its Effect on the Fuel Loading of Aluminum-base Fuel Elements, ORNL-2476, Sept. 19, 1958. (Unclassified AEC report.)
31. H. A. Kraus and S. O. Samoriga, in Summary Technical Report for the Period Apr. 1, to June 30, 1958, Preparation of 75 Wt.% Aluminum–25 Wt.% Uranium Spherical Shot, NLCO-750. (Confidential AEC report.)
32. Fundamental and Applied Research and Development in Metallurgy. Progress Report for April 1958, NMI-2069, June 10, 1958. (Secret AEC report.)
33. R. W. Dayton and C. R. Tipton, Jr., Progress Relating to Civilian Applications During August 1958, BMI-1286, Sept. 1, 1958. (Unclassified AEC report.)
34. R. W. Dayton and C. R. Tipton, Jr., Progress Relating to Civilian Applications During September 1958, BMI-1294, Oct. 1, 1958. (Unclassified AEC report.)
35. W. D. Wilkinson and W. F. Murphy, "Nuclear Reactor Metallurgy," Chap. 4, p. 74, D. Van Nostrand, Inc., 1958.
36. Reactor Technology Quarterly Report No. 4, Metallurgy and Materials, KAPL-2000-1, January 1958. (Unclassified AEC report.)
37.* U. Merten et al., The Preparation and Properties of Zirconium-Uranium-Hydrogen Alloys, A/CONF./15/P/789.
38. H. S. Kalish, The Powder Metallurgy of Zirconium-Uranium Alloys, *Transactions of the American Society for Metals*, 50: 271 (1958).
39. U. S. Atomic Energy Commission, 1958. (Unpublished.)
40. R. D. Nelson, Transformation Kinetics of Plutonium, Part I—A Study of the Beta to Alpha and Alpha to Beta Transformations, HW-55778, Apr. 17, 1958. (Unclassified AEC report.)
41. U. S. Atomic Energy Commission, 1958. (Unpublished.)
42. J. H. Kittel and L. R. Kelman, Effects of Irradiation on Some Uranium-Plutonium Alloys, ANL-5706, June 1958. (Unclassified AEC report.)
43. U. S. Atomic Energy Commission, 1958. (Unpublished.)
44. W. D. Wilkinson and W. F. Murphy, "Nuclear Reactor Metallurgy," Chap. 13, D. Van Nostrand, Inc., 1958.
45. J. R. Murray, The Uranium-Thorium System and Some Aspects of the Uranium-Thorium Zirconium System, AERE-M/R-2500, March 1958. (Unclassified British report.)
46. F. A. Rough and A. A. Bauer, Constitution of Uranium and Thorium Alloys, BMI-1300, June 1958. (Unclassified AEC report.)
47. Atomic Energy of Canada, Ltd., 1958. (Unpublished.)
48. R. W. Dayton and C. R. Tipton, Jr., Progress Relating to Civilian Applications During June 1958, BMI-1273, July 1958. (Unclassified AEC report.)
49. W. K. Barney, W. E. Ray, and H. G. Sowman, Development of Ferritic Stainless Steel–UO_2 Dispersion Fuel Elements, KAPL-1908, Jan. 30, 1958. (Unclassified AEC report.)
50.* J. Belle, Properties of Uranium Dioxide, A/CONF./15/P/2404.
51.* H. R. Hoesksta and S. Siegel, The Uranium-Oxygen System: U_3O_8 to UO_3, A/CONF./15/P/1548.
52.* G. H. Chalder et al., The Fabrication and Properties of Uranium Dioxide, A/CONF./15/P/192.
53.* J. A. L. Robertson et al., Behavior of Uranium Oxide as a Reactor Fuel, A/CONF./15/P/193.
54.* W. K. Barney, Irradiation Effects in UO_2, A/CONF./15/P/615.
55. R. F. S. Robertson and G. M. Allison, Irradiation of Compacted and Sintered Uranium Oxide on the X-2 Loop Tests X-2-f and X-2-i, CRDC-718, May 1958. (Unclassified Canadian report.)
56.* U. Runfors, R. Kiessling, and N. Schonberg, The Production of Uranium Dioxide Bodies for Fuel Elements, A/CONF./15/P/182.
57. Fuel Elements Conference, Paris, Nov. 18–23, 1957, TID-7546 (Book 2), March 1958. (Unclassified AEC report.)
    a. C. D. Harrington, Preparation and Properties of Uranium Dioxide Powders, p. 369.
    b. L. C. Watson, Production of Uranium Dioxide for Ceramic Fuels, p. 384.
58. V. J. Tennery, Review of Thermal Conductivity and Heat Transfer in UO_2, CF-58-9-24, Sept. 3, 1958. (Unclassified AEC report.)
59. R. Scott, Thermal Conductivity of UO_2, AERE-M/R-2526, March 1958. (Unclassified British report.)
60. J. D. Eichenberg, An In-pile Measurement of the Effective Thermal Conductivity of UO_2, WAPD-200, September 1958. (Unclassified AEC report.)
61.* J. Flinta, The Thermal Conductivity of UO_2, A/CONF./15/P/141.
62. W. C. Cohen and D. F. Molino, Behavior of UO_2 Bodies Subjected to Temperature Transients, KAPL-1873, July 1, 1957. (Unclassified AEC report.)
63. H. Nowotny et al., The Binary Systems: UC with TiC, ZrC, VC, NbC, TaC, Cr_3C_2, Mo_2C, and WC, *Monatshefte für Chemie*, 88(3): 336-343 (1957).
64. N. Brett, D. Law, and D. T. Livey, Some Investigations on the Uranium–Thorium–Carbon

System, AERE M/R 2574, June 1958. (Unclassified British report.)

65. R. J. Gray, W. C. Thurber, and C. K. H. DuBose, Preparation of Arc-melted Uranium Carbides, *Metal Progress*, 74(1): 65-70 (July 1958).
66. A. E. Austin and A. F. Gerds, The Uranium–Nitrogen–Carbon System, BMI-1272, June 23, 1958. (Unclassified AEC report.)
67. J. F. Drummond and G. A. Welch, The Preparation and Properties of Some Plutonium Compounds. Part VI, Plutonium Dioxide, *Journal of the Chemical Society*, 79: 4781-4785 (December 1957).
68.* C. F. Holley, Jr., et al., Thermodynamic and Phase Relationships for Plutonium Oxides, A/CONF./15/P/701.
69. J. H. Drummond et al., The Preparation and Properties of Some Plutonium Compounds. Part VII, Plutonium Carbides, *Journal of the Chemical Society*, 79: 4785-4789 (1957).
70.* J. T. Waber, The Corrosion Behavior of Plutonium and Uranium, A/CONF./15/P/699.
71. R. W. Dayton and C. R. Tipton, Jr., Progress Relating to Civilian Applications During May 1957, BMI-1189, June 1, 1957. (Confidential AEC report.)
72. J. Weissbart, P. E. Blackburn, and E. A. Gulbransen, Further Studies on the Mechanism of Oxidation of Uranium Oxide. Research Report 100FF942-R3, AECU-3729, June 6, 1957. (Unclassified AEC report.)
73.* L. L. Seigle and L. S. Castleman, Mechanism of Irradiation Induced Dimensional Instability of Uranium, A/CONF./15/P/618.
74.* B. R. Hayward and G. G. Bentle, Effect of Burn-up on Metallic Fuel Elements Operating at Elevated Temperature, A/CONF./15/P/617.
75.* A. H. Willis, Sources of Fuel-element Instability, A/CONF./15/P/616.
76. W. V. Johnston, The Effects of Transients and Longer Time Anneals on Irradiated U-Zr Alloys, KAPL-1965, June 1, 1958. (Unclassified AEC report.)
77. A. T. Churchman, R. S. Barnes, and A. H. Cottrell, Effects of Heat and Pressure on the Swelling of Irradiated Uranium, AERE-M/R-2510, March 1958. (Unclassified British report.)
78.* R. S. Barnes and G. W. Greenwood, The Effect of Gases Produced by Irradiation in Reactor Materials Other Than Uranium, A/CONF./15/P/29.
79. K. E. Zimen and L. Dahl, The Diffusion of Fission Xenon From Metallic Uranium, AERE-LIB/Trans-769, March 1958. (Unclassified British report.)
80. R. B. Kehoe, Nonequilibrium Beta Retention in Fuel Elements, IGR-TN/C-855, 1958. (Unclassified British report.)
81. *Reactor Core Materials*, Vol. I, No. 2, May 1958. (Available from the Superintendent of Documents, U. S. Government Printing Office, Washington 25, D. C.
82. D. W. White, A. P. Beard, and A. H. Willis, Irradiation Behavior of Dispersion Fuels, KAPL-1909, Oct. 1, 1957. (Unclassified AEC report.)
83. W. K. Barney and B. D. Wemple, Metallography of Irradiated UO_2-containing Fuel Elements, KAPL-1836, Jan. 15, 1958. (Unclassified AEC report.)
84. J. D. Eichenberg et al., Effects of Irradiation on Bulk UO_2, WAPD-183, October 1957. (Unclassified AEC report.)
85. D. A. Young, The Etching of Radiation Damage in Lithium Fluoride, AERE-C/M-340, May 1958. (Unclassified British report.)

---

*Second United Nations International Conference on the Peaceful Uses of Atomic Energy, Geneva, September 1958. (Available from the Office of Technical Services, Dept. of Commerce, Washington 25, D. C.)

Graphite

Hanford irradiations of grades TSGBF and CSF graphite at 30°C indicate that the thermal conductivity of these materials is not altered by exposures beyond 3000 Mwd/ton. However, their electrical resistivity continues to change. Up to 8400 Mwd/ton, the electrical resistivity of CSF graphite apparently increases with increasing dosage at a rate of 0.6×10^{-4} ohm-cm per 1000 Mwd/ton. After reaching a maximum value of 45×10^{-4} ohm-cm for transverse (to the axis of extrusion) samples and 36×10^{-4} ohm-cm for parallel samples at 500 Mwd/ton, the electrical resistivity of TSGBF graphite appears to decrease. At 5500 Mwd/ton, average values for transverse samples are 38×10^{-4} ohm-cm, whereas average values for parallel samples are 32×10^{-4} ohm-cm.

Studies of distortion in graphite caused by irradiation at 500 to 600°C have indicated that the rate of dimensional contraction varies inversely with the degree of development of graphite structure.[1] The materials with poor development of graphitic structure which appear to be dimensionally stable under irradiation at 30°C exhibit a high rate of contraction when irradiated at 500 to 600°C. Measurement of apparent crystallite sizes and changes in c_0 spacing indicate that this contraction does not result from further development of graphite structure.

Experimental graphites produced by the Speer Carbon Company and the National Carbon Company have been tested for nuclear purity in the Hanford Test Reactor. Results indicate that the total capture cross section is unaffected by the following fabrication variables: (1) incorporation of certain carbon-base additives in the base mix to increase density, (2) substitution of chlorine purification for the "F" process, (3) increasing the size of the furnace loading over that normally used, and (4) using bar sizes of $16\frac{1}{2}$ by $16\frac{1}{2}$ by 50 in. rather than the usual dimensions of 4 by 4 by 48 in. It also was found that resin impregnation, used to decrease permeability, did not affect purity when followed by AGOT regraphitization. However, where resin impregnation was followed by baking at 950°C without regraphitization, an appreciable decrease in nuclear purity was noted.

In support of the Brookhaven materials-development program for the Liquid Metal Fuel Reactor Experiment (LMFRE), several types of graphite were tested for bismuth penetration.[2] Graphite samples, degassed at 900°C, were submerged in bismuth at 250 psi and 550°C. The uptake in grams of bismuth per cubic centimeter of graphite varied from 0.5 to about 1.5, depending on the type of graphite used. The National Carbon Company is attempting to produce samples that have lower permeability than those tested to date.

The effect of radiation on the reaction between graphite and hydrogen has been studied in the British BEPO reactor.[3] Results indicate that pile radiation causes an increase in the rate of reaction. At temperatures of 500 to 600°C, methane is the main product of the reaction, and the rate of reaction appears to be proportional to the pressure of hydrogen.

A comparison of the 300°C oxidation rate of AGOT graphite after irradiation at 25 to 50°C to 4×10^{20} nvt thermal flux with the 300°C oxidation rate of unirradiated AGOT graphite indicates a far greater rate for the irradiated samples.[4] This is true of samples oxidized both in the absence of irradiation and in a 200,000 r/hr gamma flux. Similar effects were obtained in natural graphite. Results of in-pile oxidation studies indicated that, although combustion of graphite is accelerated by irradiation below 300°C, at higher temperatures the reaction may be retarded by irradiation. More experiments in this area are needed.

Investigation of methods of reducing the permeability of graphite revealed that impregnants are required that have lower viscosities and better wetting action than conventional pitches.[5] Such materials do a better job of filling the pores as well as the larger open volumes reached by conventional pitch. By using special proprietary impregnants, graphite permeability

can be reduced by several orders of magnitude. The behavior of unfueled graphite containing these impregnants under irradiation at about 400°C does not differ appreciably from that of reactor-grade graphite.

Some physical properties of graphite fueled with UO_2 (maximum bake temperature 1450°C) and with UC (maximum bake temperature 2800°C) have been measured.[5] The presence of 0.38 g/cm^3 of uranium in the form of UO_2 resulted in a significant reduction in flexural strength and electrical conductivity; however, thermal conductivity and compressive strength were less dependent on uranium content. In the graphitized bodies containing UC, thermal and electrical conductivities appeared to be higher than in the unfueled graphite. The cause of this could be a promotion of more complete graphitization by the uranium. At a uranium content of 0.67 g/cm^3, the flexural and compressive strengths of these samples were reduced by almost 50 per cent.

(W. C. Riley)

Beryllium Metal and Alloys

Work continues at Nuclear Metals[6] to produce beryllium sheet with some third-dimensional ductility. The ductility in the thickness direction is being evaluated by bend tests using specimens 3 in. long, 0.088 in. thick, and having width-to-thickness ratios from 1 to 44.

Research has been done at Harwell[7] to determine the expansion behavior of cast and extruded beryllium when injected with helium. Samples were bombarded in a cyclotron with 40 Mev alpha particles. Specimen temperatures did not exceed 500°C during irradiation. Annealing treatments were carried out at various temperatures and for various times after bombardment. It was shown that the grain boundaries in beryllium provide a source of the vacancies which seem to be required before helium can precipitate and that they also act as a short-circuit path for subsequent diffusion of the helium. This concept is strengthened by the fact that helium precipitation and volume expansion were found to occur less rapidly in cast metal than in extruded material, which has a considerably smaller grain size (and, hence, more grain boundaries per unit volume).

Beryllium alloys containing 1 to 25 wt.% magnesium can be prepared by impregnating a skeletonized beryllium-powder compact with molten magnesium, according to a British patent (J. Williams and J. W. S. Jones for the United Kingdom Atomic Energy Authority).[8]

A continuous electrolytic process for the preparation of beryllium metal has been described by Holden, Kells, and Whitman.[9] In this process an equimolar mixture of molten NaCl and $BeCl_2$ is electrolyzed at 300 to 350°C over a mercury cathode. An amalgam containing up to about 2 wt.% beryllium can be prepared. The beryllium can be separated from the mercury by a preliminary expressing operation, followed by vacuum distilling or vacuum hot pressing of the residue. The hot-pressed compacts were reported to have an oxygen content of less than 0.8 wt.%. The fresh amalgam has a bright appearance, but darkens quickly on standing in air, probably indicating an ultrafine beryllium particle size. No mechanical-property data were reported for the hot-pressed beryllium compacts. It would, of course, be of extreme interest to know the effect of ultrafine grain size on strength and ductility since grain refinement appears to be one practical method of mitigating the apparently intrinsic brittleness of beryllium.

Interest in beryllium as a structural material continues to be evidenced by a steady stream of review articles and surveys in the technical and trade literature. Because of their completeness, attention is called to reports of the Materials Advisory Board,[10,11] an Institute of Metals review,[12] and a state-of-the art report issued by the Defense Metals Information Center.[13]

(A. J. Griest)

Beryllium Compounds

X-ray determinations of the crystallographic thermal expansion of BeO and Al_2O_3 were made by Atomics International.[14] Within the limits of experimental accuracy, the crystallographic ratios c/a for alpha Al_2O_3 and BeO were constant between 20 and 1750°C, indicating isotropic thermal expansion for these hexagonal lattices. Some unexplained deviations in the c/a ratio for BeO were observed above 1000°C, and some diffraction lines disappeared above 1800°C. It appears that this observed change of structure in BeO at high temperature might be related to the reducing conditions of the experiment, analogous to the structural changes reported by the

Russians for Al_2O_3 exposed to reducing conditions at high temperature.[15]

Initial experiments on inhibiting crystal growth of BeO during sintering and subsequent heating in air were carried out by Battelle. Average BeO crystal sizes ranged from 2.5 to 22 μ in compacts sintered to near-theoretical density at temperatures between 2600 and 3100°F. Heating the sintered compacts in air for 15 hr at 2750°F caused crystal growth, to average diameters of 16 to 30 μ. The mean growth rate during heating in air was lowest for the compacts sintered at the highest temperature, 3100°F. Chemical additives to inhibit the BeO crystal growth and improve the high-temperature stability of BeO ceramics are being sought. (J. F. Quirk)

Solid Hydrides

Research in the hydride-moderator program continues to be directed toward zirconium hydride and hydrides of zirconium-uranium alloys. The phase diagrams and the problem of hydrogen migration are the aspects receiving the most attention.

Zirconium Hydride

Studies of the hydriding of zirconium and Zircaloy-2 at Hanford[16,17] in monoisopropylbiphenyl (MIPB) have shown that the process is dependent on both the hydrogen pressure and the temperature. Table II-1 gives the results of the investigation.

A critical review of the literature through March 1958, on the hydriding of zirconium and its alloys, has been prepared by Hanford.[18] This review, which contains 50 references, presents a hypothesis for necessary conditions of hydriding and also describes failures of tubes and fuel-element jackets.

Alloy Hydrides

Hydrogen-absorption isotherms have been measured at Battelle[19] to determine the phase diagram of the zirconium – 25 wt.% uranium alloy hydride system. Table II-2 presents the data that have been obtained to date. High-temperature X-ray diffraction studies are being made to ascertain the phases present at these temperatures. (H. H. Krause)

Table II-1 RESULTS OF HYDRIDING ZIRCONIUM AND ZIRCALOY-2 IN MIPB FOR SIX DAYS AT 100 PSI*
(Initial H_2 concentration, 3 to 12 ppm)

	Final H_2 concentration in metal, ppm	
Temp., °C	Hydrogen pressure, 5 psi	Hydrogen pressure, 1 psi
400	700-8700	200-370
350	140-975	30-90
300	5-38	2-3
250	10-11	1
210	10	
150		

* Data by Hanford Atomic Products Operation.[16,17]

Table II-2 PHASE BOUNDARIES IN THE ZIRCONIUM–25 WT.% URANIUM ALLOY HYDRIDE SYSTEM*

	710°C		748°C		776°C	
Phase boundary	Hydrogen absorption, cm^3/g	Pressure, cm of Hg	Hydrogen absorption, cm^3/g	Pressure, cm of Hg	Hydrogen absorption, cm^3/g	Pressure, cm of Hg
1	39.6	0.55	36.7	1.06	36.2	1.84
2	62.7	0.59	57.4	1.20	50.8	1.84
3	86.1	1.24	87.2	3.37	88.3	6.70
4	128.8	1.30	129.2	3.50	129.8	6.75

*Data by Battelle Memorial Institute.[19]

References

1.* R. E. Nightengale, J. M. Davidson, and W. A. Snyder, Damage Effects To Graphite Irradiated up to 1000°C, A/CONF./15/P/614.

2. F. Maslan, ed., Progress Report, Nuclear Engi-

neering Department, Oct. 1–Dec. 31, 1957, BNL-491, May 1958. (Unclassified AEC report.)
3. N. S. Corney and R. B. Thomas, The Effect of Pile Radiation on the Reaction Between Hydrogen and Graphite, AERE-C/R-2502, June 1958. (Unclassified British report.)
4.* G. R. Hennig, G. J. Dienes, and W. Kosiba, Radiation Effects on the Oxidation Rate and on Other Chemical Properties of Graphite, A/CONF./15/P/778.
5.* W. P. Eatherly et al., Physical Properties of Graphite for Nuclear Applications, A/CONF./15/P/708.
6. Fundamental and Applied Research and Development in Metallurgy, Progress Report for May 1958, NMI-2070, June 20, 1958. (Secret AEC report.)
7. R. S. Barnes and G. B. Redding, The Injection of Helium into Cast Beryllium, AERE-M/R-2332A, May 1958. (Unclassified British report.)
8. J. Williams and J. W. S. Jones, Beryllium Alloys, British Patent 788,239; *Nuclear Engineering*, 3: 272 (June 1958).
9.* R. B. Holden, M. C. Kells, and C. I. Whitman, A Continuous Electrolytic Process for the Preparation of Beryllium Metal, A/CONF./15/P/717.
10. Report of the Panel on Toxicity of Beryllium, MAB-135-M, July 31, 1958. National Research Council, Washington 25, D. C.
11. Report of the Panel on Beryllium, MAB-129-M, June 25, 1958. National Research Council, Washington 25, D. C.
12. J. Williams, The Fabrication and Properties of Commercially Pure Beryllium, *Metallurgical Reviews*, 3(9): 1-44 (1958).
13. W. Hodge, Beryllium for Structural Applications, DMIC Report 106, Aug. 15, 1958. Battelle Memorial Institute.
14. D. J. Klein, Measurements of the Crystallographic Thermal Expansion of Alpha Alumina and Beryllia To Elevated Temperatures Emphasizing Anisotropic Effects, NAA-SR-2542, Aug. 1, 1958. (Unclassified AEC report.)
15. N. Ye. Filonenko et al., Note on Alumina Spinel, $AlO \cdot Al_2O_3$ (in Russian), *Doklady Akademii Nauk*, 115(3): 583-585 (1957).
16. U. S. Atomic Energy Commission, 1958. (Unpublished.)
17. U. S. Atomic Energy Commission, 1958. (Unpublished.)
18. D. W. Shannon, Conditions for the Hydriding of Zirconium and Zircaloy-2, An Interpretative Literature Survey, HW-55460, Apr. 7, 1958. (Unclassified AEC report.)
19. R. W. Dayton and C. R. Tipton, Jr., Progress Relating to Civilian Applications During September 1958, BMI-1294, Oct. 1, 1958. (Unclassified AEC report.)

*Second United Nations International Conference on the Peaceful Uses of Atomic Energy, Geneva, September 1958. (Available from the Office of Technical Services, Dept. of Commerce, Washington 25, D. C.)

Control-rod Alloys

Boron Alloys

Phillips Petroleum Co. has irradiated 18-8 stainless steel–1 wt.% boron alloys, enriched 93 per cent in B^{10}, to 15 and 25 at.% burn-up in the Materials Testing Reactor (MTR).[1] Effects of irradiation on tensile properties are shown in Table III-1. Voids were observed adjacent to the boride phase inclusions. These are probably a result of helium-gas pockets and preferential dissolution of lithium upon etching.

Table III-1 TENSILE TEST RESULTS FOR IRRADIATED STAINLESS STEEL–B^{10} ALLOY*

Irradiation, nvt thermal	B^{10} burn-up, at.%	Hardness, R_C	Ultimate tensile strength, psi	Yield strength (0.2% offset), psi	Total elongation in 1 in., %
0	0	30	121,900	93,400	15.6
2.6×10^{20}	15	37	153,500	149,500	3.4
4.4×10^{20}	25	42	137,100		1.6

* Data by Phillips Petroleum Co.[1]

Bettis has prepared iron–1 and 2 wt.% boron, ferritic stainless steel–2 wt.% boron, and austenitic stainless steel–2 wt.% boron as part of a program to develop a burnable-poison material. These were induction melted successfully in BeO crucibles and chill cast into water-cooled copper molds.

Silver-Indium-Cadmium Alloys

It has been found that adherent coatings of ductile metal can be plated satisfactorily on silver-base control alloys.[2] This plate provides corrosion protection to the alloys in reactor water of low or high oxygen content without impairing any of their desirable properties. The silver–15 wt.% indium–5 wt.% cadmium alloy has been found to be sensitive to water with high oxygen content. The plated specimens, corrosion-tested in dynamic (10 fps), high pH (9.5 to 10.5 with LiOH), 550°F oxygenated (4.0 to 6.0 ppm) water, exhibited weight changes of −0.03 to +0.02 mg/cm² in 28 days, compared with losses of 58 to 60 mg/cm² for bare specimens. Defected plated samples had about the same weight change as those with continuous plates, indicating that pinholes in the coating have little effect on its ability to retard corrosion. By eliminating the need for tin additions to prevent internal oxidation, plating will result in control rods with greater effectiveness and longer life.

Coarsening of grain size of wrought silver–15 wt.% indium–5 wt.% cadmium alloy from ASTM No. 5 to ASTM No. 2 sufficiently improves creep resistance to meet design requirements.[3] Although the coarse-grained alloy has a yield strength of only 7000 to 8600 psi at 550°F at low rates of loading (0.05 in./min), the yield strength of 10,900 psi at 550°F at high rates of loading (2 in./min) appears adequate. This is of concern in applications where resistance to thermal and mechanical shock is important.

(V. W. Storhok)

Dispersion-control Materials

Bettis is investigating dispersions of B^{10} in austenitic and ferritic stainless steels as well as in iron for possible use as burnable-poison materials.[3] Four-micron-diameter B^{10} powder and $< 44\ \mu$-diameter stainless powder are blended, cold-pressed at 45 tsi, and sintered at 1200°C to 90 per cent of theoretical density. Optimum sintering conditions have not been established, but dry hydrogen, argon, or helium atmospheres may result in some boron loss. Vacuum sintering appears promising.

Because hafnium is not readily available for control rods, Yankee[4] has investigated B_4C-silver dispersions and has reached the conclusion that pressing and sintering techniques are applicable for producing compacts. At a pressure of 125,000 psi, green densities decreased from 91 to 73 per cent of theoretical as B_4C loadings increased from 5 to 32 wt.%. Furthermore, sintering at 1400°F caused expansion of compacts pressed at 86,000 and 125,000 psi but increased the density of compacts pressed at 29,000 and 57,000 psi. The highest density after sintering was 88 per cent of theoretical for 5 wt.% B_4C pressed at 29,000 psi. Change in density was negligible after 2 hr at either 1400 or 1650°F.

A dispersion type reactor-poison component containing neutron-absorbing glass particles as the dispersed phase is being developed at Knolls.[5] A large number of vitreous structures based on B_2O_3 as a glass former have been examined. Cadmium borates and cadmium–rare earth borates were considered promising since the incorporation of two or more poison materials can give a wider range of blackness. Also, the vitreous structure should provide more vacant lattice sites than a crystalline structure, and thus possibly more helium and lithium atoms produced by the n-α reaction in B^{10} can be accommodated in the lattice. A glass containing 25 wt.% CdO, 25 wt.% Gd_2O_3, 30 wt.% B_2O_3, and 20 wt.% CaO with a density of 4.0 g/cm^3 was selected as the most promising material. Titanium was used as the matrix material, and an extrusion method developed for other dispersions[6] was satisfactory for producing clad triflute configurations. (G. W. Cunningham)

References

1. H. T. Watanabe and W. O. Schaffnit, Radiation Damage Studies of Boron–Stainless Steel, IDO-16483, Sept. 18, 1958. (Unclassified AEC report.)
2. I. Cohen, Westinghouse Atomic Power Division, Sept. 15, 1958. (Unpublished.)
3. Technical Progress Report, Pressurized Water Reactor (PWR) Project for the Period Apr. 24, 1958, to June 23, 1958, WAPD-MRP-74, 1958. (Unclassified AEC report.)
4. L. Lewis, Silver–Boron–Carbide Cermets, YAEC-58, June 18, 1958. (Unclassified AEC report.)
5. Reactor Technology Quarterly Report No. 4, Metallurgy and Materials, KAPL-2000-1, January 1958. (Unclassified AEC report.)
6. W. E. Ray and P. R. Mertens, The Development of Stainless-steel Clad Model Control Rods with Stainless-steel Rare-earth Oxide Cores, KAPL-1644. (Confidential AEC report.)

Corrosion

Zirconium

Two aspects of zirconium corrosion, namely, the pickup of hydrogen during exposure to high-temperature water and the stringer type corrosion phenomenon, continue to receive major attention.

Studies at Bettis[1] have indicated that, unlike nickel diffusion-bonded specimens, copper and iron diffusion-bonded Zircaloy-2 samples exhibit hydrogen absorption characteristics during exposure to high-temperature water similar to those of unbonded Zircaloy. Furthermore, no adverse effects on the corrosion behavior of Zircaloy-2 have been noted in the presence of 1 wt.% copper or iron.

Additional studies have confirmed earlier observations that (1) vacuum melting will produce corrosion-resistant Zircaloy-2 ingots and (2) increasing the amount of hot work results in some improvement in the high-temperature-water corrosion resistance of atmosphere (helium or argon) melted Zircaloy-2.

A research program at Battelle[2] has had as its objective the development of a high-strength zirconium alloy having satisfactory corrosion resistance. Nine series of ternary and quaternary zirconium-base alloys were studied. Zirconium-base alloys exhibiting the most promising combination of good corrosion resistance and high hardness were those containing:

1. 2 wt.% Sn–0.5 wt.% Mo
2. 2 wt.% Sn–2 wt.% Nb–0.1 wt.% Fe–0.5 wt.% Ni
3. 2 wt.% Sn–3 wt.% Nb–0.1 wt.% Fe–0.5 wt.% Ni
4. 3 wt.% Sn–0.1 wt.% Fe–0.5 wt.% Ni
5. 3 wt.% Sn–0.5 wt.% Mo–0.1 wt.% Fe–0.5 wt.% Ni
6. 3 wt.% Sn–0.5 wt.% Mo–1 wt.% Nb–0.1 wt.% Fe–0.5 wt.% Ni
7. 4 wt.% Sn–0.5 wt.% Mo

To obtain a corrosion-resistant surface, it is necessary to pickle zirconium-base materials in HNO_3-HF baths. However, rapid and thorough rinsing is needed after the etch; otherwise, accelerated attack may occur on subsequent exposure to high-temperature water. The fluoride ion is the offending material which the rinse must remove. Studies at Hanford have shown that aluminum nitrate in the form of a 15 per cent solution of $Al(NO_3)_3 \cdot 9H_2O$ in 15 per cent HNO_3 is a very effective rinsing agent for the fluoride ion. This must be followed by a rinse in either hot or cold running water. (W. K. Boyd)

Stainless Steel

Probably the outstanding problem encountered in the use of stainless steels in nuclear power plants is the susceptibility of the steels to chloride and caustic stress-corrosion cracking. Sodium nitrate additions have been found to be effective in preventing cracking in rocking autoclave studies with 500 ppm chloride water at 500°F. Recent data from Bettis, however, have demonstrated that such a treatment does not eliminate stress cracking in the crevice areas of model boilers. Stress-cracking failures of the martensitic type 410 stainless steel exposed to low-oxygen water (0.5 to 2 ppm) at 300°F and H_2-NH_3 water at 300°F have been reported by Knolls. (W. K. Boyd)

Niobium

Significant improvements in oxidation resistance, as compared with that of previously known niobium alloys, are apparent in new niobium alloys recently patented by Du Pont.[3–5] These alloys are based on niobium-titanium, niobium-aluminum-iron, and niobium-aluminum-chromium and oxidize at rates representing up to a 2000-fold improvement over pure niobium. The best of these alloys oxidize slower than 80 wt.% nickel–20 wt.% chromium, a representative commercial heat-resistant alloy, as seen in Table IV-1. The excellent oxidation resistance of these alloys is probably due to the formation of complex spinel type scales, such as Al_2FeO_4. Spinel type scales are normally

Table IV-1 WEIGHT GAINS OF NIOBIUM ALLOYS DURING AIR OXIDATION*

Alloy composition, wt.%	Weight gain, mg/cm² 1000°C, 16 hr	1200°C, 16 hr
100 Nb	350	1100
80Ni–20Cr	0.3	2.1
Nb–29Ti–10Mo–5Mn–1Al	4.5	
Nb–16Ti–5Mo–4Al–3Be–2Fe	6.3	
Nb–19Al–10Fe	0.5	1.4
Nb–10Al–9Fe–25Ni	0.2	0.6
Nb–14Al–10Fe–15Co–4Mo–1Ce	0.2	0.8
Nb–5Al–30Cr	2.4	4.2
Nb–10Al–19Cr–15Co	0.2	1.0
Nb–10Al–10Cr–15Ni–4W–2Ce	0.3	0.8

*Data compiled from Du Pont patents.[3–5]

very adherent and impart good oxidation protection to the underlying metal. The fabricability of these alloys is apparently marginal since it was stated that oxidation resistance and fabricability "tend to oppose each other." One alloy, niobium–19 wt.% aluminum–10 wt.% iron, was capable of being forged into a nozzle shape.

Work on the development of oxidation-resistant niobium is continuing at The Ohio State University, Horizons, and Sylvania-Corning. At Ohio State[6] the oxidation behavior of a niobium–50 wt.% zirconium–2.6 wt.% titanium was found to follow the fourth-power relation

$$W^4 = kt$$

where W = weight gain, mg/cm²
k = rate constant $(mg/cm^2)^4$ hr
t = time, hr

An internal subscale found in these alloys consisted of a lamellar ZrO_2 precipitate. The outer scales were protective, but the weight gains represented less than a tenfold improvement in oxidation resistance compared to pure niobium.

At Horizons,[7] experiments are now directed toward developing protective coatings for use up to 2500°F. A flame-sprayed coating of Fecral (iron–25 wt.% chromium–5 wt.% aluminum) was protective for 1 hr at 2500°F. (W. D. Klopp)

Molybdenum

In a paper by McCloud,[8] General Electric has released some details of the coated molybdenum buckets which have successfully operated in an experimental jet engine. The forged buckets were triple plated with chromium-nickel-chromium to a total thickness of 4 mils and heat-treated to produce some homogenization of the coating. The experimental engine has been operated over 500 hr at bucket temperatures of 2000°F. One test consisted of feeding 4 pints of sand into the running engine over a 2-hr period, followed by operation for an additional 25 hr.

Work by Bartlett and Williams[9] has shown that the oxidation rate of unprotected molybdenum is greater in flowing air than in stagnant air in the range 1600 to 2200°F. The oxidation rate increased two- to threefold when the air-flow rate was raised from 0 to 13.5 ipm. This was attributed to faster removal of the volatilizing MoO_3, allowing a higher concentration of oxygen at the reaction interface. (W. D. Klopp)

Iron-Nickel Alloys

Work at the Forrestal Research Center of Princeton University, reported by Brabers and Birchenall[10] on the oxidation behavior of iron alloys containing from 37 to 48.5 wt.% nickel at 1920°F, showed that the resistance of these alloys to oxidation is about 20 times that of unalloyed iron. This was attributed to the relative instability of the more rapidly growing wüstite phase after the attainment of steady-state oxidation conditions. The wüstite formed during initial oxidation of the surface is low in nickel content and leaves a very nickel-rich subsurface layer. Upon further oxidation, the equilibrium oxide formed is a spinel that characteristically exhibits a relatively slow rate of growth.

(E. S. Bartlett)

Iron-Chromium-Aluminum Alloys

In continuing work at the National Bureau of Standards,[11–13] the oxidation kinetics of three iron-chromium-aluminum alloys in air were studied. In general, oxidation proceeded parabolically. Activation energies for the oxidation process were determined to be 71,900 cal/mole, 66,610 cal/mole, and 53,400 cal/mole for the three alloys studied. Oxidation tests at 2300 and 2500°F on the alloy having the highest activation energy resulted in very rapid oxidation in certain areas of the specimens. Generally, oxidation at 1900 and 2300°F for 100 hr resulted in a dimensional loss of about 1 mil for all alloys. Unfortunately, compositional details were available for only the alloy whose

activation energy was 53,400 cal/mole; this was an iron–24 wt.% chromium–6 wt.% aluminum alloy. The material was received in strip form, indicating that the alloys were fabricable; thus combined chromium and aluminum contents may have been at least 33 and 8 wt.%, respectively (this is the approximate composition of a hot-fabricable commercial alloy). (E. S. Bartlett)

Magnesium-base Alloys

Oak Ridge[14] recently conducted a survey and discussed conditions which would be hazardous in uses involving magnesium-alloy cladding of reactor fuel elements in CO_2-cooled reactors. Although, through the use of alloys such as Magnox C (1 wt.% aluminum, 0.05 wt.% beryllium) or Magnox E (1 wt.% aluminum, 0.05 wt.% beryllium, 0.01 wt.% calcium), the danger of ignition of the clad fuel elements would be reduced, it was concluded that cooling system failures, generation of severe nuclear-power thermal transients, and possibly the release of Wigner energy would represent conditions of hazardous operation. Several suggestions for minimizing these hazards were presented. It is felt that an intensive study of the kinetics of the oxidation of magnesium by CO_2 would be helpful in assessing the potential dangers involved.

The French[15] have observed a 10- to 100-fold increase in the oxidation rate of magnesium at temperatures from 660 to 930°F when moisture was added to the oxidizing atmosphere.

(E. S. Bartlett)

Aluminum Alloys

Because of the desirability of aluminum as a fuel-element cladding material, investigation of the hot-water corrosion behavior of aluminum alloys at Chalk River was continued. Work has progressed along two lines: (1) development of nickel coatings to protect the aluminum alloys from hot-water corrosion[16] and (2) reduction of corrosion by adding inhibitors to the environment.[17]

It was found that, although aluminum alloys containing 0.5 to 2 wt.% nickel satisfactorily resist corrosion by static water at 570°F, imparting velocity of about 20 fps resulted in about 100-fold decrease in corrosion resistance to about 50 to 100 mils per year. Static and replenished autoclave tests, as well as loop tests, showed that of the several nickel platings evaluated a 0.2 mil Kanigen electroless nickel plate gave the most promise. However, none of the coatings was satisfactory since coating defects became apparent during the course of corrosion testing. Work is continuing on precoating preparation as well as on coating processes.

Additional alloy development resulted in an aluminum alloy containing 2 wt.% nickel, 0.5 wt.% iron, 0.2 wt.% silicon, 0.04 wt.% beryllium, 0.07 wt.% zirconium, and 0.2 wt.% titanium. This alloy has resistance to corrosion in static 570°F water superior to that of other alloys tested.

In circulating-water, loop corrosion tests, some degree of inhibition of corrosion was achieved by adding 1000 ppm of dissolved silica. Further corrosion protection resulted from doping of the environment with the normal corrosion product. However, none of the loop modifications completely inhibited corrosion of the aluminum specimens. The mechanism of inhibition is being further investigated with the objective of producing an environment which will completely inhibit the corrosion of aluminum by hot flowing water. (E. S. Bartlett)

Corrosion by Liquid Metals and Fused Salts

Attention is called to three recent summaries pertinent to corrosion by liquid metals. A paper by Klamut et al.[18] summarizes findings from a research program at Brookhaven National Laboratory devoted to various corrosion problems pertinent to the uranium-bismuth fuel and the thorium-bismuth breeder blanket in the Liquid Metal Fueled Reactor (LMFR). Information contained in an Oak Ridge paper[19] pertains to basic metallurgical and corrosion problems inherent in high-temperature reactors which utilize molten fluoride salts. The coverage in a book by Wilkinson and Murphy[20] is quite broad, including liquid-metal physical and heat-transfer properties and a general treatment of corrosion.

Oak Ridge[21] has considered the suitability of lithium as a reactor coolant from the physical-property viewpoint and has summarized the available information on the corrosion resistance of various metals, alloys, and ceramics to lithium at elevated temperatures. Figures 8 and 9 summarize the general corrosion situation to 1500°F. Although many materials have satisfactory corrosion resistance to lithium in

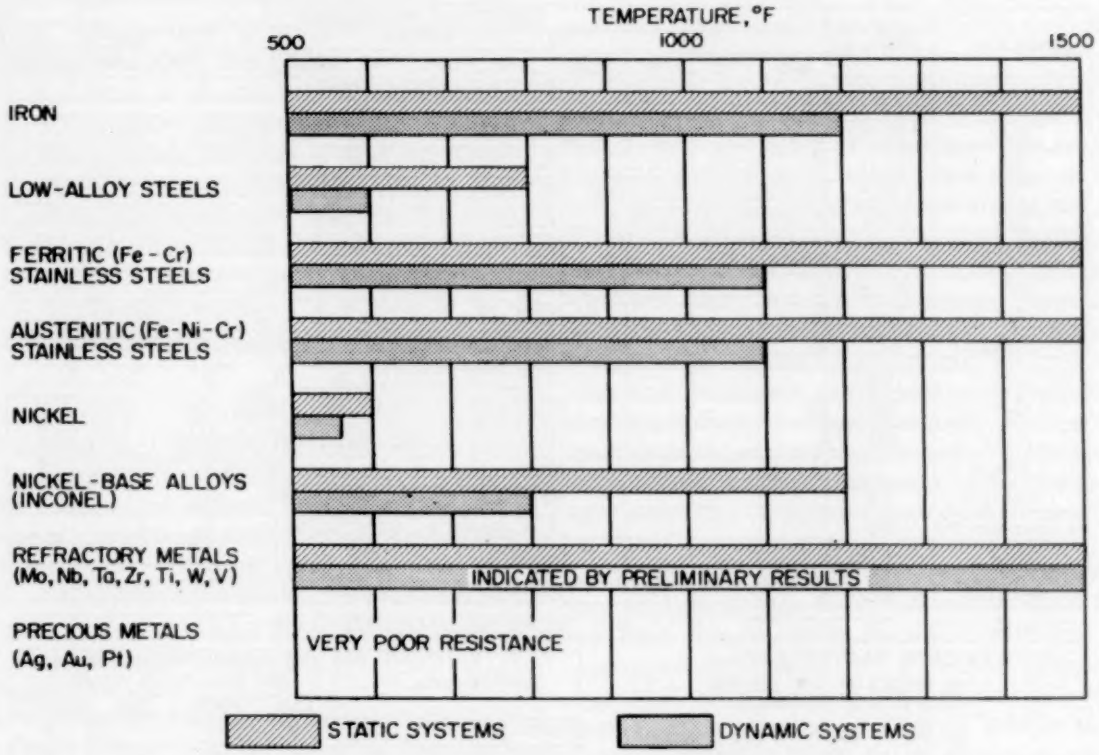

Figure 8—Corrosion resistance of various metals and alloys in lithium. Bars indicate approximate temperatures below which a system might be operated for 1000 hr with less than 0.005 in. of attack or container surface removal. Data from Oak Ridge National Laboratory.[21]

static isothermal systems up to 1500°F, none checked to date is resistant in dynamic nonisothermal systems. The austenitic and ferritic steels are the best commercially available materials, but their use is limited to 1100 or 1200°F for long-time exposure. The refractory metals have not been evaluated in dynamic systems because of the difficulty of fabricating suitable experimental systems; however, some effort along this line is being planned. The effect of impurities in lithium on its corrosivity has not been checked systematically.

Elevated-temperature thermal-gradient mass transfer by lithium has been under investigation by Nuclear Development Associates, with recent emphasis on the solution step in the corrosion process. In this connection a short-time isothermal crucible test has been developed as an expedient for obtaining data pertinent to the effect of temperature, additives, etc., on solution rates. To date, information from this type of experiment has correlated fairly well with that obtained previously from long-time thermal-convection loop experiments; this suggests that the mass-transfer process is controlled by the rate of solution rather than by the rate of deposition.

In the Molten Salt Reactor Program at Oak Ridge, the variety of studies being conducted include those to determine the corrosion behavior of potentially useful container materials for selected fuel-bearing fluoride salts at 1200°F. Inconel and INOR-8 are of prime interest, and thermal-convection loop experiments have been directed toward distinguishing fine differences in the resistance of these materials to attack. Although Inconel has displayed excellent resistance (for example, 2 mils maximum penetration in a 1200°F, polythermal system), recent information[22] indicates that the resistance of INOR-8 is even better in that attack is barely observable after several thousand hours of exposure. Experiments are also being made with in-pile molten-salt forced-circulation loops. Several such loops are in the construction stage, and the irradiation of one has recently been completed. This was an Inconel system in which a $NaF-ZrF_4-UF_4$ (60.8-27.4-

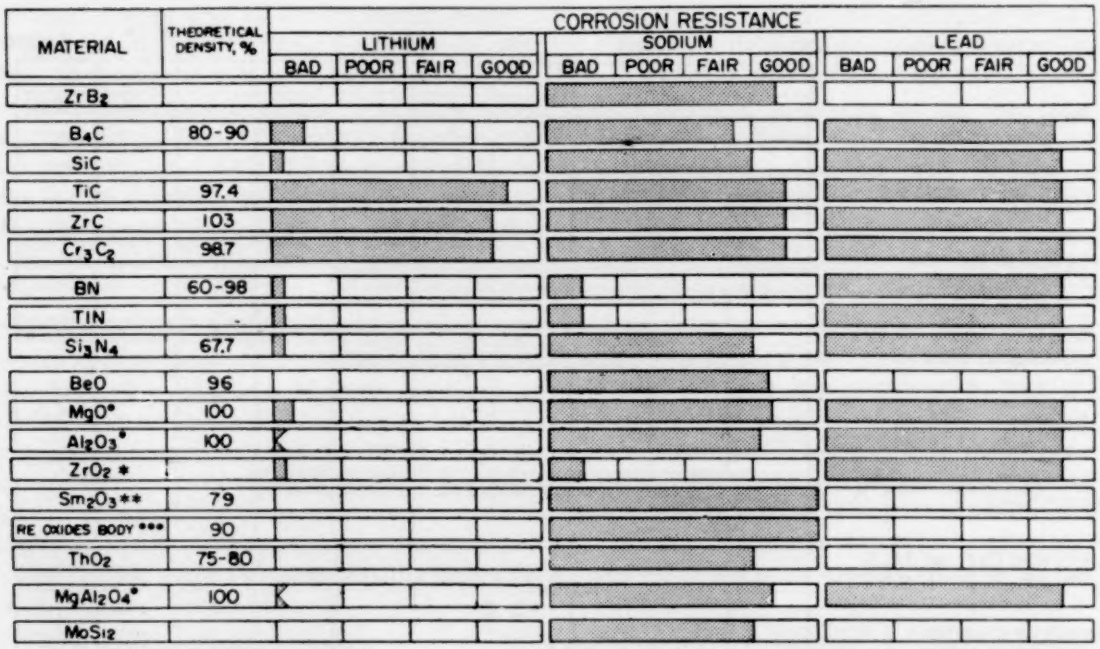

SIGNIFICANCE OF SHORTEST BARS:

▨ PIECES OF THE TESTED SPECIMEN REMAINED.

K THERE WAS NO VISIBLE TRACE OF THE TESTED SPECIMEN.

* A SPECIMEN FROM A SINGLE CRYSTAL.
* CaO-STABILIZED.
** A 1000-HR TEST.
*** A 500-HR TEST. BODY COMPOSITION: 45.0 TO 49.5% Sm_2O_3 – 22.5 TO 27% Gd_2O_3 – BALANCE PRIMARILY OTHER RARE-EARTH OXIDES.

TYPE OF DATA	ARBITRARY CORROSION RATINGS AND DATA RANGE BASES			
	BAD	POOR	FAIR	GOOD
DEPTH OF ATTACK, mils *	3	2	1	0
WEIGHT CHANGE, % **	6	4	2	0
DIMENSIONAL CHANGE, %	3	2	1	0

* MEASURED IN METALLOGRAPHIC EXAMINATIONS.
** DETERMINED BY DIRECT MEASUREMENTS AND/OR BY CALCULATIONS BASED ON THE MATERIAL(S) FOUND IN THE TEST MEDIUM BY CHEMICAL ANALYSES.

Figure 9—Corrosion resistance of various ceramics in static lithium, sodium, and lead media for 100 hr at 1500°F. Data from Oak Ridge National Laboratory.[21]

11.8 mole %) mixture was circulated. The irradiation took place in a vertical hole in the Low Intensity Test Reactor (LITR). During a 235-hr exposure, a maximum temperature of 1600°F was maintained; the temperature differential ranged from 230 to 250°F. Postirradiation examinations of selected sections indicated that the degree of corrosion was about the same (maximum depth of penetration of 4 mils) as would be expected under the same conditions in the absence of radiation.

Two recent British reports describe methods of determining oxygen levels in highly purified sodium. This is important because the corrosion rates of most materials by molten sodium are strongly dependent on the sodium purity. In the first investigation,[23] levels as low as 3 ppm (obtained by titanium gettering) were detected by the use of a vacuum-distillation technique devised by Humphries at Argonne. In the Humphries method a sodium sample is drawn into a receiver, which may be an integral part of a test system, and is distilled off by vacuum; the residue is analyzed for oxygen concentration. Insofar as is known, this method has not as yet been used for analytical work in the 0 to 10 ppm range, although there is no apparent reason why it should not be well suited for such service. The second report[24] describes a new technique which is particularly adaptable to a flowing system. This method, which theoretically could be used for detecting contamination as low as 0.1 ppm, is based on the fact that the attack of niobium by sodium depends on oxygen level; the attack is negligible with pure sodium but increases as the contamination increases. Two orifice plates, identical except for materials of construction (one of stainless steel and one of

niobium), are located in parallel flow lines. The temperature of the plates is raised to 600°C and flow rates adjusted so that they are initially equal. As oxide-containing sodium attacks the niobium, the flow area is increased and the resulting difference in the parallel flow is indicated by a signaling device. About 6 hr is required for a strong signal with gettered sodium flowing at 600°C; however, a large inleakage of oxygen is detected quickly. Calibration is performed with a vacuum distillation unit.

(J. H. Stang)

Zirconium-Water Reactions

The Bureau of Mines[25] recently published additional results of their zirconium-hazards research study. Although only exploratory results with regard to reaction rates are available, the study is making progress in determining the reasons, conditions, and mechanisms of zirconium explosions.

In the experiments performed, treatment of zirconium foil samples in hydrogen, nitrogen, or carbon dioxide caused extreme brittleness. Subsequent treatment by steam caused a complete breakup accompanied by a color change variously described as dark gray and blue-black. Under conditions when the surface of the zirconium foil sample acquired a blue-black oxide, the edges were almost invariably coated with a white oxide, which presumably indicates a more complete reaction at the edges.

Different methods of cleaning the samples resulted in significantly different rates of reaction, indicating the importance of initial surface condition. For example, a sample cleaned by pretreating in argon at 800°C and 760 mm had a weight gain of 17.5 per cent when exposed to steam at 500°C and 220 mm for 93.3 hr, whereas a similar sample cleaned by etching in an HNO_3-HF solution gained 9.7 per cent by reaction with steam at 500°C and 235 mm for 143.5 hr. This amounts to about half the weight gain in about twice the time for the acid-etched sample as compared with the argon-pretreated sample when both were reacted with steam at about the same temperature and pressure.

Tests by Columbia University[26] were made to determine the extent of metal-water reaction under conditions of simulated nuclear thermal transients. Reactor periods of the order of a few milliseconds were simulated, and the metal samples were destroyed by "electrical explosion" produced by direct-current electrical heating.

Two types of behavior were observed. Evidence was not found of self-sustained metal-water reactions or of bubble formation at the surface of unvaporized specimen fragments for silver, aluminum, copper, tin, and zinc when subjected to fast transient heating and explosion. Uranium and zirconium specimens exhibited continued generation of bubbles at the surface of unvaporized specimen fragments for several tenths of a second. In the case of uranium this was attributed to a high heat capacity. In addition, in the case of zirconium, a strong afterglow of the unvaporized fragments of the samples persisted for a period of 0.8 to 1 sec. For similar "explosions" of zirconium specimens in oil rather than in water, the afterglow remained for periods of only 0.4 to 0.5 sec, or about half as long. Postreaction examination of the unvaporized fragments of a heated zirconium specimen showed significant reaction with 75°F water, a penetration of 0.001 to 0.0015 in. of the metal taking place during an estimated interval from 0.8 to 2 msec when the glowing fragment was being quenched. A representative heated zirconium fragment 0.040 in. thick showed three zones: a nonmetallic gray-black layer 0.001 in. thick at the surface; an intermediate nonmetallic white layer 0.0008 in. thick; and, finally, the zirconium metal which has a Widmänstatten structure indicative of rapidly quenched metal. It was concluded from this evidence that a self-sustained metal-water reaction was not observed for uranium but that this tendency existed for zirconium. However, for zirconium, further experimental proof is required.

Aerojet[27] has performed additional tests in their explosion dynamometer to explore the reaction between a uranyl sulfate solution (HRT fuel) and molten Zircaloy-2 droplets. No appreciable difference was found between the uranyl sulfate solution and water as an oxidant, as evidenced by the data given in Table IV-2, which were read from a straight line, log-log graphical correlation in the report.

Additional conclusions are:

1. The reaction with aqueous solutions is not self-sustaining when the droplets are larger than 20 μ in diameter and there is an excess of the aqueous solution.

Table IV-2 EXTENT OF REACTION OF MOLTEN ZIRCALOY-2 DROPLETS*

Original droplet diameter, μ	Reaction in Water,† wt.%	Reaction in Uranyl sulfate fuel solution,‡ wt.%
3000	12	10
200	32	29
20	72	64

* Data from Aerojet General Corp.[27]
† Molten Zircaloy-2 originally at 2077°C.
‡ Molten Zircaloy-2 originally at 2066°C.

2. Minor alloying additions in zirconium-base alloys do not materially affect the extent of the reaction.

3. The data provide additional evidence to support earlier conclusions that the zirconium-water reaction is a process involving chemisorption of oxygen molecules on the surface of the metal. The fact that the addition of small amounts of electrolytes to the water has only a second-order effect on the reaction rate is consistent with this conclusion.

(A. W. Lemmon, Jr.)

Selected Metallurgical Aspects of Cladding and Structural Materials

Nickel

Ames Laboratory[28] reports a eutectic occurring at 18 to 20 wt. % nickel between yttrium and an unidentified compound; it melts at 950°C.

Zirconium and Zircaloy-2

Bettis[29] has stated that the cooling rate during postfabrication heat-treatment of Zircaloy-2 is critical to corrosion life in 750°F, 1500 psi steam. Cooling rates of greater than 90°F/min through the alpha-plus-beta phase region are necessary to give acceptable corrosion rates following heat-treatments in the beta or alpha-plus-beta range.

Niobium

The self-diffusion of niobium is being studied by Sylvania,[30] employing Nb^{95} in $NbCl_5$ to measure self-diffusion, using diffusion couples. Values for the diffusion coefficient of 3.2×10^{-9} cm^2/sec at 2000°C and 1.7×10^{-10} cm^2/sec at 1800°C were obtained with a 1-hr anneal.

Investigation of the tantalum-niobium alloy system[31] confirms the existence of an unbroken series of solid solutions. No evidence of a solid transformation was found in any of the alloys. The solidus line is reported to rise from the melting point of niobium, 2420°C, to the melting point of tantalum, 2940°C, and the liquidus is found to follow quite closely the path taken by the solidus.

Work on niobium-base alloys at Battelle[32] indicates that niobium-chromium alloys appear to possess the necessary metallurgical characteristics for precipitation hardening in the compositional range of 5 to 12 wt.% chromium.

(J. A. DeMastry)

Selected Mechanical Properties of Cladding and Structural Materials

Zircaloy-2 and -3

Evaluation of vacuum-skull-melted reactor components of Zircaloy-2 cast from suitable reactor-grade scrap has been made at Bettis.[33] Tensile and impact specimens were prepared from the walls of two square-walled castings and tested in the as-cast condition at room temperature and 260°C. These data are shown in Table IV-3, along with typical data from wrought Zircaloy-2 for comparison. Fusion-welded Zircaloy-2 subassembly side plates, annealed for 8 hr at 800°C and furnace-cooled, showed ultimate and yield strengths 5000 psi less than those in the as-welded condition. However, annealing increased the ductility approximately 10 to 20 per cent.

The effect of hydrogen on the mechanical properties of Zircaloy-2 at room and elevated temperatures is being investigated at Knolls. The effects of 12, 150, and 500 ppm of hydrogen on the ultimate strength, 0.2 per cent offset yield strength, and total elongation at temperatures in the 75 to 100°F range are shown in Figs. 10 and 11. The creep properties of Zircaloy-2 tested longitudinally to the rolling direction at temperatures up to 1000°F are summarized in Table IV-4 and Fig. 12.

(F. R. Shober)

Table IV-3 COMPARISON OF TENSILE AND IMPACT PROPERTIES OF CAST AND WROUGHT ZIRCALOY*

Tensile properties

	Test temp., °C	No. of specimens and direction	Yield strength (0.2% offset), psi	Tensile strength, psi	Elongation in 2 in., %	Reduction in area, %
Cast	RT	15	55,500	74,500	21.6†	29.3
	260	13	30,000	42,100	25.5†	45.2
Wrought	RT	Longitudinal	35,000	60,000	14.0	23.0
	RT	Transverse	51,000	57,000	15.0	31.0
	260	3, longitudinal	20,700	34,800	36.0	64.0
	260	3, transverse	25,500	34,100	32.5	49.5

Impact properties

	Test temp., °C	No. of specimens and direction	Ft-lb
Cast	RT	16	6.6
	260	16	24.2
Wrought	RT	3, longitudinal	5.2
	RT	3, transverse	2.0
	260	3, longitudinal	22.8

* Data taken from Bettis.[33]
† Elongation, per cent in ¾ in.

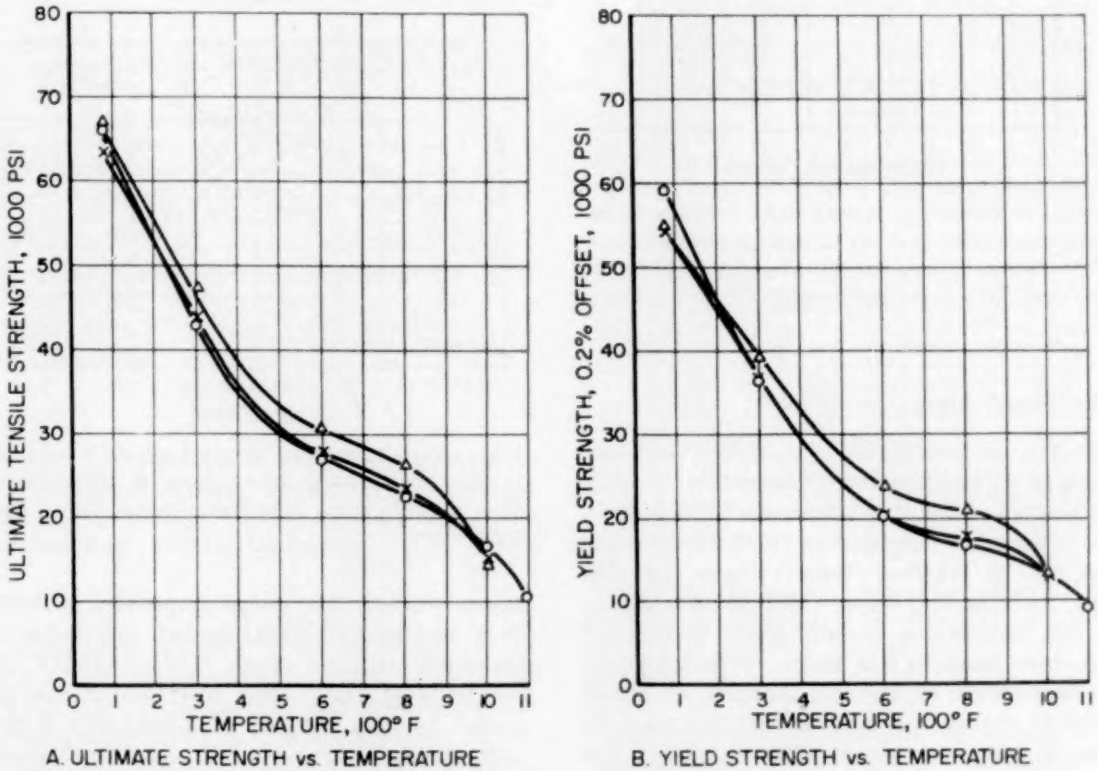

Figure 10 — Zircaloy-2 tensile tests (transverse direction, argon atmosphere). Hydrogen content: ○, 12 ppm; ×, 150 ppm; △, 500 ppm. Data from Knolls Atomic Power Laboratory.

Table IV-4 CREEP TEST RESULTS ON ANNEALED ZIRCALOY-2 TESTED LONGITUDINALLY TO THE ROLLING DIRECTION*

Temp., °F	Stress, psi	Loading strain, %	Time, hr, for indicated total deformation, %					Minimum creep rate, %/hr
			0.1	0.5	1.0	3	5	
300	32,000	1.52						1.3×10^{-4}
600	25,000	2.88				400		5.7×10^{-5}
800	8,000	0.148		725	2775			2.2×10^{-4}
1000	5,000	0.117		16	41.5		678	5.6×10^{-3}
1000	4,000	0.620	187	63	163		926	3.8×10^{-3}

*Data by Knolls Atomic Power Laboratory.

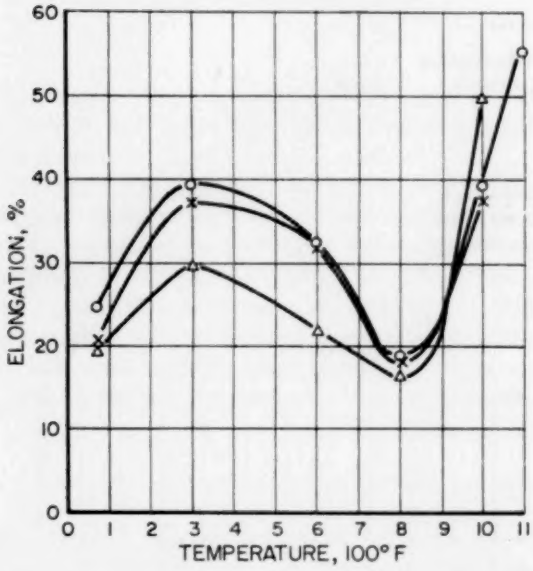

Figure 11 — Zircaloy-2 tensile tests (transverse direction, temperature versus elongation, argon atmosphere). Hydrogen content: ○, 12 ppm; ×, 150 ppm; △, 500 ppm. Data from Knolls Atomic Power Laboratory.

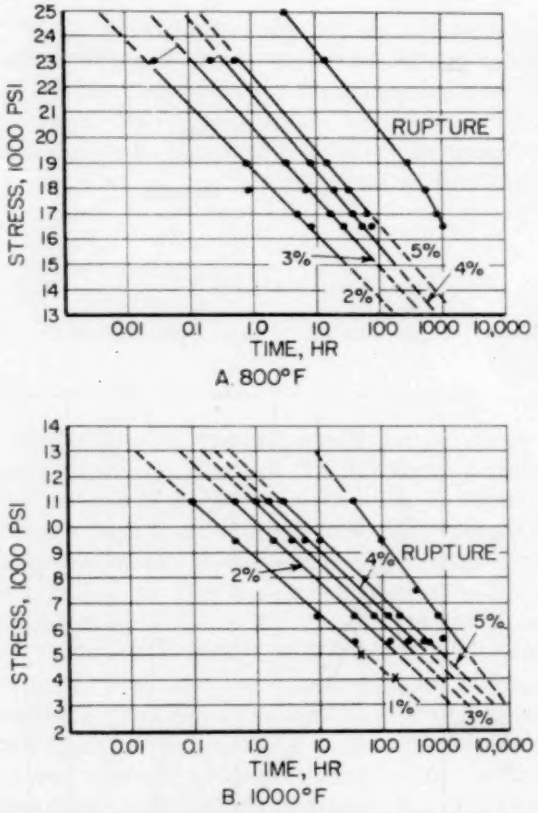

Figure 12 — Zircaloy-2 stress-rupture tests (stress versus time for total deformation). ●, stress-rupture data; ×, creep data. Data from Knolls Atomic Power Laboratory.

Nickel-base Alloys

The tensile properties of a nickel-base molybdenum alloy (nominal composition 17 wt.% molybdenum – 7 wt.% chromium – 5 wt.% iron, balance nickel, designated as INOR-8) have been measured at various temperatures by Oak Ridge, Battelle, and Haynes Stellite. A compilation and comparison of data, shown in Figs. 13 to 15, were made by Oak Ridge.[22] The temperature dependence of Young's modulus is shown in Fig. 16. Relaxation curves on INOR-8 for 0.1% strain at temperatures of 1200 to 1600°F are shown in Fig. 17. At 1400°F and above, relaxation occurs quite rapidly, while at 1300°F and below an incubation period was evident before creep started. The creep properties of INOR-8 in a molten-salt environment are being determined over the range 1100 to 1500°F. Data for tests at 1100, 1200, and 1300°F are presented in Figs. 18 and 19. Creep data at these same temperatures were obtained by Haynes in air. These data are shown in Fig. 20. Room-temperature tensile data indicate that aging in the 100 to 1400°F range up to 2000 hr produces

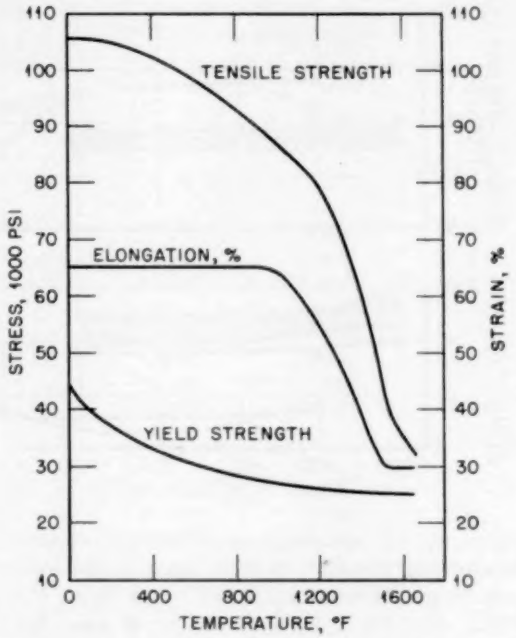

Figure 13 — Tensile properties of INOR-8 as a function of temperature. Data from Oak Ridge National Laboratory.[22]

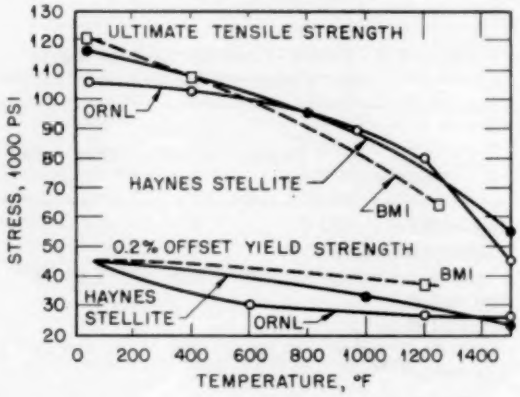

Figure 14 — Comparison of tensile properties of INOR-8 obtained at ORNL, Haynes Stellite Company, and BMI. ○, ORNL; □, BMI; ●, Haynes Stellite. Data from Oak Ridge National Laboratory.[22]

no significant changes in the properties of the alloy. The lower carbon-content alloy (Heat SP-19, 0.06 wt.% carbon) had greater tensile ductility than an alloy containing higher carbon (Heat 8M-1, 0.14 wt.% carbon). Figure 21 shows a comparison of these data with those of Hastelloy B, which, though somewhat stronger, is considerably less ductile.

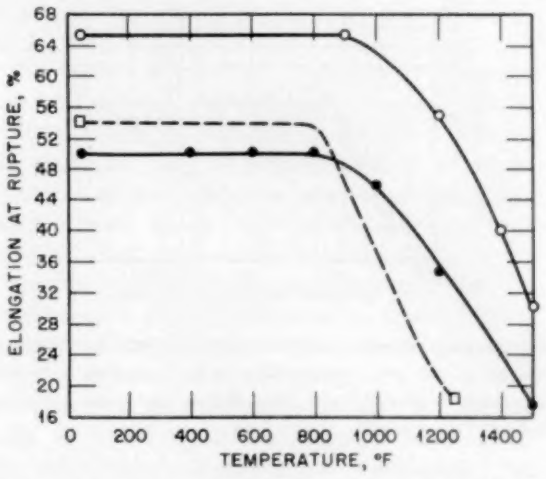

Figure 15 — Comparison of tensile elongations of INOR-8 specimens tested at ORNL, Haynes Stellite Company, and BMI. ○, ORNL; □, BMI; ●, Haynes Stellite. Data from Oak Ridge National Laboratory.[22]

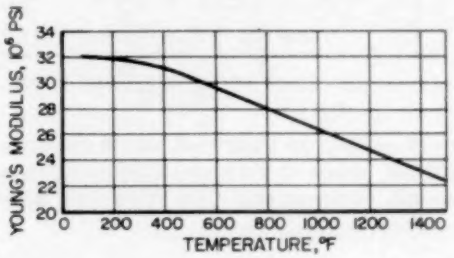

Figure 16 — Young's modulus for INOR-8 as a function of temperature. Data from Oak Ridge National Laboratory.[22]

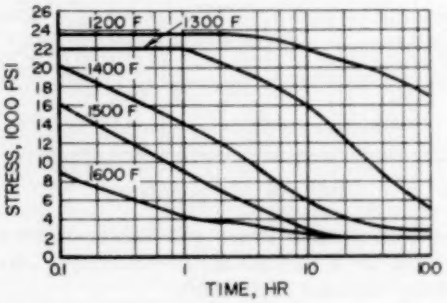

Figure 17 — Relaxation curves for INOR-8 stressed to 0.1 per cent strain at temperatures from 1200 to 1600°F. Data from Oak Ridge National Laboratory.[22]

An investigation of the hot ductility of Inconel and Inconel X was made at Oak Ridge.[34] The ductility of both alloys increased with increased test temperatures up to 2200°F, the embrittling temperature, beyond which the ductility was

Table IV-4 CREEP TEST RESULTS ON ANNEALED ZIRCALOY-2 TESTED LONGITUDINALLY TO THE ROLLING DIRECTION*

Temp., °F	Stress, psi	Loading strain, %	Time, hr, for indicated total deformation, %					Minimum creep rate, %/hr
			0.1	0.5	1.0	3	5	
300	32,000	1.52						1.3×10^{-4}
600	25,000	2.88				400		5.7×10^{-5}
800	8,000	0.148		725	2775			2.2×10^{-4}
1000	5,000	0.117		16	41.5		678	5.6×10^{-3}
1000	4,000	0.620	187	63	163		926	3.8×10^{-3}

*Data by Knolls Atomic Power Laboratory.

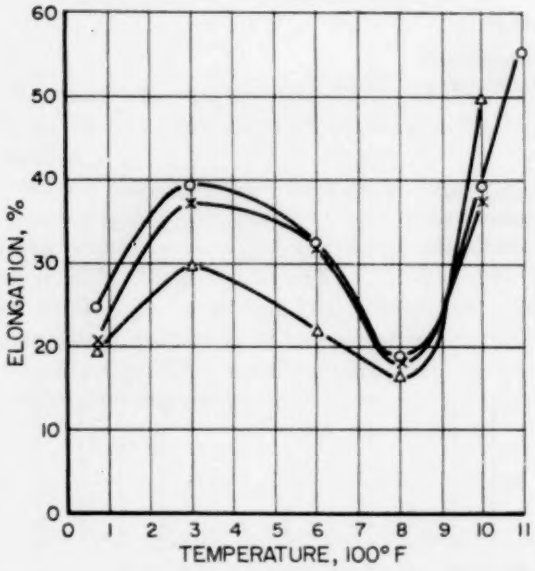

Figure 11—Zircaloy-2 tensile tests (transverse direction, temperature versus elongation, argon atmosphere). Hydrogen content: ○, 12 ppm; ×, 150 ppm; △, 500 ppm. Data from Knolls Atomic Power Laboratory.

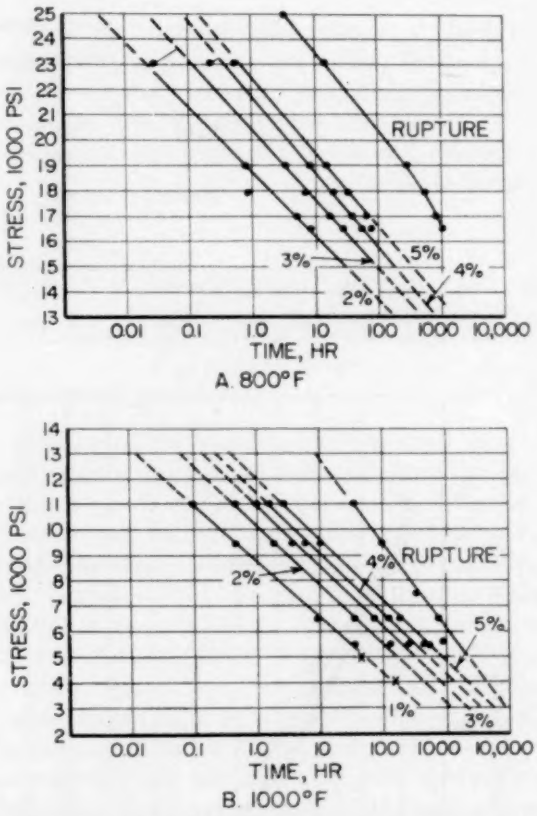

Figure 12—Zircaloy-2 stress-rupture tests (stress versus time for total deformation). ●, stress-rupture data; ×, creep data. Data from Knolls Atomic Power Laboratory.

Nickel-base Alloys

The tensile properties of a nickel-base molybdenum alloy (nominal composition 17 wt.% molybdenum–7 wt.% chromium–5 wt.% iron, balance nickel, designated as INOR-8) have been measured at various temperatures by Oak Ridge, Battelle, and Haynes Stellite. A compilation and comparison of data, shown in Figs. 13 to 15, were made by Oak Ridge.[22] The temperature dependence of Young's modulus is shown in Fig. 16. Relaxation curves on INOR-8 for 0.1% strain at temperatures of 1200 to 1600°F are shown in Fig. 17. At 1400°F and above, relaxation occurs quite rapidly, while at 1300°F and below an incubation period was evident before creep started. The creep properties of INOR-8 in a molten-salt environment are being determined over the range 1100 to 1500°F. Data for tests at 1100, 1200, and 1300°F are presented in Figs. 18 and 19. Creep data at these same temperatures were obtained by Haynes in air. These data are shown in Fig. 20. Room-temperature tensile data indicate that aging in the 100 to 1400°F range up to 2000 hr produces

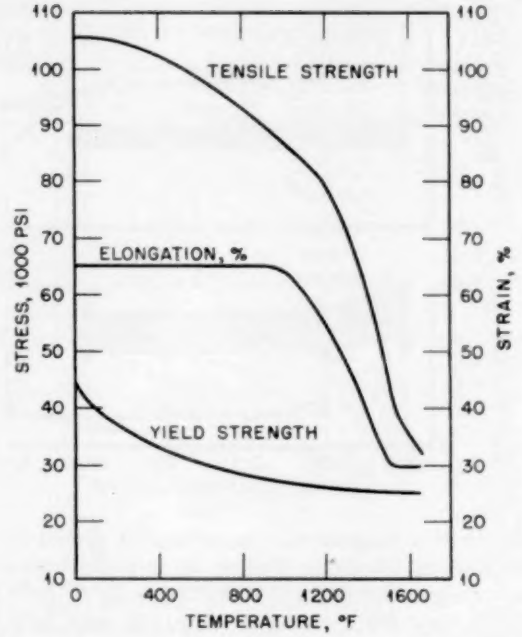

Figure 13 — Tensile properties of INOR-8 as a function of temperature. Data from Oak Ridge National Laboratory.[22]

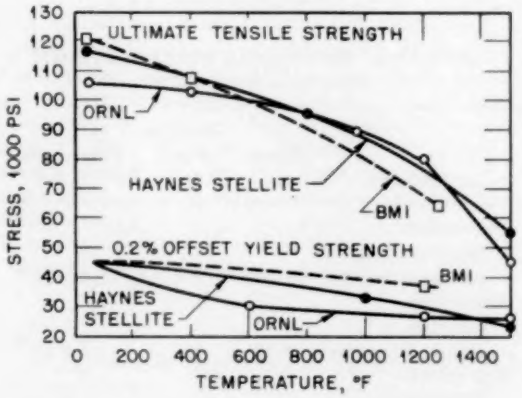

Figure 14 — Comparison of tensile properties of INOR-8 obtained at ORNL, Haynes Stellite Company, and BMI. ○, ORNL; □, BMI; ●, Haynes Stellite. Data from Oak Ridge National Laboratory.[22]

no significant changes in the properties of the alloy. The lower carbon-content alloy (Heat SP-19, 0.06 wt.% carbon) had greater tensile ductility than an alloy containing higher carbon (Heat 8M-1, 0.14 wt.% carbon). Figure 21 shows a comparison of these data with those of Hastelloy B, which, though somewhat stronger, is considerably less ductile.

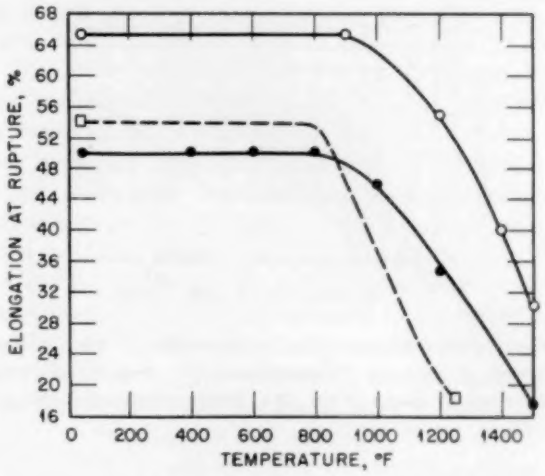

Figure 15 — Comparison of tensile elongations of INOR-8 specimens tested at ORNL, Haynes Stellite Company, and BMI. ○, ORNL; □, BMI; ●, Haynes Stellite. Data from Oak Ridge National Laboratory.[22]

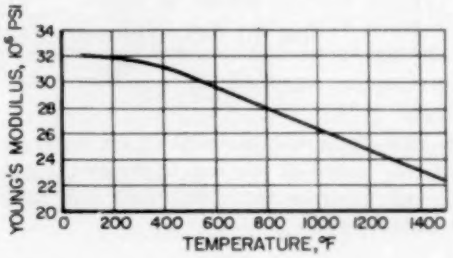

Figure 16 — Young's modulus for INOR-8 as a function of temperature. Data from Oak Ridge National Laboratory.[22]

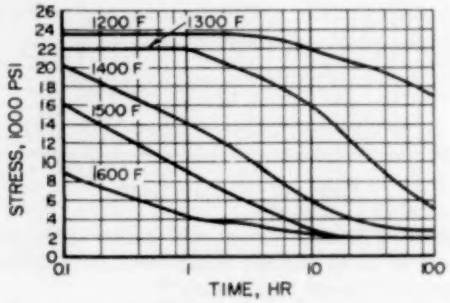

Figure 17 — Relaxation curves for INOR-8 stressed to 0.1 per cent strain at temperatures from 1200 to 1600°F. Data from Oak Ridge National Laboratory.[22]

An investigation of the hot ductility of Inconel and Inconel X was made at Oak Ridge.[34] The ductility of both alloys increased with increased test temperatures up to 2200°F, the embrittling temperature, beyond which the ductility was

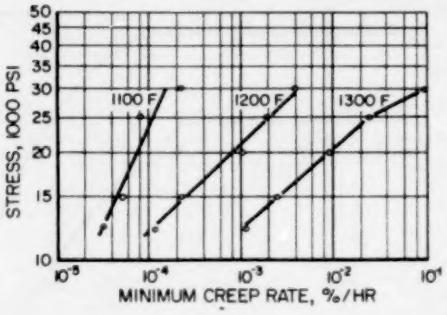

Figure 18 — Creep rates versus stress for INOR-8 tested at various temperatures in a molten-salt environment. Data from Oak Ridge National Laboratory.[22]

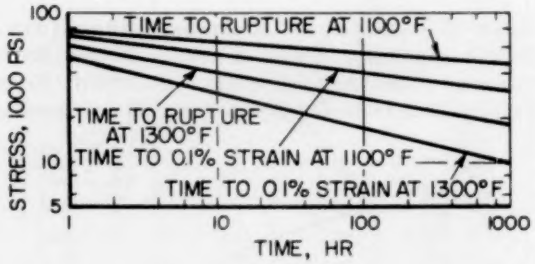

Figure 19 — Time to 1 per cent strain versus stress for INOR-8 tested at various temperatures in a molten-salt environment. Data from Oak Ridge National Laboratory.[22]

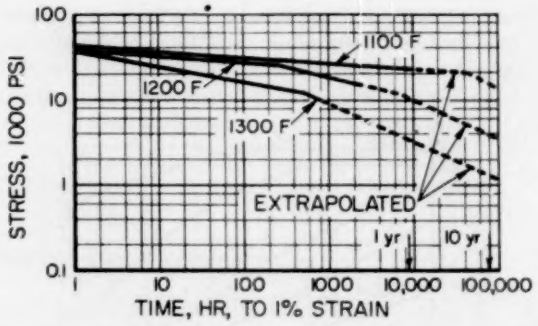

Figure 20 — INOR-8 creep and stress-rupture data obtained in air by Haynes Stellite Company. Data from Oak Ridge National Laboratory.[22]

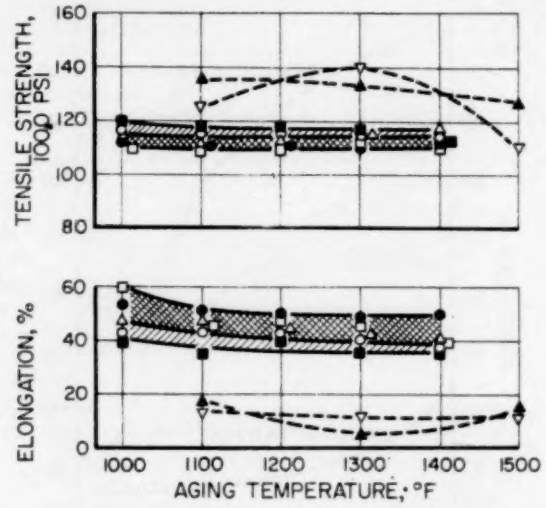

Figure 21 — Room-temperature tensile properties of INOR-8 and Hastelloy B after aging in the temperature range 1000 to 1400°F for times up to 2000 hr. ▨, Heat 8M 1; ○, aged 500 hr; ■, aged 2000 hr. ▩, Heat SP-19; ●, aged 500 hr; △, aged 1000 hr; □, aged 2000 hr. ---, Hastelloy B; ▽, aged 500 hr; ▲, aged 1000 hr. Data from Oak Ridge National Laboratory.[22]

Table IV-5 SHORT-TIME CREEP TESTS FOR 6057 ALLOY AT 212°F*

Condition	Stress, psi	Duration of test, hr	Creep rate,† %/hr
Hot-rolled (perpendicular to rolling direction)	11,000	450	2.4×10^{-5}
Hot-rolled (parallel to rolling direction)	15,000	350	5×10^{-4}
Hot-rolled (parallel to rolling direction)	16,000	300	1×10^{-3}

* Data by Atomic Energy of Canada, Ltd.[35]
† Not secondary creep rates.

observed to decrease rapidly. The ultimate strength decreased with increasing temperature from 1500°F to the embrittling temperature. Metallographic examination of the fractured specimens showed that the loss of ductility is accompanied by grain-boundary melting in Inconel X. (F. R. Shober)

Other Materials

The results of short-time creep tests of an aluminum–3.5 wt.% magnesium alloy (6057) at 212°F obtained by Canadian workers[35] are presented in Table IV-5.

Mechanical properties of AISI type 347 stainless steel nitrided in sodium at 75, 850, and 1000°F were determined at Knolls.[36] The re-

Table IV-6 TENSILE PROPERTIES OF AS-RECEIVED AND NITRIDED SPECIMENS*

Test temp., °F	Yield strength (0.2% offset), psi	Ultimate strength, psi	Elongation in 1 in., %
	As received†		
75	34,600	84,900	49.2
850	21,400	62,100	26.6
1000	19,400	55,900	25.0
	Nitrided 26 days‡		
75	55,500	75,900	13.0
850	29,500	51,800	5.8
1000	28,200	49,700	9.4
	Nitrided 53 days		
75	67,600	72,400	12.5
850	34,700	54,200	3.6
1000	35,100	52,100	

*Data from Knolls Atomic Power Laboratory.[38]
†Average of two tests.
‡Average of three tests.

Table IV-7 CREEP DATA ON THERMALLY DEGASSED FINE-GRAINED SINTERED TANTALUM SHEET TESTED AT 1200°F IN A HELIUM ATMOSPHERE*

Stress, psi	Time in progress, hr	Initial deformation, %	Total deformation, %	Minimum creep rate, %/hr
10,000	960.7	0.051	0.090	Nil
12,000	1200.0	0.012	0.098	0.0001
14,000	1032.3	0.058	0.158	0.000025
16,000	1001.8	0.12	0.201	0.0004

*Data by Battelle Memorial Institute.[2]

sults and the effect of nitriding are shown in Table IV-6.

The creep properties of thermally degassed fine-grained sintered tantalum sheet at 1200°F, as determined by workers at Battelle,[2] indicate that there is little difference between this type of tantalum and annealed arc-cast tantalum. Results from creep tests on the sintered material at 1200°F are given in Table IV-7.

Tensile properties of annealed (1 hr at 1600°C) niobium-base alloys determined at 25 and 1093°C by the Aviation Gas Turbine Division of Westinghouse[37] indicate that vanadium and zirconium are effective strengtheners at 1093°C. The results of these tests are given in Table IV-8. The 100-hr rupture strength of annealed niobium as determined at Battelle[32] was 8100 and 5800 psi at 1200 and 1260°C, respectively. Additions of 1.1 wt.% chromium increased the 100-hr rupture strength to approximately 9300 psi at 1260°C, while the addition of 1 wt.% oxygen, 1.8 wt.% zirconium, and 4.0 wt.% zirconium increased the 100-hr rupture strength to approximately 6800 psi at the same temperature.

(F. R. Shober)

Radiation Effects in Nonfuel Materials

Basic Studies

Several studies have been reported on defect formation and annealing processes in metals. They have shown similarities and differences caused by electron irradiation, fast-neutron

Table IV-8 MECHANICAL PROPERTIES OF NONCONSUMABLE-ARC-MELTED NIOBIUM ALLOYS*

Nominal composition, wt.%	Test temp., °C	Proportional limit, psi	Yield strength (0.2% offset), psi	Ultimate tensile strength, psi	True stress at fracture, psi	Elongation in 1 in., %	Reduction in area, %
99Nb–1V	25	42,680	47,780	52,750	85,750	26.2	97.8
95Nb–5V	25	61,500	74,400	86,150	174,700	27.2	72.3
95Nb–5V	1093		33,500	36,900		37.4	
99Nb–1W	25	35,800	44,200	48,150		35.9	74.8
99Nb–1W	1093		10,800	11,590		25.0	
95Nb–5W	25	43,950			53,300	0.28	
95Nb–5W	1093		11,500	13,990		22.8	
90Nb–10HF	25	45,050	53,000		66,900	2.9	8.6
99Nb–0.5Zr–0.5Ti	25	34,080	38,400	53,500	146,600	31.9	77.4
99Nb–0.5Zr–0.5Ti	1093		21,000	26,130		21.6	
97Nb–1Zr–1Ti–HF	1093		43,200	44,280		9.9	

*Data by Westinghouse Electric Corp.[37]

irradiation, quenching, and cold work. The annealing processes have been followed by measurements of resistivity, lattice expansion and strain, density change, and stored energy.

Considerable information has been reported on molybdenum and tungsten. Hanford[38–40] has carried out further annealing studies on molybdenum irradiated by fast neutrons from 6.5×10^{16} nvt to 1.2×10^{20} nvt. The annealing effect up to 170°C is interpreted as a first-order process with activation energy of 0.285 ev.[38] Close interstitial vacancy pairs are believed to disappear in this process. At higher temperatures, up to 600°C, the initial rate of defect removal is proportional to defect concentration, and equilibria at lower concentrations are reached at each higher temperature.[39] Density measurements[40] of molybdenum have shown a decrease from the initial value of 10.210 ± 0.005 g/cm^3 to 10.150 ± 0.005 g/cm^3 at 1.2×10^{20} nvt.

Kinchin and Thompson[41] have studied the neutron irradiation and annealing of molybdenum and tungsten wire by resistivity and stored-energy measurements. Wires were irradiated at 30°C and −196°C up to 1.3×10^{19} nvt. The metals irradiated at −196°C displayed annealing peaks at −170°C for molybdenum and at −80°C for tungsten, while specimens irradiated at 30°C had annealing peaks at 150°C for molybdenum and 320°C for tungsten. Stored-energy release for molybdenum was a maximum at 180 to 200°C. The derived activation energies were 0.25 ev at −170°C and 1.23 ev at 150°C for molybdenum and 0.5 ev at −80°C and 1.7 ev at 320°C for tungsten. For an irradiation of 10^{18} nvt, the fractional number of displaced atoms was estimated to be 2.6×10^{-5} from the total stored energy of 0.063 cal/g and assuming 10-ev energy release. This estimate gives a resistivity of 28 μohm-cm for 1 per cent interstitials and vacancies. The authors interpret the low-temperature annealing on the basis of migration of interstitials, with some interstitials annihilating vacancies and some being trapped. The high-temperature annealing effect is attributed to vacancy migration.

Adam and Martin[42] have measured the lattice and physical expansion of molybdenum after neutron irradiation. They found the physical expansion to be linear up to 250 ppm at 2×10^{19} nvt. The lattice expansion was similar but about three times smaller. Annealing stages were found at 180°C, where 40 per cent recovery occurred, and at 550°C. These observations agree essentially with the results of Hanford.

Piercy[43] has investigated the formation of point defects in platinum by quenching, cold work, and neutron irradiation. He measured these effects in terms of resistivity, density, lattice strain, and hardness. Quenching from 1600°C produced divacancies, with activation energy for migration of 1.13 ev. Neutron irradiation produced single vacancies with activation energy of 1.43 ev and having an annealing peak at about 250°C. Specimens were cold-worked at −196°C; these showed a range of annealing with partial recovery of resistivity below 100°C and hardness decrease above 400°C.

Morgan[44] has proposed the formation of dislocation loops to account for the effect of neutron irradiation on the critical shear stress. The dislocation loops may be formed as a result of plastic deformation around thermal or displacement spikes. He predicts a dependence upon the cube root of the integrated flux and fits his theory with prior data on copper.

Sosin and Meechan[45] have studied defect production in copper and nickel by electron bombardment and cold work in liquid helium. For 1 Mev electrons, the resistivitiy increases were 10.6×10^{-27} ohm-cm/electron/cm^2 for nickel and 3.6×10^{-27} ohm-cm/electron/cm^2 for copper. The metals were cold-worked by elongation of 15 per cent. Annealing was followed by resistivity measurement. There was no sharp recovery stage below 100°K. This confirms prior conclusions that the low-temperature (35°K) recovery in irradiated copper is caused by close-pair combination. Annealing stages for the cold-worked specimens occurred at 0 and 150°C for copper and at 100 and 300°C for nickel. The first stage was interpreted as a result of interstitial migration and the second stage as vacancy migration.

Gilman and Johnston[46] have studied, by micrographic techniques, the formation and movement of dislocations and point defects in neutron-irradiated lithium fluoride. The micrographic technique revealed dislocations and defect clusters by means of their etching behavior. Neutron doses greater than 10^{15} nvt produce a uniformly fine etching effect which is interpreted as being due to defect clusters less than 50 A in size but larger than single vacancies. Annealing above 400°C produces dislocation loops which grow and disappear above 500°C. Crystallographic

Table IV-9 EFFECTS OF IRRADIATION AND ANNEALING ON THE MECHANICAL PROPERTIES OF ZIRCALOY*

Test	Unirradiated	Irradiated†	Average property change, %
Hardness, Rockwell A	52.9 ± 0.02	.9 ± 0.05	+9.5
Yield strength (0.2% offset), 1000 psi	42	85–95	+114
Ultimate tensile strength, 1000 psi	67	90–98	+40
Uniform elongation, %	12	>0–3	−75
Reduction in area, %	42–45	22–32	−20

Summary of changes in properties after 1-hr postirradiation anneal at:

	400°C	500°C	600°C
Hardness	No change	Approximately unirradiated values	Approximately unirradiated values
Yield strength	No change	Approximately unirradiated values	Approximately unirradiated values
Ultimate strength	No change	Approximately unirradiated values	Approximately unirradiated values
Elongation	4% increase	Approximately unirradiated values	Approximately unirradiated values
Reduction of area	No change	16% increase	Not available

*Data by Bettis.
†Flux not given.

Table IV-10 ROOM-TEMPERATURE TENSILE-TEST RESULTS ON UNIRRADIATED AND IRRADIATED ZIRCALOY-3*

Integrated fast flux, nvt	Capsule	MTR cycles	MTR position	Direction to rolling	Yield strength (0.2% offset), psi	Ultimate tensile strength, psi	Uniform elongation in 1.26 in., %	Total elongation in 1.26 in., %	Reduction in area, %
Preirradiated				Longitudinal	40,000	62,000	17.2	28.9	41.3
Preirradiated				Longitudinal	35,300	61,300	17.4	28.6	43.3
Preirradiated				Longitudinal	35,400	61,900	17.1	27.7	44.9
Preirradiated				Transverse	49,700	59,300	11.3	30.6	42.0
Preirradiated				Transverse	49,700	60,000	11.6	24.5	44.8
1.2×10^{20}	7-12-3	10	L-49SW	Longitudinal	69,700	73,300	3.6	20.2	50.6
1.2×10^{20}	7-12-3	10		Longitudinal	68,700	72,700	4.0	11.9	44.0
1.2×10^{20}	7-12-3	10		Transverse	78,300	78,300	0	16.5	52.6
1.2×10^{20}	7-12-3	10		Transverse	78,000	78,000	0	14.4	62.0
1.8×10^{20}	7-12-1	5	L-47	Longitudinal	66,100	71,000	4.2	13.3	43.3
1.8×10^{20}	7-12-1	5		Longitudinal	67,300	72,000	3.8	13.6	46.6
1.8×10^{20}	7-12-1	5		Transverse	81,900	81,900	0	6.9	56.6
1.8×10^{20}	7-12-1	5		Transverse	78,000	78,000	0	6.7	50.0
3.3×10^{20}	7-12-4	5	L-49NW	Longitudinal	68,000	72,000	3.5	16.0	41.3
3.3×10^{20}	7-12-4	5	L-49NW	Longitudinal	70,700	75,300	4.0	12.6	41.3
3.3×10^{20}	7-12-4	5	L-49NW	Transverse	78,000	78,000	0	7.6	51.3
3.3×10^{20}	7-12-4	5		Transverse	77,300	77,300	0	9.8	48.0
3.4×10^{20}	7-12-2	10	L-49NW	Longitudinal	69,300	72,300	4.1	17.5	42.0
3.4×10^{20}	7-12-2	10		Longitudinal	69,300	73,700	4.0	12.4	43.3
3.4×10^{20}	7-12-2	10		Transverse	81,500	81,500	0	6.0	42.0
3.4×10^{20}	7-12-2	10		Transverse	82,000	82,000	0	6.4	51.3

*Data by Knolls Atomic Power Laboratory.

Table IV-11 RESULTS OF TESTS OF NOTCHED-BEND SPECIMENS OF DUCOL W.30 STEEL PLATES AND WELDS*

Specimen	Irradiation temperature, °C	Transition temperature, °C, at indicated irradiation		
		No irradiation	Irradiated to 4×10^{19} nvt	Irradiated to 7.6×10^{19} nvt
Base plate	50–60	3	38	75
	130–140	3	70	75
Weld metal	50–60	30	58	105
	130–140	30	75	105

*British data.[47]

Table IV-12 EFFECT OF 1516-MWD IRRADIATION ON TRANSITION TEMPERATURE OF HY-65 STEEL IN THREE HEAT-TREATMENT CONDITIONS*

Heat-treatment	Preirradiation hardness, R_C	Effect of irradiation on transition temperature
Normalize at 1750°F, temper 1 hr at 1225°F	16.3	Raised 196°C
Austenitize at 1750°F, brine quench, temper 1 hr at 1225°F	29.7	Raised 137°C
Austenitize at 1750°F, austemper at 700 to 800°F, temper 1 hr at 1225°F	25.9	Raised 176°C

*Canadian data.[48]

cavities are formed above 600°C, appearing first at subgrain boundaries. They are flat with sides parallel to (1 0 0) planes. The authors suggest that the cavity is an agglomeration of excess vacancies resulting from loss of fluorine. The yield stress, hardness, and resistance of dislocation movement increase for neutron doses above 10^{12} nvt. These effects are related to cluster formation rather than to point defects.

(A. E. Austin)

Effects of Irradiation on Mechanical Properties

Hardness measurements and tensile tests were performed by Bettis on Zircaloy specimens, as-irradiated and after postirradiation annealing at 400, 500, and 600°C. The results are summarized in Table IV-9. Knolls findings on the effects of irradiation on the mechanical properties of Zircaloy-3 are given in Table IV-10. The data indicate that the exposures used were sufficient to produce saturation of irradiation effects. It is significant that the uniform transverse elongation for all postirradiation specimens is zero. The material has apparently lost all capacity for work hardening in the direction of rolling.

Studies of the effects of irradiation on the mechanical properties of mild steels showed that the notched-bar transition temperature could be increased appreciably by irradiation. Notched specimens from unwelded plate and from welds in Ducol W.30 steel were tested in England.[47] They were irradiated to 4×10^{19} and 7.6×10^{19} nvt at 50 to 60°C and at 130 to 140°C. The results of slow-bending tests on these specimens are summarized in Table IV-11. Findings from a similar Canadian study[48] on HY-65 steel are presented in Table IV-12. For comparison with a steel of standard construction, unirradiated HY-65 in the normalized condition has a transition temperature about 26°C lower than that of ASME type 201 mild steel. In addition to raising the transition temperature, irradiation also reduces the notched-bar energy absorption at temperatures where ductile behavior occurs.[47–49]

It has been found that grain size has an influence on the irradiation-induced increase in transition temperature in steels. This is demonstrated by the difference in behavior between wrought plate and welds.[47,49] The increase in transition temperature is greater for the weld than for the base plate. Hull and Mogford[50] discuss Cottrell's method of estimating, from tensile tests, increases in notched-bar transition temperature (ΔT) with irradiation dose (ϕ). A constant $\Delta T/\phi^{1/3}$ is calculated for four different grain sizes of Em-2 steel. This calculated

value agrees reasonably well with a value derived experimentally. In general, these studies point out the definite advantage of using fine-grained steels for resistance to radiation-induced embrittlement.

In a Geneva Conference report, Bartz[51] discusses in some detail the performance of structural components, fuel elements, control rods, high-pressure piping, and pressure vessels. Information is presented on the effects of irradiation on the properties of aluminum alloys, beryllium, stainless steel, carbon steels, Croloys, Hastelloy X, Inconel 702, Inconel X, and K monel. For some materials, behavior after exposure to integrated fluxes as high as 3.76×10^{22} nvt is reported. (D. C. Martin)

References

1. Technical Progress Report, Pressurized Water Reactor (PWR) Project for the Period June 24, 1958, to Aug. 23, 1958, WAPD-MRP-75, August 1958. (Unclassified AEC report.)
2. R. W. Dayton and C. R. Tipton, Jr., Progress Relating to Civilian Applications During August 1958, BMI-1286, Sept. 1, 1958. (Unclassified AEC report.)
3. H. B. Hix, Compositions of Matter, U. S. Patent 2,822,268 (assigned to E. I. du Pont de Nemours and Company), Feb. 4, 1958.
4. T. N. Rhodin, Jr., Niobium-base High-temperature Alloys, U. S. Patent 2,838,395 (assigned to E. I. du Pont de Nemours and Company), June 10, 1958.
5. T. N. Rhodin, Jr., Metal Production, U. S. Patent 2,838,396 (assigned to E. I. du Pont de Nemours and Company), June 10, 1958.
6. R. Speiser, Development of an Oxidation-resistant Columbium Alloy, Status Report No. 17 for the Period Apr. 16, 1958, to Aug. 15, 1958, Aug. 18, 1958. Ohio State University Research Foundation, Columbus, Ohio.
7. E. C. Hirakis, Research for Coatings for Protection of Niobium Against Oxidation at Elevated Temperatures, Quarterly Report No. 3 for Jan. 1, 1958, May 1958. Horizons, Inc., Cleveland, Ohio. Ohio.
8. J. L. McCloud, Molybdenum Is Here to Stay, *Metal Progress*, 74(2): 75-78 (August 1958).
9. E. S. Bartlett and D. N. Williams, The Oxidation Rate of Molybdenum in Air, *Transactions of the American Institute of Mining and Metallurgical Engineers*, 212(2): 280-281 (April 1958).
10. M. J. Brabers and C. E. Birchenall, High-temperature Oxidation of Iron-Nickel Alloys, *Corrosion*, 14(4): 33-36 (April 1958).
11. National Bureau of Standards, July 1958. (Unpublished.)
12. National Bureau of Standards, July 1958. (Unpublished.)
13. National Bureau of Standards, 1958. (Unpublished.)
14. J. L. Scott, An Analysis of the Magnesium-CO_2 Reaction in Terms of a Reactor Environment, CF-58-5-100, May 15, 1958. (Unclassified AEC report.)
15. L. Boussion, L. Grall, and R. Caillat, Atmospheric Oxidation of Magnesium Between 350 and 500°C, CEA-701, 1957. (Unclassified French report.); also *Revue de métallurgie*, 54(3): 185-188 (1957).
16. G. J. Biefer, Atomic Energy of Canada, Ltd., May 8, 1958. (Unpublished.)
17.* F. H. Krenz, G. J. Biefer, and N. A. Graham, Chalk River Experience with Zircaloy-2 and Aluminum-Nickel-Iron Alloys in High-temperature Water, A/CONF./15/P/194. (AECL-604.)
18.* C. J. Klamut et al., Material and Fuel Technology for an LMFR, A/CONF./15/P/2406.
19.* W. D. Manly et al., Metallurgical Problems in Molten Fluoride Systems, A/CONF./15/P/1990.
20. W. D. Wilkinson and W. F. Murphy, "Nuclear Reactor Metallurgy," Chap. 16, pp.263-288, D. Van Nostrand Co., Inc., April 1958.
21. Oak Ridge National Laboratory, 1958. (Unpublished.)
22. Molten Salt Reactor Program Quarterly Progress Report for Period Ending June 30, 1958, ORNL-2551, Sept. 24, 1958. (Unclassified AEC report.)
23. M. Davis and A. D. Marsh, The Corrosion of Niobium in Oxygen Bearing Sodium, IGR-TN/C-608, June 21, 1957. (Unclassified British report.)
24.* M. Davis and A. Draycott, Compatibility of Reactor Materials in Flowing Sodium, A/CONF./15/P/25.
25. J. A. Herickes et al., Zirconium Hazards Research. Progress Report No. 2 for Sept. 1, 1957, to Feb. 28, 1958, AECU-3682, Feb. 28, 1958. (Unclassified AEC report.)
26. A. J. Bendler, J. K. Roros, and N. H. Wagner, Fast Transient Heating and Explosion of Metals Under Stagnant Liquids, AECU-3623, Feb. 12, 1958. (Unclassified AEC report.)
27. H. M. Higgins, Reaction of Zircaloy-2 with Water and with Uranyl Sulfate Fuel Solution, Fourth Monthly Progress Report for Oct. 1 Through Oct. 31, 1958, AGC-AE-39, Nov. 27, 1957. (Unclassified AEC report.)
28. Semiannual Summary Research Report in Chemistry for July to December 1957, ISC-976, Mar. 15, 1958. (Unclassified AEC report.)

29. Zirconium Highlights, WAPD-ZH-8, June 1958. (Unclassified AEC report.)
30. R. Sesnick, L. S. Castleman, and L. Seigle, The Self-Diffusion of Niobium II, Second Annual Progress Report, SEP-248, June 30, 1958. (Unclassified AEC report.)
31. D. E. Williams and W. H. Pechin, The Tantalum-Columbium Alloy System, *Transactions of the American Society for Metals*, 50: 1081-1089 (1958).
32. E. J. Jablonowski, F. R. Shober, and R. F. Dickerson, Battelle Memorial Institute, July 1958. (Unpublished.)
33. Zirconium Highlights, WAPD-ZH-10, August 1958. (Unclassified AEC report.)
34. E. A. Pigan, An Investigation of Hot Ductility of Inconel and Inconel X, ORNL-2571, Sept. 19, 1958. (Unclassified AEC report.)
35. Atomic Energy of Canada, Ltd., 1958. (Unpublished.)
36. Reactor Technical Quarterly Report No. 4, Metallurgy and Materials, KAPL-2000-1, January 1958. (Unclassified AEC report.)
37. R. T. Begley, Westinghouse Electric Corp., Aug. 15, 1958. (Unpublished.)
38. Fuels Development Operation Quarterly Progress Report for July, August, and September, 1957, HW-53488, October 1957. (Secret AEC report.)
39. Fuels Development Operation Quarterly Progress Report for October, November, and December, 1957, HW-54702, Jan. 15, 1958. (Secret AEC report.)
40. Fuels Development Operation Quarterly Progress Report for January, February, and March, 1958, HW-56029, Apr. 15, 1958. (Secret AEC report.)
41. G. H. Kinchin and M. W. Thompson, Irradiation Damage and Recovery in Molybdenum and Tungsten, *Journal of Nuclear Energy*, 6(4): 275 (May 1958).
42. J. Adam and D. G. Martin, Measurements of Unit Cell and Physical Dimension Changes of Molybdenum After Neutron Irradiation, AERE-M/M-197, July 1958. (Unclassified British report.)
43. G. R. Piercy, Point Defects in Platinum, CR MET-782, 1958. (Unclassified Canadian report.)
44. C. E. Morgan, Effect of Neutron Irradiation on the Critical Shear Stress of Metal Single Crystals, NARF-58-9-T, May 20, 1958. (Unclassified USAF report.)
45. A. Sosin and C. J. Meechan, Defect Production and Migration in Copper and Nickel, NAA-SR-2062, November 1957. (Unclassified AEC report.)
46. J. J. Gilman and W. G. Johnston, Dislocations, Point-Defect Clusters, and Cavities in Neutron Irradiated LiF Crystals, *Journal of Applied Physics*, 29(6): 877 (June 1958).
47. R. C. Burnett, J. M. N. Allen, and D. R. Harries, Examination of a Welded Ducol W.30 Steel Plate of $4\frac{5}{8}$-in. Thickness, AERE-M/R-2536, April 1958. (Unclassified British report.)
48. Atomic Energy of Canada, Ltd., 1958. (Unpublished.)
49.* M. J. Makin et al., The Mechanical Properties, Embrittlement, and Stability of Irradiated Metals and Alloys, A/CONF./15/P/80.
50. D. Hull and I. L. Mogford, Estimation of the Increase in Notched Transition Temperature of Steels Irradiated with Neutrons, AERE-M/R-2555, April 1958. (Unclassified British report.)
51.* M. H. Bartz, Performance of Metals During Six Years Service in the Materials Testing Reactor, A/CONF./15/P/1878.

*Second United Nations International Conference on the Peaceful Uses of Atomic Energy, Geneva, September 1958. (Available from the Office of Technical Services, Dept. of Commerce, Washington 25, D. C.).

Melting, Casting, Heat-treatment, and Hot Working

The recovery of unalloyed scrap uranium by melting it under a molten salt cover in air has been studied over the years by a number of investigators.[1–5] Since heavy scrap (croppings, reject slugs, etc.) can be handled quite satisfactorily in the presently used vacuum-remelt operation, the scrap form that provides the greatest incentive for recovery is the "saw dust" and "turnings" from the cutoff and fuel-slug machining operations. If this high-surface scrap is included in the vacuum remelt, oxide contents are high and metal quality suffers.

Most recently Mallinckrodt has been examining the feasibility of producing acceptable quality billets in a single, scrap-remelting, air operation.[5] Small-scale (2500 g) experiments were conducted, and the results resolved, to some extent, the problem areas. Some of the conclusions are as follows:

1. High-yield, low-impurity uranium billets were obtainable by melting turnings from dingot (as-reduced) uranium under a salt cover.

2. Lithium fluoride, magnesium fluoride, calcium chloride, and calcium fluoride provided adequate protection from air for molten uranium. The best results were obtained with LiF-CuF_2 (1:1, molar), MgF_2-CaF_2 (1:1, molar), and LiF-MgF_2-CaF_2 (35:41:24, wt.%). The alkali fluorides, with the exception of lithium fluoride, react with molten uranium, alone or in combination with magnesium or calcium fluoride.

3. Pretreatment (by pickling) of the chips did not improve the metal product.

4. Relatively low hydrogen content metal was produced. However, the minimum content was 2.1 ppm, and helium purging was not effective.

5. Erosion of the graphite crucible was not reduced by the application of crucible dressings (MgO-MgF_2 and Al_2O_3-SiO_2-$MgCl_2$), and their use lowered the metal yields.

Shape casting of unalloyed uranium, uranium-base alloys, and uranium-containing alloys of zirconium is receiving considerable attention for a number of reasons. Hare and Dickerson reported on the feasibility of casting intricate-shaped fuel elements from a uranium–5 wt.% chromium alloy.[7] However, most of the interest lies in the casting of shapes from which the desired fuel-element components can be conveniently fabricated.

The demand for small-diameter zirconium tubing as specifically used for the cladding of uranium dioxide fuel pellets prompted a recent study by Nuclear Metals.[8] In this study the problems present in the fabrication of zirconium alloys are commented on in terms of the critical chemical and dimensional specifications for the final tube product. Specific comments are given on contamination by lubricants and removal of the contaminants by chemical means. Further comments are given on annealing, drawing speeds, and the mechanical and corrosion properties of the final product.

(E. L. Foster)

Cladding

Cladding by Drawing and Roll Bonding

Nuclear Metals[9] is investigating "cable cladding" as a method of cladding extended tubular surfaces of uranium with aluminum. The method would include cladding and bonding by a process of drawing which could become a very economical process for fabricating tubular fuel elements. It is intended that the drawing action will take place on both the inner and outer surfaces of the element. The outside aluminum clad will be deformed by a die, and the inside aluminum clad will be deformed by a ball or tube mandrel. Lubricants for the drawing of aluminum over nickel-plated uranium are being studied preparatory to the cladding studies.

(E. S. Hodge)

Pressure Bonding

Diffusion-bonding studies conducted at Sylvania[10] have revealed that the growth of a bond interface between two metallic systems is affected by pressure. In the most recent bonding studies of aluminum to uranium, it was shown that the formation of the UAl_3 layer is accelerated by an increase in pressure. In other bond systems the opposite effect was observed. There are several theories that explain the effects of pressure on the growth of a bond interface; however, at the present time, they have not been sufficiently proven that prediction of behavior is possible.

The results of gas-pressure-bonding studies conducted at Battelle during the past several years were summarized in a Geneva Conference paper.[11]

Studies are continuing on the development of the gas-pressure-bonding technique for the preparation of flat-plate Zircaloy-clad UO_2 fuel elements.[12] The UO_2 is compartmented by Zircaloy ribs which are bonded to the Zircaloy cladding. In previous studies the fuel-element components were assembled into a Ti-Namel jacket which was evacuated, sealed, and pressure bonded. In the recent work the components are assembled, and the Zircaloy edges are fusion welded to form a gastight assembly. This assembly is then pressure bonded directly, resulting in a cost reduction and elimination of the Ti-Namel-Zircaloy reaction. The elements are being bonded at 1550 and 1750°F with 10,000 psi of helium. After bonding, they are subjected to a 5-min treatment at 1850°F. This completes the transformation of the Zircaloy and promotes grain growth across the bond interface.

Studies have been initiated to utilize the gas-pressure-bonding technique for the cladding and bonding of niobium and molybdenum fuel elements and assemblies.[12–14] The initial phase is concerned with the determination of optimum conditions for the self-bonding of these elements. Ductile bonds with grain growth across the interface were obtained for molybdenum plates bonded 3 hr at 2100°F with 10,000 psi of helium. Niobium plates bonded under the same conditions possessed a weak brittle bond.

Several basic studies of pressure bonding are being conducted to supplement the fuel-element development programs. One study involves the determination of the conditions under which the mating surface will deform sufficiently to produce the intimate contact required for diffusion and bonding.[12–14] The objective of this study is to relate the optimum conditions of bonding for any given material to its known mechanical or physical properties. In another study the bonds are being evaluated by X-ray diffraction and electron microscopy to determine characteristics of the bond interface. Many of the pressure bonds appear to possess a foreign contaminant at the bond interface when viewed at low magnification; however, observation under the electron microscope suggests that the imperfections are voids, not contaminants. (S. J. Paprocki)

Diffusion Bonding

A brazing technique is being investigated by Bettis for the bonding of Zircaloy-clad compartmented flat-plate uranium dioxide fuel elements. The components to be clad are fabricated to final size prior to assembly. Perforated Zircaloy-2 frames are plated with thin deposits (approximately 0.00022 in. thick) of nickel, copper, or iron by a chemical replacement technique. The oxide fuel, pressed into strips, is placed in the compartmented Zircaloy frames. Covers are applied, and the assembly is sealed by resistance seam welding. The sealed elements, placed in mechanical jigs, are bonded by a diffusion-brazing operation consisting of a heat-treatment for 2 hr at 1010°C, which is above the eutectic temperatures for the zirconium-nickel, zirconium-copper, and zirconium-iron binary systems.[15,16] Cold-rolled Zircaloy plates vapor blasted and pickled for a short time (about 15 sec) in the standard hydrofluoric-nitric-water solution serve as an excellent base for continued processing. Tests have indicated that cold-rolled or cold-rolled and annealed Zircaloy plates are equally suitable for cladding components.[17] Graphite coating of the fuel plates has been effective in eliminating the fuel-cladding interaction.[18]

Fabricated elements are being evaluated by helium leak testing, corrosion tests in 680°F water and 750°F steam, internal pressure tests, water-logging tests, thermal cycling, and metallographic examination of bonds. Intentionally defected samples without a graphite barrier layer at the fuel-cladding interface were exposed to 680°F water and 750°F steam for periods up to 55 days with no loss in fuel-

element integrity and only minor swelling (less than 0.005 in.) due to the fuel-cladding interaction.[19] However, no corrosion swelling of defected elements incorporating a graphite barrier layer has been observed in short-time tests.[20] Internal-pressure tests have indicated high cladding bursting pressures, in excess of 3000 psi for 0.025-in.-thick cladding. Water-logging tests (with 0.005-in.-diameter cladding defects) show rupture in some samples and cladding deflections up to 0.122 in. without rupture in others. Thermal-cycling tests of fuel-element samples between room temperature and 1700°F have shown no dimensional changes after 100 cycles.[21] Metallographic examination of bond interfaces indicates bonds of good quality.[20] Bonds have shown some bond-line voids which may be due to entrapment of chemical films within pores of the deposits and the subsequent ineffective wetting in these areas during plating. Variations in bath agitation, which affects the characteristics of the deposit, are being investigated as a means of eliminating these voids which appear more extensive when large areas of Zircaloy-2 are diffusion bonded.[18]

Chemical analysis of the concentrations of copper and iron as a function of distance from the original bond interface of diffusion-bonded fuel elements indicates that the highest concentration does not exceed 1 wt.% and occurs at the bond interfaces. At the external cladding surfaces (0.020-in.-thick cladding), the concentrations are 0.03 to 0.14 wt.% copper and about 0.3 wt.% iron. Iron is higher at the surface because of its higher level in the original cladding.[18]

The effect of bonding times between 5 and 15 min at 1000°C and 15 psig by simultaneous resistance heating and diffusion bonding of Zircaloy-clad compartmented flat-plate uranium dioxide fuel elements has been investigated.[20] Each element was composed of a punched receptacle plate, plated with copper or iron and sandwiched between two 0.025-in.-thick Zircaloy-2 cover plates. Uncoated natural uranium dioxide fuel inserts were used as fillers Pressure testing of the elements at 700 psig showed a sporadic occurrence of leaks which bore no direct relation to the bonding time but appeared to have resulted either from lack of bonding at a plating discontinuity or in areas where molten eutectic was pressed away from the rib-cover plate interface. Metallographic examination of the elements showed: (1) at short bonding times, 5 min, the diffusion of iron appeared to be more complete than that of the copper; (2) where molten eutectic (zirconium-copper or zirconium-iron) formed pockets of relatively large volume, such pockets were not completely diffused at 15-min bonding time; and (3) there was no evidence of fuel-cladding interaction for 5-min bonding time, but 10-min bonding time produced the fuel-cladding interaction. (M. A. Gedwill, Jr.)

Coextrusion

Through an initial study made by Nuclear Metals,[22] the process of coextrusion followed by swaging has been demonstrated as being feasible for the production of pin type fuel elements of uranium−10 wt.% molybdenum clad with tantalum. In this limited program two fuel pins consisting of a 0.150-in.-diameter core with a 0.004-in. thickness of tantalum cladding were produced successfully. These fuel pins were produced from billet assemblies which were sealed into evacuated heavy-walled iron jackets and extruded with glass lubrication through 0.375- and 0.340-in.-diameter dies (14× and 17× reductions). Coextrusion was accomplished at 1800°F from a 1.400-in.-diameter liner in a 300-ton press. Cold swaging of these extruded rods through reductions up to 61.5 per cent was accomplished without difficulty. A qualitative destructive test indicated that metallurgical bonding existed between the core and cladding.

The coextrusion technique[9,23,24] is being applied to the manufacture of Zircaloy-2-clad tubes of uranium−2 wt.% zirconium. These fuel tubes are being fabricated and examined at Nuclear Metals with further metallurgical tests being made by Savannah River. Three problems encountered in earlier experimental work which had a great effect upon the yield of high-quality tubes were investigated. The six experimental billets used for this investigation were extruded at the American Brass Company. These problems and the solutions are as follows:

1. Mandrels failed by ductile fracture during extrusion. It was found that mandrels with a hardness R_C 55 retain their hardness and physical dimensions so that the ductile failure of the mandrel will probably not occur.

2. "Dog-boning" of the Zircaloy at the front end of the extrusion billet into the copper can

sometimes resulted in breakthrough of the Zircaloy. This problem appears to have been solved by machining a $\frac{1}{4}$-in. radius on the front outer edges of the Zircaloy front plate.

3. Bowing of the tubes during the cooling period occurred after extrusion. Better support and facilities for rolling the heated tube onto a plane surface immediately after extrusion reduce the bowing considerably.

Four tubes of uranium–2 wt.% zirconium clad with Zircaloy-2 were completely processed and selected as candidates for irradiation testing. The diametral dimensions of these four typical full-size power-reactor fuel tubes indicate that dimensional specifications on the tube diameters can be satisfied with little difficulty. A program has been laid out to investigate the effect of several variables on outer-surface smoothness, core-cladding interface, and end-shape cladding thinning.

Nuclear Metals[23] coextruded the first of five Zircaloy-clad uranium composite billets for Hanford from a 4-in. liner through a 1.055-in. die, an area reduction of 14.8. Examination of the rod showed the Zircaloy cladding to be within the specified tolerance of 0.020 ± 0.003 and the Zircaloy-to-uranium bond to be satisfactory. The as-extruded rod surface and core-to-cladding interface, however, were irregular. Swaging did not entirely remove the surface irregularities. Heat-treatment of the Zircaloy and uranium stock for the remaining billets is being tried in an attempt to improve the surface and interface of the remaining rods.

Several aluminum and aluminum–4 wt.% magnesium clad uranium tubes have been produced by the multitemperature extrusion technique.[9] The tube extrusions exhibited generally the same mechanical behavior as the rod extrusions.[25] Both forged ingots and forged dingots of uranium were used in these tubes. The core-cladding interface resulting from the use of the forged dingot was very smooth, whereas the interface resulting from the use of the forged ingot was jagged.

Attempts at making integral end seals for these tubes proved successful. It appears that end seals can be integrally made if some reasonable taper in the end seal is acceptable.

Cracking of aluminum–4 wt.% magnesium when it is used as the inner cladding material was observed. This was anticipated and can be avoided by the use of 2S aluminum as the inner cladding material.

Thirty-two enriched rods with Zircaloy-2 cladding and integral Zircaloy-2 end seals have been extruded, etched, and swaged.[23] Of these 32 rods, 16 have been beta treated, radiographed, and straightened. The front end-seal defect of these 16 rods is between $1\frac{1}{4}$ and $1\frac{3}{4}$ in. long, whereas the rear defect is between $\frac{1}{2}$ and 1 in. long. The over-all length, measured from tip to tip, of enriched-uranium rods is between $34\frac{1}{4}$ and $34\frac{3}{4}$ in. Bond tests of the Zircaloy-2 cladding and the Zircaloy end seals indicate no bonding difficulties, and no blisters were formed on the rods during the beta heat treating. (C. B. Boyer)

Extrusion Cladding

Chalk River[26] reported that, in an earlier trial production run of 145 extrusion-clad uranium plates, numerous defects occurred in the cladding. In this case the cladding thickness was 25 mils. It was believed that many of these defects might be eliminated by extruding the original cladding oversize and then machining it to the required 25-mil thickness.

To test the oversized-cladding technique, another trial production run was completed where over 1100 uranium plates were clad with an oversize sheath. The following extrusion conditions were used for the run:

Die temperature, 525 ± 10°C
Billet temperature, 525 ± 10°C
Core preheat temperature, 300°C
Extrusion speed, 8 to 10 fpm

Argon atmosphere was used for preheat, and billets were upset in vacuum.

The average cladding production rate was about 6 plates per hour. The dimensional accuracy of the oversize sheath was such that only 0.25 per cent of the plates was not acceptable for subsequent machining. Neither interfacial blisters (those located at the cladding-core interface) nor aluminum blisters (those located within the aluminum cladding itself) were found in the sheath. Elimination of the interfacial blisters was attributed to reduced core contamination through improved handling and packaging procedures. The avoidance of aluminum blisters, which were suspected to be related to air entrapment, was achieved by

evacuating the die block prior to upsetting the billets.

Core breakage in this trial production run was not encountered as in the "on-size" cladding run. The problem of core breakage was apparently overcome by using the oversize-cladding approach (because of less extrusion pressure exerted on the core), as well as by improving die alignment and core-to-mandrel slot clearances.

To aid in the machining of the oversized aluminum cladding, Chalk River uses three different types of inspection instruments to determine the location of the uranium plate with respect to the sheath. With these instruments, the rejection rate of unsatisfactorily machined clad plates was down to 2 per cent after 500 plates were processed.

The preliminary cost figures using the oversized-sheath approach indicate that the operation will fall below $1.20 per lb of uranium. This figure includes machining, labor, materials, machine rentals, administration, inspection, and overhead costs. The cost of machining alone was reported to be about $0.20 per lb of uranium.

A brief study on the effect of nickel-plate aging on cladding-to-core bond strengths was also conducted.[26] The results indicated that bond strengths are better when the nickel plate is applied to the core shortly before cladding. In one case, for example, the average bond strength was about 7900 psi for a clad uranium core plated two days before cladding. By comparison, a clad core plated 248 days before cladding exhibited an average bond strength of about 4700 psi. In this same study it was also noted that the bond strength appears to increase with the higher preheat temperatures. The preheat temperatures were 200, 300, and 400°C.

In its work on extrusion cladding of uranium plates, Battelle[27] made an effort to determine the general configuration and character of the billet-to-billet seams formed in the aluminum cladding. The experiments were conducted using the "right-angle" extrusion equipment, in which the extrusion ram moves perpendicularly to the plate during cladding. To aid in locating the seams, the initial tests were conducted by extruding successive billets of red and white Plasticine over standard-sized steel plates. The results of similar tests conducted later with aluminum billets appeared to correlate very well with those obtained with Plasticine. It was found that the original 2-in.-diameter-billet end surfaces were stretched out over cladding lengths greater than 25 ft. In addition, it was observed that some portions of the seam in the aluminum cladding were thicker than others; this appeared to be related to the increased amount of stretching the original surface had undergone. The results of a few tensile tests of claddings containing seams suggested that the presence of these seams did not have a marked effect on the tensile properties.

Battelle[27] also found that, for the limited number of plates tested, bond strengths with median values in the range from 20,000 to 26,000 psi were achieved between the cladding and uranium. Median values from 8000 to 17,000 psi were obtained between aluminum and sintered-aluminum-powder (SAP) end plugs.

(R. J. Fiorentino)

Canning

Attempts by Battelle to can fueled graphite with Inconel X have not been successful. Welds ruptured during long-time thermal cycling. However, graphite coated with silicon and canned in type 316 stainless steel appears to have good possibilities.

Sulzer Brothers, Ltd., of Switzerland have demonstrated[28] that hollow uranium fuel cylinders, internally clad with Zircaloy-2, can be produced by simple means, using a zone-melting process in a vacuum. The component parts are placed in a multisectional permanent mold of graphite and slowly drawn through the coils of an induction furnace. The metallic bond produced between the uranium and Zircaloy-2 shows satisfactory mechanical strength and corrosion resistance. (P. H. Bonnell)

Nonelectrolytic Chemical-plating Techniques

Vitro Laboratories[29] investigated electrophoretic methods of applying oxidation-resistant coatings to molybdenum. The optimum combination was a multilayer coating of Nichrome, cermet, and undensified Nichrome. For example, with nickel-bonded niobium carbide as the cermet, specimens withstood, without visible damage, four hundred 45-sec cycles between 200 and 2000°F with a 30-sec hold at 2000°F, after which they withstood 2000°F static air for 10 hr before failure.

Sylvania-Corning explored the possibility of coating uranium dioxide powders with niobium

films by the hydrogen reduction of niobium pentachloride in a fluidized bed of the powder. The work was terminated before satisfactory coatings were obtained.

Uranium dioxide powders were coated with tungsten films at Battelle[30] by hydrogen reduction of the chloride in a fluidized bed. Less than 0.1 per cent of the powder remained uncoated when, at 400°C, tungsten was deposited to the extent of 20 per cent of the total weight of the bed.

The coating of Croloy-2¼ with molybdenum was undertaken[12–14,31] with partial success. In the hydrogen reduction of molybdenum pentachloride at 800°C, a flash deposit of electroless nickel was found necessary to avoid the lack of adherence caused by the formation of a surface layer of lower chlorides or oxidation products on the Croloy-2¼. Molybdenum coating by reduction with Grignard reagents of solutions of molybdenum pentachloride in organic solvents was unsuccessful, incomplete reduction having been obtained. Reduction of surface coatings of molybdenum oxide by liquid sodium, sodium alloys, or ether solutions of lithium aluminum hydride was also unsuccessful.

Uniform, adherent coatings of niobium carbide, tantalum carbide, and zirconium carbide on graphite were obtained[32,33] by thermal decomposition of halide vapors in a range of pressure-temperature conditions thermodynamically unfavorable for the formation of the metal but favorable for the formation of carbide. In this way the rate of coating formation was made dependent on the rate of diffusion of carbon from the base, which resulted in good surface conformity and uniformity of thickness. The adherence of the coatings was shown[33] to depend upon a mechanical bond between the graphite and the carbide, which, in turn, depended upon the surface condition of the graphite base. An etching procedure was developed for the treatment of dense graphite prior to coating to ensure coating adherence.

(J. M. Blocher, Jr.)

Ceramic Coatings

For a general treatment of the state of the art, attention is directed to a paper[34] by Richmond et al. of the National Bureau of Standards. This is summarized in the recent Wilkinson and Murphy book, *Nuclear Reactor Metallurgy*.[35]

The difficulties encountered in attempting to coat type 420 stainless steel with ceramic coatings are described by Bradley[36] of Georgia Institute of Technology. The metal, after receiving the heat-treatment necessary to fire the coating, exhibits a marked change in thermal expansion at about 550°F. On cooling from 1500 to 550°F, the metal shrinks at a uniform rate of 12.4×10^{-6}/°F. From 550°F to room temperature, the metal expands at an average rate of about 8×10^{-6}/°F. This expansion develops tensile stresses sufficient to cause crazing in the ceramic coating. No solution to the problem is given, but a number of suggestions are made.

(B. W. King)

Welding and Brazing

Extensive information on welding and brazing programs at Knolls is presented in a Reactor Technology Quarterly Report.[37] Sections of this report pertinent to reactor core technology are reviewed below.

Effect of Welding Atmosphere and Pickling on the Corrosion Resistance of Welded Zircaloy-2 and -3

To produce Zircaloy-2 or -3 welds which will have good corrosion resistance in 680°F water, a vacuum shielding chamber is necessary. However, there were indications during this investigation that a shielding atmosphere somewhere between the best atmosphere in the vacuum chamber and that of the Plexiglas chamber might be suitable. Therefore it was recommended that there be additional study to determine whether corrosion-resistant welds can be made using pressures higher than 0.03 μ and back flushing with helium.

Joining of Zircaloy-2 to Austenitic Stainless Steel

Studies of most conventional joining processes produced negative results. Some processes rejected in this study might appear more promising with improvements in equipment and technique. Brazing with pure silver produced joints suitable for applications involving moderate stress, low impact, and low strain.

Investigation of the Feasibility of Diffusion Bonding Zircaloy Sheets Using a Stainless-steel Diffusion Layer

Preliminary tests indicate that this is a promising method of joining Zircaloy-2. However, joint corrosion resistance and ductility have not been determined.

Hanford and Bettis[18,20] are conducting programs on electron-beam welding of aluminum and Zircaloy, respectively. Hanford has successfully used an a-c power supply instead of the conventional direct current. No clear preference was indicated for one type of current. However, it should be noted that that an electron-beam gun will operate as a half-wave rectifier when supplied with a-c power. It would be expected that, on a-c, energy would be delivered to the weld pool in a series of conventional half-wave pulses.

Bettis is working with two units whose characteristics are listed below:

	Carl Zeiss	Westinghouse Electron Tube Division
Beam potential, volts	50,000–100,000	2,000–10,000
Beam current, amp	0–0.020	0–1.3
Beam power, kw	1	15
Focal distance, in.	1–2	¾–1
Focal spot diameter, in.	Less than 1/10	1/16 to ¼
Size of beam generator (approx.), in.	10 diam. × 30 length	3¼ diam. × 3 length

The Zeiss unit requires less energy and is much more precise in control than the Westinghouse unit. It is also four times as expensive ($60,000 versus $15,000). (R. E. Monroe)

Nondestructive Testing

The high standards of integrity demanded for nuclear components, especially fuel elements, have resulted in continued efforts to develop and improve nondestructive testing techniques. These efforts have been directed more toward the refinement of standard ultrasonic, eddy-current, X-ray, and gamma-ray techniques into more accurate and highly automated systems than toward basically new techniques. In a paper[38] presented at the Second Geneva Conference, McGonnagle and Paul have described many of these developments.

Ultrasonics appears to be the most widely used and rapidly developing nondestructive test method with many applications reported. At Hanford,[39] ultrasonic equipment has proved feasible in detecting unbonded areas as small as 2 to 5 mils in diameter on irradiated cylindrical fuel elements. At Knolls,[37] immersion ultrasonic equipment has been developed to test core-to-cladding bonds routinely on irradiated oval fuel elements. A process has been developed by Los Alamos[40] for the application of a thin vinyl plastic coating to graphite plates to prevent absorption of the coupling fluids used in ultrasonic inspection. There is no significant attenuation of ultrasonic impulses by the coating. After inspection, the vinyl sheath may be easily stripped from the plates.

Recent developments in industrial applications of isotopes to gauging and nondestrustive testing were reported at the Geneva Conference by Aebersold and Fowler.[41] The extension of gauging and radiographic techniques to meet industrial requirements has been mainly in the improvement of technique and component equipment rather than in development of new types of sources. Exceptions have been the source technology development of Kr^{85} and efforts to develop low-energy photon and beta-excited X-ray sources.

Two devices have been developed at Battelle to measure and record the channel spacing between stacked fuel plates in subassemblies. One is based on the use of strain gauges on deforming members, the other on the use of a liquid-filled expandable element and hydraulic system. The recorded output of both gauges is directly proportional to the actual plate separation and is reproducible within 1 mil over the range 65 to 105 mils. (C. V. Weaver)

References

1. R. M. Lang et al., Large-batch Melting of Uranium, BMI-932, Aug. 2, 1954. (Unclassified AEC report.)
2. G. W. Rengstorff and H. W. Lownie, Jr., Further Studies of Large-batch Melting of Uranium, BMI-1015, July 1[illegible], 1955. (Confidential AEC report.)

3. J. W. Simmons, ed., Summary Technical Report for the Period Apr. 1, 1957, to June 30, 1957, NLCO-685, July 19, 1957. (Confidential AEC report.)
4. J. W. Simmons, ed., Summary Technical Report for the Period July 1, 1957, to Sept. 30, 1957, NLCO-690, Oct. 21, 1957. (Confidential AEC report.)
5. J. W. Simmons, ed., Summary Technical Report for the Period Oct. 1, 1957, to Dec. 1, 1957, NLCO-715, Feb. 7, 1958. (Confidential AEC report.)
6. J. Nelson, ed., Process Development Quarterly Report (Part I, Laboratory Work), MCW-1415, July 1, 1958. (Confidential AEC report.)
7. A. W. Hare and R. F. Dickerson, A Method of Casting Radiator Type Fuel Elements for a Nuclear Reactor, *Modern Castings*, 33: 112-114 (May 1958).
8. N. R. Gardner and P. Loewenstein, The Cold Working of Extruded Zircaloy Tubing, NMI-1194, Apr. 30, 1958. (Unclassified AEC report.)
9. Fundamental and Applied Research and Development in Metallurgy. Progress Report for April 1958, NMI-2069, June 10, 1958. (Secret AEC report.)
10. L. S. Castleman and L. Seigle, Fundamentals of Diffusional Bonding—III, SEP-251, June 30, 1958. (Unclassified AEC report.)
11.* S. J. Paprocki, E. S. Hodge, and C. B. Boyer, Preparation of Reactor Components by a Gas-pressure Bonding Technique, A/CONF./15/P/788.
12. R. W. Dayton and C. R. Tipton, Jr., Progress Relating to Civilian Applications During September 1958, BMI-1294, Oct. 1, 1958. (Unclassified AEC report.)
13. R. W. Dayton and C. R. Tipton, Jr., Progress Relating to Civilian Applications During July 1958, BMI-1280, Aug. 1, 1958. (Unclassified AEC report.)
14. R. W. Dayton and C. R. Tipton, Jr., Progress Relating to Civilian Applications During August 1958, BMI-1286, Sept. 1, 1958. (Unclassified AEC report.)
15. Pressurized Water Reactor (PWR) Project Technical Progress Report for the Period Apr. 24, 1957, to June 23, 1957, WAPD-MRP-68. (Unclassified AEC report.)
16. Pressurized Water Reactor (PWR) Project Technical Progress Report for the Period Aug. 24, 1957, to Oct. 23, 1957, WAPD-MRP-70. (Unclassified AEC report.)
17. Pressurized Water Reactor (PWR) Project Technical Progress Report for the Period Oct. 24, 1957, to Dec. 23, 1957, WAPD-MRP-71. (Unclassified AEC report.)
18. Pressurized Water Reactor (PWR) Project Technical Progress Report for the Period June 24, 1958, to Aug. 23, 1958. WAPD-MRP-75. (Unclassified AEC report.)
19. Pressurized Water Reactor (PWR) Project Technical Progress Report for the Period Feb. 24, 1958, to Apr. 23, 1958, WAPD-MRP-73. (Unclassified AEC report.)
20. Pressurized Water Reactor (PWR) Project Technical Progress Report for the Period Apr. 24, 1958, to June 23, 1958, WAPD-MRP-74. (Unclassified AEC report.)
21. Pressurized Water Reactor (PWR) Project Technical Progress Report for the Period Dec. 24, 1957, to Feb. 23, 1958, WAPD-MRP-72. (Unclassified AEC report.)
22. J. J. Pickett and L. R. Aronin, Investigation of Coextrusion as a Method of Producing Tantalum-clad Uranium–10 Wt.% Molybdenum Pin Type Fuel Elements, NMI-4404, Jan. 23, 1958. (Unclassified AEC report.)
23. Fundamental and Applied Research and Development in Metallurgy. Progress Report for May 1958, NMI-2070, June 20, 1958. (Secret AEC report.)
24. L. Isakoff, comp., Heavy Water Moderated Power Reactors Quarterly Progress Report for February, March, and April, 1958, DP-295, June 1958. (Unclassified AEC report.)
25. Fundamental and Applied Research and Development in Metallurgy. Progress Report for March 1958, NMI-2068, Apr. 29, 1958. (Secret AEC report.)
26. W. M. Barss and N. J. Donahue, comps., Savannah River Operations Office, February 1958. (Unpublished.)
27. R. J. Fiorentino et al., Battelle Memorial Institute, Aug. 22, 1958. (Unpublished.)
28.* P. Sulzer, E. Bodmer, and P. de Haller, The Manufacture of Internally Cooled Pressurized-tube Elements of Metallic Uranium by a Zone Melting Process, A/CONF./15/P/240.
29. A. C. Werner and R. J. Abelson, Preparation of Protective Coatings by Electrophoretic Methods, WADC-TR-58-11, February 1958. (Unclassified USAF report.)
30. J. H. Oxley et al., Coating of Uranium Dioxide Powders with Metallic Tungsten Films, BMI-1297, Oct. 8, 1958. (Unclassified AEC report.)
31. R. W. Dayton and C. R. Tipton, Jr., Progress Relating to Civilian Applications During June 1958, BMI-1273, June 1958. (Unclassified AEC report.)
32.* J. M. Blocher, Jr., and I. E. Campbell, Carbide Coatings for Graphite, A/CONF./15/P/1428.
33. J. M. Blocher, Jr., et al., Niobium Carbide Coating of Graphite Tubes, BMI-1296, Oct. 6, 1958. (Unclassified AEC report.)
34. J. C. Richmond et al., Ceramic Coatings for Nuclear Reactors, *Journal of the American Ceramic Society*, 38(2): 72-80 (February 1955).

35. W. D. Wilkinson and W. F. Murphy, "Nuclear Reactor Metallurgy," pp. 300-301, D. Van Nostrand Company, Inc., 1958.
36. E. L. Bradley, Problems in Simultaneous Heat-Hardening and Ceramic Coating of Type 420 Stainless Steel, *American Ceramic Society Bulletin*, 37(5): 222-226 (May 1958).
37. Reactor Technology Quarterly Report No. 4, Metallurgy and Materials, KAPL-2000-1, Aug. 1, 1958. (Unclassified AEC report.)
38.* W. J. McGonnagle and R. S. Paul, New Developments in Nondestructive Testing of Reactor Fuel Elements, A/CONF./15/P/2378.
39. K. P. Bokish, Ultrasonic Bond Testing of Irradiated Fuel Elements, HW-56028, May 9, 1958. (Secret AEC report.)
40. J. S. Church et al., Vinyl Coating of Graphite Plates for Ultrasonic Inspection, LAMS-2211, Mar. 25, 1958. (Unclassified AEC report.)
41.* P. C. Aebersold and E. E. Fowler, Recent Developments in Industrial Applications of Isotopes; Gauging and Nondestructive Testing, A/CONF./15/P/1794.

*Second United Nations International Conference on the Peaceful Uses of Atomic Energy, Geneva, September 1958. (Available from the Office of Technical Services, Dept. of Commerce, Washington 25, D. C.)

☆ U. S. GOVERNMENT PRINTING OFFICE : 1959 O -480406 (3)